



Chair of Thermal Processing Technology

Master's Thesis



Risk assessment on fire hazards in the
collection of waste portable batteries in
Austria

Tobias Berthold Grassauer, BSc

November 2022

MONTANUNIVERSITÄT LEOBEN
Department für Umwelt- und Energieverfahrenstechnik
Lehrstuhl für Thermoprozesstechnik

Risk assessment on fire hazards in the collection of waste portable batteries in Austria

Risk analysis and numerical approach on the probability of short circuits in battery bulks

MASTER'S THESIS

submitted by

Ing. Tobias Berthold Grassauer, BSc

approved by

Dipl.-Ing. Michael Hohenberger

Dipl.-Ing. Dr.mont. Thomas Nigl

Univ.-Prof. Dipl.-Ing. Dr.techn. Harald Raupenstrauch

Leoben, November 2022

Affidavit

I declare in lieu of oath, that I wrote this thesis and performed the associated research myself, using only literature cited in this volume.

Eidesstattliche Erklärung

Ich erkläre an Eides statt, dass ich diese Arbeit selbstständig verfasst, andere als die angegebenen Quellen und Hilfsmittel nicht benutzt und mich auch sonst keiner unerlaubten Hilfsmittel bedient habe.

Leoben, November 2022



Ing. Tobias Berthold Grassauer, BSc

Acknowledgement

I would like to thank everyone who supported and motivated me in the preparation of this Master's thesis. Univ.-Prof. Harald Raupenstrauch, Head of the Chair of Thermal Processing Technology, for the supervision and the opportunity to write this thesis. I would like to thank Dipl.-Ing. Michael Hohenberger for his active support in the preparation of the thesis. The numerous suggestions and constructive criticism helped me a lot. Dr. mont. Thomas Nigl I would like to express my special thanks for supporting me with his expertise.

Abstract

The collection of portable batteries at end-of-life is the first step in waste management and circular economy towards material recycling and recovery of raw materials. The collection facilities are placed as close as possible to the end user. The safety of intermediate storage facilities must be ensured.

The increasing amount of lithium-based batteries in many waste streams poses a fire safety challenge for waste management. Just a small number of hazard assessments, as for other material streams available, are found for portable battery collection. The growing proportion of lithium in the amounts placed on the market is already apparent in the composition of the collected masses. Due to their composition, lithium batteries and lithium-ion accumulators cause a significantly higher hazard than other battery types.

Factors influencing the occurring fire risk and the possible consequences are investigated. The expected causes for ‘thermal runaways’ differ from those for the operational phase. The waste nature of the batteries leads to different characteristics. Some impact factors have not been studied qualitatively or quantitatively in the evaluated literature. The effects of battery collection fires are comparable to typical fires in the same scale.

Studies on the probability of short-circuits in battery piles are not yet available. This thesis presents a new approach using rigid body dynamics in the free software ‘blender’ for investigation of the geometrical arrangement of batteries in random fills. The formed short circuits are detected and characterised further. A simplified electrical model is used to estimate the heat generation of each battery and to describe the likelihood of subsequent ignition within the bulk. The influence of different parameters is investigated in several test series and a sensitivity analysis is presented.

The simulation results indicate that the main impact factor on the formation of short circuits is the proportion of button cell batteries. If the fraction is 5 %, the evaluation results in a short circuit rate of about 0.4 % of the cells. In a pure coin battery fraction, this proportion is approx. 83 %. Based on the number of batteries in interconnected networks and the calculated electrical currents, it can be shown that the formation of short circuits across many cells in serial connection can be considered as highly unlikely. With the correlations found, an estimate about the distribution of heat release within the bulk can be made.

Kurzfassung

Die Sammlung von Gerätebatterien am Ende der Lebensdauer stellt in der Abfall- und Kreislaufwirtschaft den ersten Schritt zum stofflichen Recycling und der Rückgewinnung von Rohstoffen dar. Die Rückgabemöglichkeiten werden möglichst nah am Endnutzer platziert, aus diesem Grund ist die Sicherheit der Zwischenlager zu gewährleisten.

Die steigende Menge an Lithium-basierten Batterien in vielen Abfallströmen stellt eine brand-schutztechnische Herausforderung für die Abfallwirtschaft dar. Gefahrenbetrachtungen wie für andere Stoffströme, liegen für die Gerätebatteriensammlung nur in geringer Zahl vor. Der wachsende Lithium-Anteil der in Verkehr gesetzten Mengen zeigt sich bereits in der Zusammensetzung der Sammlung. Aufgrund ihres Aufbaus stellen Lithiumbatterien und Lithium-Ionen-Akkumulatoren eine wesentlich größere Gefahr als andere Batterietypen dar.

Es werden die Einflussfaktoren auf das entstehende Brandrisiko und die möglichen Folgen untersucht. Die erwarteten Ursachen für 'Thermal runaways' weichen von jenen für die Nutzungsphase ab. Die Abfalleigenschaften der Batterien führen zu anderen Charakteristiken. Einige der Einflussfaktoren wurden in der ausgewerteten Literatur bisher weder qualitativ noch quantitativ untersucht. Die Auswirkungen eines Brandes in der Gerätebatteriensammlung sind mit typischen Bränden derselben Größenordnung vergleichbar.

Betrachtungen zur Wahrscheinlichkeit von Kurzschlüssen in Batterieschüttungen liegen bisher nicht vor. In dieser Arbeit wird ein neuartiger Ansatz mittels Starrkörpersimulation in der freien Software 'Blender' vorgestellt, mit dem die geometrische Anordnung von Batterien in zufälligen Schüttungen untersucht werden kann. Die gebildeten Kurzschlüsse werden erfasst und weiter charakterisiert. Durch ein vereinfachtes elektrisches Model kann die entstehende Wärme jeder einzelnen Batterie abgeschätzt und die Wahrscheinlichkeit einer darauffolgenden Entzündung innerhalb der Schüttung beschrieben werden. In mehreren Versuchsreihen wird der Einfluss verschiedener Parameter untersucht. Eine Sensitivitätsanalyse wird präsentiert.

Die Simulationsergebnisse deuten darauf hin, dass der wichtigste Einflussfaktor auf die Bildung von Kurzschlüssen der Anteil an Knopfzellenbatterien ist. Beträgt dieser 5 %, ergibt die Auswertung eine Kurzschlussrate von etwa 0.4 % der Zellen. In einer reinen Knopfbatteriefraktion beträgt dieser Anteil ca. 83 %. Anhand der Anzahl der Batterien in zusammenhängenden Netzwerken und den errechneten Strömen zeigt sich, dass die Bildung von Kurzschlüssen über viele Zellen in Serienschaltung als sehr unwahrscheinlich erachtet werden kann. Mit den gefundenen Zusammenhängen lässt sich eine Abschätzung über die Verteilung der Wärmefreisetzung innerhalb der Schüttung treffen.

Contents

| | |
|--|-----------|
| 1. Introduction | 1 |
| 2. Theory & literature review | 2 |
| 2.1. Principles of electrical networks | 2 |
| 2.1.1. Basic electrical components | 2 |
| 2.1.1.1. Ideal connection | 2 |
| 2.1.1.2. Ideal resistor | 2 |
| 2.1.1.3. Ideal voltage source | 3 |
| 2.1.2. Kirchhoff's circuit laws | 3 |
| 2.1.2.1. Current law | 4 |
| 2.1.2.2. Voltage law | 4 |
| 2.1.3. Calculation of electrical networks | 5 |
| 2.2. Batteries | 6 |
| 2.2.1. Chemical fundamentals | 6 |
| 2.2.2. Electrical fundamentals | 7 |
| 2.2.2.1. Voltage | 7 |
| 2.2.2.2. Capacity | 8 |
| 2.2.2.3. Internal resistance | 8 |
| 2.2.2.4. Short circuit | 9 |
| 2.2.3. Battery types and categories | 9 |
| 2.2.3.1. Primary cells and batteries | 10 |
| 2.2.3.2. Secondary cells and batteries | 10 |
| 2.2.4. Hazardous properties | 11 |
| 2.3. Battery collection in Austria | 12 |
| 2.3.1. Legal framework in Austria | 12 |
| 2.3.1.1. Austrian legislation for collection and treatment of waste bat- teries | 12 |
| 2.3.1.2. Definitions | 14 |
| 2.3.1.3. Waste holder | 15 |
| 2.3.1.4. Stakeholders | 18 |
| 3. Risk analysis | 21 |
| 3.1. Problem formulation | 21 |
| 3.1.1. System description | 21 |

| | | |
|-----------|--|-----------|
| 3.2. | Causes | 22 |
| 3.2.1. | Thermal runaway of a lithium battery | 22 |
| 3.2.1.1. | Mechanical abuse | 23 |
| 3.2.1.2. | Thermal and electrical abuse | 23 |
| 3.2.2. | Heat release of a battery | 25 |
| 3.2.2.1. | Serial short circuit of many batteries | 26 |
| 3.2.2.2. | Parallel short circuit of many batteries | 27 |
| 3.2.3. | Fire causing input material | 28 |
| 3.3. | Effects | 28 |
| 3.3.1. | Fear and panic reactions | 28 |
| 3.3.2. | Release of toxic gases | 29 |
| 3.3.3. | Spread inside the battery bulk | 29 |
| 3.3.4. | Expansion out of the container | 29 |
| 3.3.5. | Release of chemical substances | 30 |
| 3.3.6. | Explosion | 30 |
| 3.4. | Results and discussion of the risk analysis | 30 |
| 3.5. | Conclusion of the risk analysis | 32 |
| 4. | Numerical study on electrical short circuits in battery bulks | 33 |
| 4.1. | Problem formulation | 33 |
| 4.2. | Algorithm development | 33 |
| 4.2.1. | Geometrical models | 34 |
| 4.2.1.1. | Batteries | 34 |
| 4.2.1.2. | Containers | 36 |
| 4.2.2. | Physical model | 38 |
| 4.2.2.1. | Standard battery types composition | 40 |
| 4.2.3. | Electrical model | 41 |
| 4.2.4. | Time discretization and iterations | 42 |
| 4.2.5. | Analysis | 43 |
| 4.2.5.1. | Batteries and bulk | 43 |
| 4.2.5.2. | Short circuits in bulk | 44 |
| 4.2.5.3. | Electrical currents and released heat | 46 |
| 4.2.5.4. | Simulation stability and accuracy | 48 |
| 4.3. | Design of experiments | 49 |
| 4.4. | Results of the numerical study | 50 |
| 4.4.1. | Parameter tests | 50 |
| 4.4.2. | Various bulk sizes with constant parameters | 51 |
| 4.4.2.1. | Bulk density ρ_{bulk} | 51 |
| 4.4.2.2. | Bulk void fraction ε_{bulk} | 52 |
| 4.4.2.3. | Number of batteries $N_{batts,bulk}$ | 52 |
| 4.4.2.4. | Movement at the end of the settle time | 53 |
| 4.4.2.5. | Pole contacts of batteries | 53 |
| 4.4.2.6. | Short circuits | 54 |
| 4.4.2.7. | Electrical currents and heat release | 57 |

| | | |
|-----------|---|------------|
| 4.4.3. | Pure button cell bulks | 59 |
| 4.4.3.1. | Bulk density ρ_{bulk} | 59 |
| 4.4.3.2. | Number of batteries $N_{batts,bulk}$ | 59 |
| 4.4.3.3. | Short circuits | 60 |
| 4.4.3.4. | Distribution of heat release | 62 |
| 4.4.4. | Variation of battery types | 62 |
| 4.4.5. | Influence of the mean battery voltage | 64 |
| 4.4.6. | Computational time | 65 |
| 4.4.7. | Parameter sensitivity tests | 66 |
| 4.5. | Discussion of the numerical study | 67 |
| 4.5.1. | Approximations | 67 |
| 4.5.1.1. | Rigid body simulation | 67 |
| 4.5.1.2. | Geometrical modelling | 67 |
| 4.5.1.3. | Physical modelling | 68 |
| 4.5.1.4. | Electrical modelling | 68 |
| 4.5.2. | Results of the simulation | 69 |
| 4.5.3. | Application limits | 69 |
| 4.5.3.1. | Limits of the model | 69 |
| 4.5.3.2. | Limits of interpretation of the results | 70 |
| 4.6. | Conclusions of the numerical study | 71 |
| 5. | Conclusions | 75 |
| 6. | Outlook and Suggestions | 76 |
| 6.1. | Suggestions for further work | 77 |
| | Bibliography | 80 |
| | Bibliography | 81 |
| | List of Figures | 85 |
| | List of Tables | 87 |
| A. | Standard battery distribution from sample | I |
| B. | Implemented container sizes and types | II |
| C. | Sensitivity parameters | III |

1. Introduction

On the basis of EU legislation, efforts are currently being made in Austria to increase the collection rates for waste batteries. The aim is to recover raw materials and conserve natural resources by establishing a circular economy.

The increasing collection rates, together with the rapidly increasing quantities of lithium-based battery systems placed on the market, have led to a change in the risk situation in the area of collection. Until now, the collected quantities consisted mainly of non-critical types like the widely used "alkaline" battery. Because of their high energy density and highly flammable ingredients, lithium batteries pose a fire hazard. The wide range of applications has already led to detailed studies of the potential dangers in the use phase. In the field of waste collection, the focus is on batteries that occur in waste streams other than battery collection and regularly lead to fire incidents there.

Detailed hazard analyses for the specific collection of batteries are lacking so far. Some possibilities are mentioned in the legal requirements, but for most of them there is no reliable knowledge about the probability of occurrence and effects. Since waste management is always lagging behind the market, an increasing fire risk can be expected.

In order to make the offer as low-threshold as possible for the end consumer, collection takes place at various locations, close to the waste producer. Therefore, it is important that the collection is carried out safely.

In this thesis, the risk in the collection of spent portable batteries in Austria will be assessed. For this purpose, possible causes of fires are to be identified and subsequently evaluated qualitatively and quantitatively.

2. Theory & literature review

In this chapter the literature, legislation in Austria and the theoretical background will be presented shortly.

2.1. Principles of electrical networks

The main concepts of electrical engineering regarding the topic of this work will be summarized in this section. Batteries are usually low voltage direct current (DC) voltage sources. Therefore the focus will be on DC and effects for high voltage, currents or alternating current (AC) will be neglected. Fast switching on and off processes are also not considered.

2.1.1. Basic electrical components

In electrical engineering all components are substituted by simple ideal representations with well defined behaviour. Under the above restrictions for typical batteries, three simple components: ideal connection, ideal resistance and ideal voltage source are sufficient to describe networks of batteries.

2.1.1.1. Ideal connection

An ideal connection is a electrically perfect conduction connection. The voltage drop is zero regardless the length of the connection. In circuit diagrams it is represented by a line.

2.1.1.2. Ideal resistor

At an ideal resistor the voltage drop U is proportional to the current I . The proportionality factor is the resistance R measured in Ω , as shown in Ohm's law (equation (2.1)).

$$U = R \cdot I \tag{2.1}$$

The power dissipation P is converted into heat. It can be calculated using equation (2.2). For a resistor the electrical power dissipation is equal to the heat release rate \dot{Q} .

$$P = \dot{Q} = U \cdot I = I^2 \cdot R = \frac{U^2}{R} \tag{2.2}$$

Following the common sign convention, voltage and current point in the same direction and have the same sign. The dissipated heat has a positive sign. The used symbol for circuit diagrams and the convention for voltage and current direction is shown in figure 2.1.

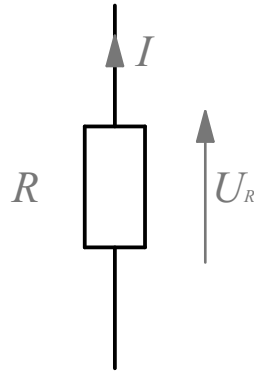


Figure 2.1.: Symbol for an ideal electrical resistor (EN 60617-2)

2.1.1.3. Ideal voltage source

Ideal DC voltage sources are assumed to maintain a voltage difference between the poles at all times. Heat dissipation is assumed to be zero and the voltage is independent of the current. Current and voltage are pointing in the opposite direction. Conventional the direction of the electrical current points out of the plus pole and towards the minus pole of the source. Calculating the power according to equation (2.2) give a negative value, so the power is transferred into the circuit. Figure 2.2 shows the symbol for a voltage source.

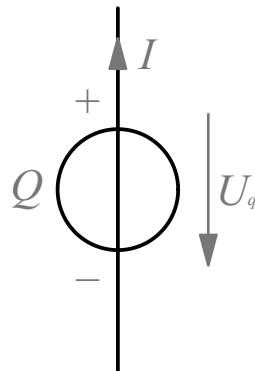


Figure 2.2.: Symbol for an ideal voltage source (EN 60617-2)

2.1.2. Kirchhoff's circuit laws

Kirchhoff's circuit laws are two basic formulas for calculation of electrical networks. When an electrical network just consists of connections, voltage sources and resistors, the two laws of Kirchhoff together with Ohm's law give enough equations to calculate the whole network.

2.1.2.1. Current law

This law states that the sum of all electrical currents entering a junction point is equal the sum of all currents leaving. If positive values are used for entering and negative values for leaving currents, the law can be formulated as the sum of all currents in a junction N is zero (equation (2.3)). In a network linear independence of all equations set up by this law is valid for all but one junction. The equation of the last junction results from the others.

$$\sum^{i \text{ in } N} I_i = 0 \quad (2.3)$$

Figure 2.3 gives an example of a junction with three currents. The current law is applied in equation (2.4).

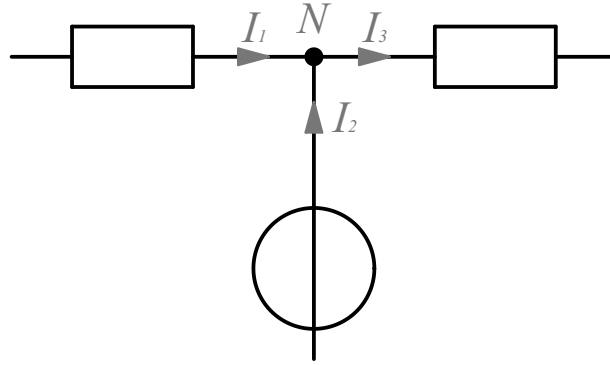


Figure 2.3.: Electrical currents entering and leaving the junction

$$I_1 + I_2 - I_3 = 0 \quad (2.4)$$

2.1.2.2. Voltage law

For each closed loop L in a network, the sum of all source voltages and voltage drops is zero (equation (2.5)). Voltages are taken positive, if they point the same direction as the loop is directed and negative if opposite.

$$\sum^{i \text{ in } L} U_i = 0 \quad (2.5)$$

Figure 2.4 gives an example for a loop with four voltages and equation (2.6) the formulation of the voltage law.

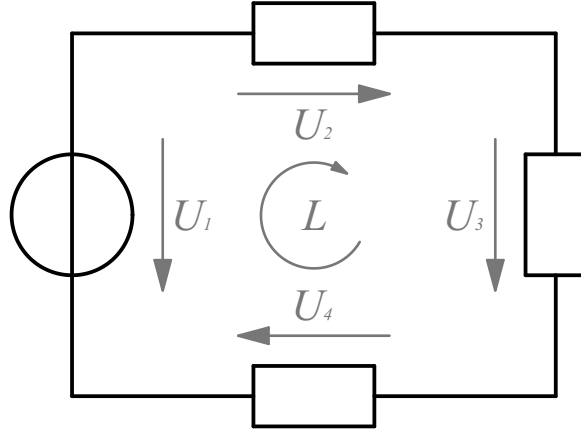


Figure 2.4.: Sum of all voltages around a loop equals zero

$$-U_1 + U_2 + U_3 + U_4 = 0 \quad (2.6)$$

2.1.3. Calculation of electrical networks

A number of methods are available for the calculation of electrical networks. In this work, an approach using graph theory is adapted. Only networks build of ideal voltage sources and resistances are used. The voltage and resistance values are given and the currents, including the direction have to be calculated.

When investigating a real scenario, the electrical properties of all components get modelled by ideal representations. The components are joined by connections and junctions. This gives an electrical circuit diagram, which can be described as a mathematical graph. Between components connected directly without any branches, is a so-called edge. The edge i has electrical properties source voltage U_{S_i} , resistance R_i and current I_i .

As explained in section 2.2.2.3, a battery can be modelled by a voltage source and an internal resistance serially connected. Each battery is an edge with the U_i is the battery voltage and R_i the internal resistance. The edge connects two nodes, each on representing a pole of the battery. The direction of the current will be assumed from the minus to the plus pole and the source voltage in the opposite direction. When poles of two batteries touch, an additional node connected with two edges between them is added. The voltage source of these edges is 0 V and R_i the connective resistance. The direction of the current is set arbitrarily.

Graph theory provides algorithms for the detection of paths, loops and connected and unconnected parts of the graph. The python library 'networkx' ([1]) is used for investigation of the graphs. The graph is separated in its connected compounds and equations are set for each individually. Equation (2.3) is written for each junction point, except one. The voltage law is formed by adding the source voltages and the voltage drops of the resistors, using the correct sign. The set of equations is solved by linear algebra and all currents are calculated. This way all currents through all batteries and connections are found. If a battery current is negative, it means the battery gets charged, positive it gets discharged. Using equation (2.2) all heat releases of all resistors can be calculated.

2.2. Batteries

Batteries are devices used as power supply for different devices. [2] defines a battery as one or more cells, forming a unit with provisions for external connections. A cell in context of this work is an electrochemical device consisting of positive and negative electrodes, a separator and an electrolyte ([2]). A battery cell is an electrochemical cell that is used to generate and store electrical energy. In Austrian and EU legislation batteries are simply defined as sources of electrical energy which is obtained by a direct conversion of chemical energy, which can consist of one or more, primary or secondary cells ([3, 4]). A primary cell or battery is designed for single use and cannot be recharged, while secondary cells or batteries can be recharged and be used multiple times. The chemical reaction is reversible([2]). The term battery refers either to an electrochemical cell in a design that is used as such for the respective application, or to several cells connected in series or in parallel in such a housing. For most practical applications, the actual number of cells is irrelevant to the user as long as the total voltage is known. Within this work a the term batteries is used regardless of the number of cells. The main terms regarding batteries are defined in the standards of IEC (e.g. [5, 6, 7, 8, 9, 10]).

2.2.1. Chemical fundamentals

A spontaneous redox reaction, where reduction and oxidation are locally separated, transforms the chemical energy in a flow of electrons. This is called a ‘Galvanic cell’ and the basic principle of a battery cell. Figure 2.5 gives a schematic drawing. The main components regarding chemistry are the anode, the electrolyte and the cathode. In many practical applications also a separator and cover materials are needed.

The anode is connected to the negative terminal of the cell and is made from a less noble material than the cathode. The cathode forms the positive terminal. Both electrodes are connected inside the cell with an ion conductor and an external electron conductor. The combination of anode and cathode materials and the difference of their electrochemical potential define the cells voltage.

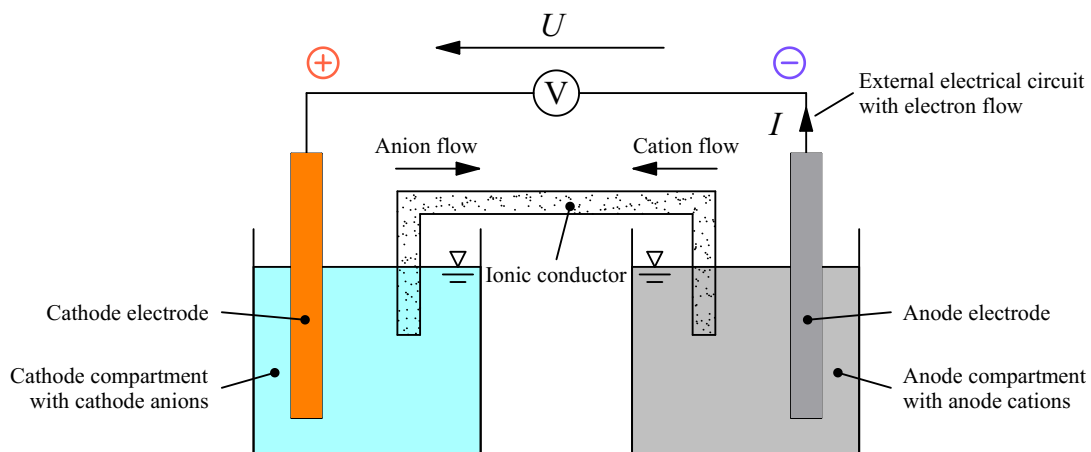


Figure 2.5.: Schematic structure of the chemical system of a battery

2.2.2. Electrical fundamentals

In electrical engineering, portable batteries are used as voltage supply for low voltage direct current supply. The symbol used in circuit diagrams is shown in figure 2.6.

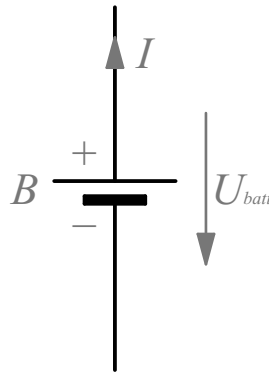


Figure 2.6.: Symbol for a battery (EN 60617-2)

2.2.2.1. Voltage

The voltage of the battery means the electrical potential difference between the two poles of the battery, which is usually called ‘terminal voltage’ (U_T), shown in figure 2.7. For various reasons the measured voltage does not remain constant.

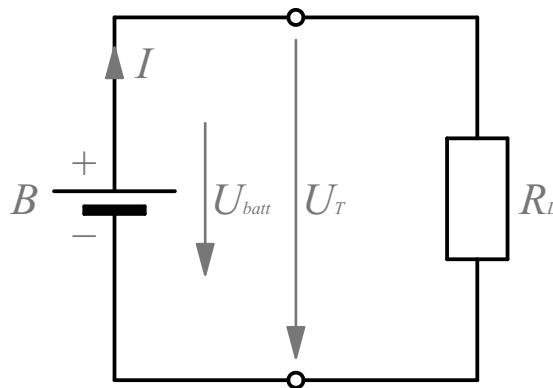


Figure 2.7.: Terminal voltage of a battery under a load R_L

The ‘open circuit voltage’ (OCV) is the voltage at an infinite load resistance R_L . Since most of the time voltmeters are used for measuring, their very high internal resistance is assumed to be infinite. The highest possible OCV of a battery (OCV_{max}) is the terminal voltage of a fully charged battery without any load ($R_L \approx \infty$) and no current ($I \approx 0$) ([9]). OCV_{max} is the upper limit for any voltage measured at a single battery. It mostly depends on the used electrochemical system and the number of cells connected in series. The nominal voltage U_N is an approximate value used for identification the open circuit voltage of a battery ([9]). It is

the value given on the labels of batteries. The ‘closed circuit voltage’ (*CCV*) ([9]) or ‘discharge voltage’ ([2]) is the terminal voltage U_T while the battery is discharged with a current I over a load R_L . A battery is considered empty when terminal voltage drops below the ‘end-of-charge-voltage’ ([2]) or ‘end-point-voltage’ (*EV*) ([9]). The dependency of the terminal voltage to the state of charge is mostly depending on the used battery chemistry. If the characteristic is quite linear it is easier to calculate the state of charge by measuring the terminal voltage. The disadvantage is that most electrical devices need a reliable voltage supply within certain voltage levels. A very flat course with a sharp decrease towards the end allows a long usage of the battery with almost the same voltage. If the run gets too flat, measuring the remaining energy available is not possible anymore.

2.2.2.2. Capacity

The capacity of a battery is the ampere hours a fully charged battery can provide ([2]). The rated capacity is given by the manufacturer and gives an approximation of the actual capacity at a certain discharge rate and a under specific environmental conditions ([2]). The available capacity is depending on the discharge rate and the ambient conditions and if the battery has a permanent or temporary loss of capacity ([2]). The state of charge (*SOC*) is the residual capacity divided by the rated capacity ([2]).

2.2.2.3. Internal resistance

Ideal voltage sources have a constant voltage under all conditions. Real batteries cannot provide the voltage at all currents. This effect can be modelled using an internal resistance R_i in series to the source. The equivalent circuit diagram is shown in figure 2.8.

Under a load R_L , the terminal voltage drops depending on the current. This can be described by

$$U_T = U_q - R_i \cdot I = U_q \cdot \left(1 - \frac{R_i}{R_i + R_L}\right) \quad (2.7)$$

A part of the electrical power is dissipated on the internal resistor and cannot be used in the circuit:

$$P = P_{R_i} + P_{R_L} = I^2 \cdot R_i + I^2 \cdot R_L = \frac{U_q^2}{R_i + R_L} \quad (2.8)$$

While an ideal voltage source can provide a infinite current when no load is applied, for real batteries the short circuit current is limited to

$$I_{sc,max} = \frac{U_q}{R_i} \quad (2.9)$$

In reality, the effects often can be neglected as long as the currents are low and the load resistance is high compared to the internal resistance.

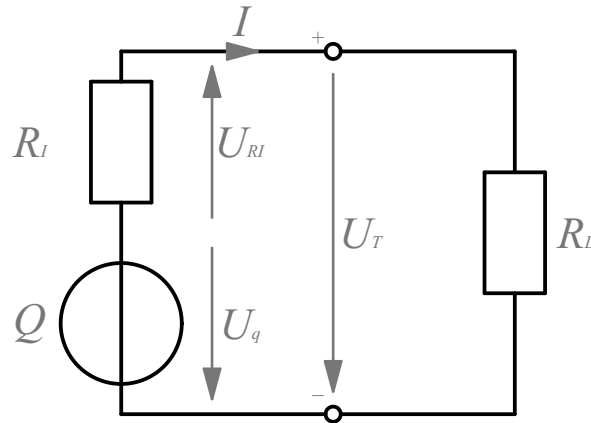


Figure 2.8.: Internal resistance model of a battery

2.2.2.4. Short circuit

Short circuiting of a battery is an unintended discharging process with a very low load resistance. This results in very high electrical current. The internal resistance cannot be neglected anymore and a heat dissipation leads to a temperature rise in the battery.

An ideal short circuit with $R_L = 0$ leads to the highest current a battery can provide and following equation (2.2) the maximum heat release on the internal resistance. The result is a thermal stress for the battery. Depending on the electrochemical system, components of the battery can get ignited. Liquid electrolytes can get heated up to the boiling point and vaporize. This results in a pressure rise if the battery is sealed. Lithium-based batteries can perform a thermal runaway.

2.2.3. Battery types and categories

The wide range of applications has led to a variety of battery types. A distinction can be made between non-rechargeable (primary) and rechargeable (secondary) batteries. Within these two, the batteries can be categorized by shape and electrochemical system. Battery types are standardised in

- IEC 60095 (Lead-acid starter batteries),
- IEC 61951-1 (Secondary cells, Nickel-Cadmium, [5]),
- IEC 61951-2 (Secondary cells, Nickel-metal hydride, [6]),
- IEC 61960-3 (Secondary cells, Prismatic and cylindrical lithium cells and batteries, [7]),
- IEC 61960-4 (Secondary cells, Coin lithium cells, [8]) and
- IEC 60086 (Primary batteries, [9, 10]).

Lead-acid batteries have a lower energy density than other battery systems, therefore they are not used in portable batteries. The collection is organized in a different way, so they will not be taken in account from here. In this chapter only the standards valid at the moment of writing will be discussed. Batteries, produced by withdrawn standards, can still show up in waste

battery collection. As an example, mercury batteries are not covered by standards anymore and the production and placing in the market is forbidden now. Further all considerations are focused on batteries used by end consumers since they are the most likely to appear in portable waste battery collection.

2.2.3.1. Primary cells and batteries

In 2021, primary batteries accounted for the majority of the collected battery mass in Germany ([11])¹. A sample from Austria shows a similar distribution. Primary batteries are categorized by electrochemical system and geometry according to [9, 10] and are grouped in six categories.

For round cells the vast majority of primary batteries in the market are using a zinc-manganese dioxide system with a potassium hydroxide electrolyte ([11, 2]). These batteries are labelled with ‘L’ in [9] and are the common type for many types of end consumer applications. Zinc-carbon are often used for low power and long life applications ([2]) and are the second most used type of primary batteries.

The fastest growing types of round cells are lithium based. Primary lithium batteries have an anode of metallic lithium alloys ([2]). For cylindrical cells mostly manganese dioxide (type ‘C’) or iron disulphide (type ‘F’) cathodes are used (compare [13, 14, 15, 16, 17, 18, 19]). Since lithium reacts with water in a dangerous way, most of the time aprotic organic solvents containing lithium salts are used as electrolytes ([20]). Propylene carbonate ([20, 21, 13]), ethylene carbonate ([20, 21]), diethyl carbonate([20, 21]), or dimethyl carbonate[21] are examples used in solvent mixtures. For primary lithium batteries lithium hexafluorophosphate and lithium trifluoromethanesulfonate are used as lithium salts in the electrolyte ([20]).

For button cells lithium (‘C’, [9]), alkaline manganese (‘L’, [9]), zinc-air (‘L’, [9]) and silver oxide (‘S’, [9]) are sold in relevant amounts ([11]). Zinc-air and alkaline manganese Silver-zinc cells are often used in small devices when long battery life and low power is needed, as in hearing aids or watches.

2.2.3.2. Secondary cells and batteries

In the case of secondary batteries, lithium-ion batteries accounts for the majority of the quantity placed on the market (82.7% of the mass in Germany 2021, [11]). Since lead batteries will be neglected, nickel–metal hydride is the second large group of secondary batteries, representing 6.3% of the mass ([11]). Further alkaline manganese and nickel cadmium are sold in smaller amounts.

¹For Austria no detailed data for the composition of batteries placed in the market or collected were found. [11] and [12] contain data for Germany. Comparability of Austrian and German market will be assumed in this thesis.

2.2.4. Hazardous properties

Lithium-based batteries combine high energy contents with flammable, organic electrolytes. Further high energy densities require low thermodynamic stabilities ([22]). Therefore, they show very different hazardous properties compared to other battery types. A typical failure mode is a so-called ‘thermal runaway’. The wide use of lithium batteries led to many publications on this topic. A review on the available literature is recently published in [23]. The following remarks base on this work.

A thermal runaway is a chain exothermic reaction inside the battery. It leads to a high heat release and temperature increase. Following the structure of the battery fails due high heat and pressure. The initial event is the failure of the separator and a short circuit between the electrodes inside the batteries. The separator can get destroyed by heat or mechanical stress.

High temperatures degrade, destabilize or melt the separator. The heat can come from outside, which is usually referred as ‘thermal abuse’, or be generated inside the battery due high currents. The second mechanism is called ‘electrical abuse’. High voltages can also lead to internal short circuits. Among others thermal abuse was investigated experimentally by [24], [25], [26] and [27]. For electrical abuse, overcharging leads to the most catastrophic failures ([28], [26], [23]). External short circuits can trigger thermal runaway when the state of charge is high enough.

Mechanical abuse was tested by nails ([26]), indentation ([29], [30]), three-point-bending and axial compression ([29]). [29] provides data for four different load cases, which makes assumptions about the required forces and deformation energies possible. The results are shown in table 2.1. Instead of integration of the F - d -function, the deformation energy E_{deform} is calculated simplified by

$$E_{deform} = \frac{F \cdot d}{2} \quad (2.10)$$

with the force F in Newton and the displacement d in metre when a thermal runaway occurred.

Table 2.1.: Forces, displacement and approximate deformation energy for internal short circuits of 18650 cylindrical lithium-ion batteries [29]

| Load conditions | F /kN | d /mm | E_{deform} /J |
|---------------------|---------|---------|-----------------|
| Radial compression | 35 | 6.1 | 107 |
| Indentation | 11 | 7.0 | 39 |
| Three-point bending | 2 | 5.0 | 5 |
| Axial compression | 7 | 4.0 | 14 |

2.3. Battery collection in Austria

The collection of waste batteries is regulated by law. The main points are presented in this section.

2.3.1. Legal framework in Austria

The legal framework for the collection of waste batteries in Austria is part of the waste legislation. The organisation and the logistics of the collections are defined and rules for fire and chemical safety are given. The Austrian waste legislation is based on EU laws. The union laws are set as Directives and therefore have to be adapted into Austrian legislation. A legally binding EU Regulation is in discussion in 2022. Since the EU legislation is not binding, only the relevant Austrian laws will be discussed.

Discussing laws requires defined legal terms. The english translations in this section are based on a comparison of the official english and german editions of EU directives dealing with waste law, if possible. Other sources are publications of official Austrian authorities.

2.3.1.1. Austrian legislation for collection and treatment of waste batteries

In matter of waste battery collection European Directives are transposed in the "waste management law" from 2002 and three following Regulations. For transportation on roads the regulations of ADR 2021 apply. The relevant legislation can be found in table 2.2.

Following the EU Directives, the "Federal law on sustainable waste management" (AWG 2002, [31]) aims for a sustainable and resource efficient waste management. Wastes should be collected separately for an optimal recycling system. Adverse impacts on humans, animals and plants should be avoided (§ 1 (1) AWG 2002). The AWG 2002 contains main definitions and guidelines for Austrian waste management. It is specified on what topics further Regulations have to be set by Austrian ministries.

The "Regulation [...] on the Waste Prevention, Collection and Treatment of Waste Batteries and Accumulators" (Batterienverordnung, [3]) specifies, beside others, a largely separate collection of waste batteries as a goal of the Regulation. A collection rate of 45 % for portable batteries is set as a minimum goal (§ 1 (3) Batterienverordnung). The Batterienverordnung elaborates the rules of the AWG 2002 in terms of the obligations of different stakeholders in waste battery collection.

Minimum criteria in terms of safety and environmental protection in waste battery collection are defined in the "Regulation [...] on Waste Treatment Obligations" (AbfallBPV, [32]). The federal ministry published explanatory notes ([33]), which will also be discussed. The "Regulation [...] on a List of waste" (Abfallverzeichnisverordnung 2020, [34]) classifies different wastes as hazardous or not.

Waste batteries are separated in three categories: portable, industrial and automotive batteries (§ 3 and Annex 3 Batterienverordnung). In this work, the main focus will be put on portable batteries.

Table 2.2.: Relevant legislation on the collection of waste batteries in Austria

| | German title | English translation | Abbreviations | Ref. |
|---|--|---|--|----------|
| 1 | Bundesgesetz über eine nachhaltige Abfallwirtschaft | Federal law on sustainable waste management | Abfallwirtschaftsgesetz 2002, AWG 2002 | [31] |
| 2 | Verordnung der Bundesministerin für Klimaschutz, Umwelt, Energie, Mobilität, Innovation und Technologie über ein Abfallverzeichnis | Regulation of the Federal Minister for Climate Action, Environment, Energy, Mobility, Innovation, and Technology on a List of waste | Abfallverzeichnisverordnung 2020 | [34] |
| 3 | Verordnung des Bundesministers für Land- und Forstwirtschaft, Umwelt und Wasserwirtschaft über die Abfallvermeidung, Sammlung und Behandlung von Altbatterien und -akkumulatoren | Regulation of the Federal Minister for Agriculture and Forestry, Environment and Water Management on the Waste Prevention, Collection and Treatment of Waste Batteries and Accumulators | Batterienverordnung | [3] |
| 4 | Verordnung des Bundesministers für Land- und Forstwirtschaft, Umwelt und Wasserwirtschaft über Abfallbehandlungspflichten | Regulation of the Federal Minister of Agriculture, Forestry, Environment and Water Management on Waste Treatment Obligations | AbfallBPV | [32] |
| 5 | Europäisches Übereinkommen über die internationale Beförderung gefährlicher Güter auf der Straße | Agreement of 30 September 1957 concerning the International Carriage of Dangerous Goods by Road | ADR | [35, 36] |

2.3.1.2. Definitions

In this section important expressions used in Austrian laws and regulations are discussed. More definitions can be found in corresponding legislation.

Battery

- A source of electrical energy consisting of one or more (non-rechargeable) primary cells or of one or more (rechargeable) secondary cells, which is obtained by direct conversion of chemical energy. (§ 3 (1) Batterienverordnung)
- Primary batteries, secondary batteries (rechargeable batteries, accumulators) and their electrochemical units (cells). (§ 3 (6) AbfallBPV)

Both definition cover both, rechargeable and non-rechargeable batteries and the number of cells is not a criterion. Unless stated otherwise, in this work batteries always refers to portable batteries.

Portable battery Portable battery are Batteries, button cells, battery packs or accumulators, that

a) are sealed,

b) can be hand-carried and

c) are neither an industrial battery nor an automotive battery, except the industrial batteries are used electrical or electronic devices in private households (§ 3 (3) Batterienverordnung)

Button cell Button cells are small, round portable batteries, with a diameter larger than their height and that are used for special cases as hearing aids, wristwatches, small portable devices, or are intended for backup power supply. (§ 3 (4) Batterienverordnung)

Waste Waste within the meaning of AWG 2002 are movable objects,

1. which the owner intends to discard of or has discarded, or
2. the collection, storage, transport and treatment of which as waste is necessary in order not to impair the public interests [...]

(§ 2 (1) AWG 2002)

Waste batteries Batteries or accumulators, which are waste according to § 2. (1) AWG 2002. (§ 3 (7) Batterienverordnung)

Problematic substances Problematic substances are hazardous waste, that usually produced in private households. Hazardous wastes produced by others are also problematic substances if they are comparable to the hazardous waste produced by households in terms of amount and characteristics.

2.3.1.3. Waste holder

The waste holder is the waste producer according to § 2 (6) (2) AWG or the person who is in possession of the waste (§ 2 (6) (1) AWG 2002). Obligations for waste holders of waste batteries are defined by the AWG 2002, Abfallverzeichnisverordnung 2020 and the AbfallBPV. In the collection of waste batteries, the person of the waste holder changes.

Waste must always be handled in a manner that complies with the goals and principles of the AWG 2002 and no public interests are affected (§ 15 (1) AWG 2002). If the waste holder is permitted and has access to approved plants and suitable place, all treatments, recoveries and disposal have to be in agreement with the applicable laws. Since the final treatment is not part of this work, at this point, reference is made to the AWG.

If the waste holder is not allowed to treat the batteries, he has to hand them over to a permitted collector or treater (§ 15 (5) AWG 2002). Records of all waste batteries must be kept (§ 17 (1) AWG 2002). Private households, carriers and some others are excluded from this obligation (§ 17 (2) AWG 2002).

Abfallverzeichnisverordnung 2020 obligates waste holders to assign the waste to a waste type in accordance with the annex 2, annex 3 and annex 4 of Abfallverzeichnisverordnung 2020 (§ 1 (2) Abfallverzeichnisverordnung 2020). The corresponding positions for waste batteries are listed in table 2.3.

Table 2.3.: Classification of waste batteries in Austria (Abfallverzeichnisverordnung 2020 Annex 1)

| | SN, waste code | Description | Hazardous | Declassification possible |
|---|----------------|-----------------------------|-----------|---------------------------|
| 1 | 35323 | Nickel-cadmium accumulators | yes | no |
| 2 | 35324 | Button cells | yes | no |
| 3 | 35335 | Zinc-carbon batteries | yes | no |
| 4 | 35336 | Alkali-manganese batteries | yes | no |
| 5 | 35337 | Lithium batteries | yes | no |
| 6 | 35338 | Batteries, mixed | yes | no |

The AbfallBPV commits the waste holder to take measures for safety (§ 2 (2) AbfallBPV). The obligations regarding batteries are listed in section 3 AbfallBPV. § 17 gives regulations regarding collection and storing, §§ 18 - 22 on the treatment. The federal ministry published extensive explanatory notes to the AbfallBPV.

Waste batteries have to be protected against effects of weather and mechanical stress (§ 17 (1) (1) and § 17 (1) (2) AbfallBPV). The explanatory notes mention protection against precipitation and excessive sunlight, against frost just in individual cases as threats. Storage outside under a roof is therefore possible, as long as no frost protection is necessary. Mechanical stress should be prevented, so the batteries are not damaged during the collection. This should

prevent the leakage of liquid electrolytes and fire and explosion hazards. This does not apply right before the treatment plant (§ 17 (1) (2) AbfallBPV).

Neither the storage of things or substances that pose a fire or explosion hazard themselves nor items or substances with an increase the potential risk in case of a fire or explosion is in the sphere of influence allowed (§ 17 (1) (3) AbfallBPV). The explanatory notes mention especially highly flammable materials, high additional fire loadings or the release of toxic gases in case of a fire.

The sphere of influence was the preferred formulation to close range around the batteries, to take in account that e. g. lithium batteries can be thrown as far as 30 m or more in case of an explosion, as the explanatory notes state. The sphere of influence is therefore also depending on the application of some safety measures such as closed collection boxes.

Additional to § 17 (1) AbfallBPV lithium batteries or battery mixtures containing lithium batteries require protection against water, moisture and extensive heat (§ 17 (4) AbfallBPV). The paragraph does not state a weight fraction threshold for the definition of battery mixtures containing lithium batteries. The explanatory notes elaborate the higher risk of lithium batteries: burst, ignition, explosion and formation of elemental hydrogen.

Extending the precautions for lithium batteries § 17 (5), (7) and (8) AbfallBPV lists three criteria defining especially dangerous batteries and battery mixtures. For these fractions further safety and fire protection measures must be taken (§ 17 (6) AbfallBPV). Reasons for the higher safety risks through lithium batteries are given in the explanation notes to AbfallBPV (explanations to § 17 (1), (4), (6) (3), (6) (4), (7)).

1. Larger or more powerful lithium batteries (§ 17 (5) AbfallBPV) The following criteria are listed:

- Lithium batteries with a mass more than 500 g,
- Lithium ion cells with more than 20 Wh capacity,
- Lithium ion batteries with more than 100 Wh capacity,
- Lithium metal cells with more than 1 g lithium and
- Lithium metal batteries with more than 2 g lithium.

These batteries must not be collected together with batteries without lithium. This category does not include most of portable batteries (compare explanations to § 17 (5) AbfallBPV).

2. Pure lithium batteries or mixtures with high lithium content (§ 17 (7) AbfallBPV) If the battery mixture exceeds a mass content of 10 % lithium batteries additional precautions are necessary. The explanatory notes elaborate, that the risk in case of a thermal runaway of a battery increases with higher lithium battery contents. The likelihood of another battery being close enough to start a thermal runaway too and the fire spreads to the whole battery bulk rises with increasing lithium battery contents.

In the explanation state, that a serious definition of a threshold for the mass content cannot be done, due to the large number of impact factors to the risk. Mixtures with lithium fractions

below 10 mass % can still show this kind of chain reactions and the explanatory notes suggest extended protection measures for bulks with more than 4 mass %. The lithium content in the collection should be kept as low as possible (compare explanations to § 17 (7) AbfallBPV).

3. Lithium batteries stronger suspicion of being damaged (§ 17 (8) AbfallBPV) This category contains lithium batteries from recalls or obviously damaged batteries which are taken over separately. These batteries may not be placed in the mixed collection (compare explanations to § 17 (8) AbfallBPV). Collection centres have to hold appropriate containers for obviously damaged batteries in reserve (§ 17 (9) AbfallBPV). The explanations to § 17 (6) (3) and (4) contain non-exhaustive list for characteristics to recognise damaged batteries.

Batteries mentioned in point 1 (§ 17 (5) AbfallBPV) or point 3 (§ 17 (8) AbfallBPV) must be kept separately, but waste battery streams from the mixed collection may fall into point 2 (§ 17 (7) AbfallBPV).

For the extended safety and fire protection measures that must be taken for these categories, § 17 (6) AbfallBPV gives a non exhaustive list and further recommendations can be found in the explanatory notes. A precise definition of the required actions is not specified in the law. The appropriateness of the respective measures must be assessed by evaluating possible risk to people (explanatory notes to § 17 (6)). The 17 (6) AbfallBPV mentions the following measures as particularly important:

1. Protection of short circuiting of the battery poles (§ 17 (6) (1) AbfallBPV) The explanatory notes suggest a range of appropriate measures, like masking of the poles or cables using insulating tape, packing of each single battery in isolating material, adding layers of non-conductive material in the bulk and avoidance of extensive shaking and electrically conductive miscasts.

2. Protection of mechanical damage (§ 17 (6) (2) AbfallBPV) Unlike § 17 (1) (2) AbfallBPV for all batteries, there is no exception for storage in context with the treatment is made. Recommendations to prevent damage by the explanations to the regulation include an avoidance of manipulations which can lead to damaging, packing and securing of batteries and avoidance of miscasts which can damage batteries.

3. Separate storage (§ 17 (6) (3) AbfallBPV) Storage of the batteries has to take place in a separate, marked location and fire protection has to be taken in account. The containers for the batteries also have to be suitable for this application.

4. Separate storage of damaged batteries (§ 17 (6) (2) AbfallBPV) Obviously damaged batteries need to be stored separated from other batteries and in appropriate containers. The area has to be marked and the fire protection has to be considered.

5. Briefing of employees Employees have to be instructed before the beginning of work about the proper handling of lithium batteries and appropriate behaviour in case of emergency.

For batteries containing liquid electrolytes in containers with more than 25 kg of batteries or batteries according to § 17 (5), (7) or (8) AbfallBPV the container has to be leak proof and resistant to the electrolytes (§ 17 (2) AbfallBPV).

2.3.1.4. Stakeholders

The legislation defines the stakeholders in battery collection. For each stakeholder regulations are set by AWG 2002, Abfallverzeichnisverordnung 2020, Batterienverordnung and AbfallBPV. If a stakeholder is in possession of waste batteries, he is the waste holder.

Producers Definitions for battery producers are given in § 12a (2) AWG 2002 and § 3a Batterienverordnung. Summarized the producer is the person who first places a battery in the Austrian market. This also counts for placing devices or vehicles with included batteries in the market. In the extended producer responsibility scheme, the Austrian law sets rules for all producers of batteries (§ 13a (2) AWG 2002 and § 10 Batterienverordnung).

The content of some substances is limited (§ 4 Batterienverordnung) and there is mandatory labelling (§ 6 Batterienverordnung). In most cases, portable batteries have to be removable from electrical devices (§ 8 Batterienverordnung). After usage the producer has to take back batteries placed in market (§ 10 (1) Batterienverordnung). The manufacturer is responsible for ensuring that the treatment of the batteries complies with the legal standards and the state of the art and is documented (§ 5 (1) Batterienverordnung).

The amounts of batteries placed in the market (§ 24 (1) Batterienverordnung) and collected, treated, recycled or exported (§ 25 (1) Batterienverordnung) has to be reported. Participation in a waste collection system is mandatory for all producers (§ 10 (2) Batterienverordnung).

Last distributor The last distributor is the person who commercially offers batteries to the consumer (§ 3 (12) Batterienverordnung). Last distributors are obligated to take back waste batteries from the consumer and give information about this possibility.

Last distributors, who have to take back batteries, do not need a permission for collecting waste, as long as the amount of taken waste batteries is not disproportionate higher than the amount of delivered batteries (§ 24a (2) (5) AWG 2002). For collection, treatment and storage of the waste batteries, the regulations of § 17. AbfallBPV have to be obeyed. If the last distributor does not hand the batteries back to the producer, he is responsible for the treatment according to legal standards and state of the art (§ 5 (3) Batterienverordnung)

Consumer Consumers acquire batteries for the usage (§ 3 (13) Batterienverordnung). After using the batteries become waste. Since waste batteries are hazardous waste (Annex 1 Abfallverzeichnisverordnung 2020) the consumer is obligated to deliver them to a certified collector or treater separately (§ 15 (5a) and § 16 (5) AWG 2002). The person of the consumer can be a private household or an organisation, like a company.

Waste collection systems As mentioned before, battery producers have to take part in waste collection systems by law. Waste collection systems are allowed to take over obligations and responsibilities from producers (§ 2 (8) (5) AWG 2002 and § 16 (1) Batterienverordnung). The system is responsible for the retrain, collection and treatment of the batteries, the information to consumers and the reporting of the amount towards the government.

For establishing a waste collection system, a permission (§ 29 (1) AWG) and an agreement with the federal ministry (§ 17 (2) Batterienverordnung) is needed. Criteria for the permission are listed in §29 AWG and § 17 Batterienverordnung. The systems need to cover the whole area of Austria, every political district and have to prove the ability they can. Waste collection systems, do not need a permission as waste collectors (§ 24a (2) (4) AWG 2002). In 2022 five systems for the collection of waste batteries are registered in Austria[^][Quote].

The collection systems licence batteries placed in the market (compare § 24 (1) Batterienverordnung and § 16 (1) (2) Batterienverordnung). They receive pick up requests from the coordination office (§ 21. (1) Batterienverordnung) or collections points (§ 11. (2) Batterienverordnung) directly and organise the transport from to collection centre to a waste treater by a carrier (§ 21. (2) Batterienverordnung).

Collection points Collection points are centres, set up and run by municipalities (§ 3 (15) (a) Batterienverordnung) or by the produces or the collection systems (§ 3 (15) (b) Batterienverordnung) where waste batteries can be returned. Municipalities (§ 28a AWG 2002) and producers (§ 13a (1) AWG 2002) are obligated to establish collection points.

Collection points have to collect batteries separated in portable, industrial and automotive batteries (§ 11 (1) Batterienverordnung). Regulation on storing and treatment of waste batteries are given in § 17 AbfallBPV. The collection points can report a pickup need to the coordination office, when it reaches a quantity threshold of 300 kg of portable batteries (Annex 3 Batterienverordnung) or does not reach it within a certain time (AWG 2002 § 28a., Batterienverordnung § 11.).

Waste collectors and treaters Waste collectors are persons who pick up, take over or legally disposes of their collection or receipt. Waste treaters are persons who recover or dispose wastes. Waste collectors and treaters need a permission (§ 24a (1) AWG 2002).

Waste collectors and treaters have to follow a complex set of rules. Next to the general obligations for waste holders according to AWG 2002, the law specifies special rules for collecting and treatment. All plants used need a permission following AWG 2002. The AbfallBPV give detailed instructions on storage and treatment of waste batteries.

Federal Ministry The ministry in charge of waste management in Austria is the "Federal Ministry for Climate Action, Environment, Energy, Mobility, Innovation, and Technology (BMK)". In some cases the agreement with the "Federal Ministry of Agriculture, Regions and Tourism (BML)" has to be reached.

The scope of duties of the BMK includes the issuance of regulations, like the Abfallverzeichnisverordnung (§ 4 AWG 2002), Batterienverordnung (§§ 13, 13a, 13b, 14, 19, 23 (1), 23 (3), 28a and 36 AWG 2002) or AbfallBPV (§ 23 (1) AWG 2002).

The ministry has to carry out coordination tasks specified in 13b (1) AWG 2002. It also can delegate these tasks to an coordination office (13b (2) AWG 2002). The ministry has made use of this possibility. Since the obligations of the ministry according to 13b (1) AWG 2002 are handed over the coordination office, they will be discussed there.

Municipalities § 28a AWG 2002 obligates municipalities to offer collection points for batteries and publish the opening hours. For collection, treatment and storage of the waste batteries, the regulations of § 17. AbfallBPV have to be followed. If the municipality does not hand the batteries back to the producer, it is responsible for the treatment according to legal standards and state of the art (§ 5 (3) Batterienverordnung).

Coordination office As mentioned before, the coordination office is commissioned by the ministry (13b (2) AWG 2002) to perform the tasks specified in 13b (1) AWG 2002. The coordination office is set in in the "Elektroaltgeräte Koordinierungsstelle Austria GmbH (EAK)". The EAK is a Not-for-profit organisation which coordinates the licensing for placing of batteries on the market, the collection, recovery and disposal and the data reporting for waste electrical and electronic equipment and waste batteries and accumulators. The EAK coordinates between the stake holders of the waste battery collection. It takes pick up requests of collection points and forwards them to the waste collection systems. The EAK takes information from the systems, producers and collectors and keeps record of all batteries produced, collected and treated in Austria.

Carriers Carriers take over the pick up, transportation and hand over of waste behalf of the waste holder. They do not become waste holders for the time of transportation. AWG 2002 describes record-keeping obligations of carriers. Transport companies get the order to collect, transport and hand over the batteries from the collection systems (§ 21 (2) Batterienverordnung). Carriers have to report information about the transport to the coordination office (§ 21 (3) and (4) Batterienverordnung). For transportation of dangerous goods on roads the regulations of ADR ([35, 36]) has to be followed.

3. Risk analysis

In this section the fire related risks in battery collection will be evaluated. Just a few studies on this topic have been found in literature. The risk assessment is based on a literature review and expert interviews.

3.1. Problem formulation

In recent years, the battery type composition shifted from almost pure non-flammable types like alkaline towards higher contents of inflammable lithium-based batteries. The even steeper increase in the masses placed on the market, indicates further rise in the future. Additionally public campaigns aim for bringing more battery amounts disposed in residual waste or other waste streams in the dedicated waste battery collection. While this improves the safety for these streams, the impact on fire hazards in waste battery collection should be studied.

The tool ‘Bow-Tie’-analysis was chosen. After a main event is defined, the cause that can lead to it are evaluated. The found causes are results of earlier causes and so on, till the root cause is found. The effects and their subsequent impacts of the main event are analysed by the same pattern. Established barriers can hinder or stop the progression of cause and effect. These barriers can be stated by law or required by authorities. They can be realised through constructive or organisational measures.

The main event in the studied case is the start of a fire. An exact definition for ‘fire’ is difficult. In this section, a fire is simply a heat source in the bulk which provides enough heat to potentially ignite inflammable miscasts, other batteries or a cardboard box.

3.1.1. System description

The analysed system is a box made of any typical material (cardboard, polymers, metal) located at a collection centre. The ambient can vary among others from private households, communal waste centres or shops. The area under consideration starts when the batteries become waste and ends right before the treatment facility.

The box is filled with a mix of different battery types and typical miscasts. The maximum battery mass is around 100 kg. Special collection schemata for larger lithium batteries are not considered.

3.2. Causes

A cause is any event that starts a chain of events resulting in a fire. Looking at the fire triangle, it is obvious that the presence of oxygen has to be assumed in all cases. Most batteries are not inflammable at all, but some contents like miscasts, lithium-based batteries or the cardboard boxes used in collection can serve as fuel. The cardboard boxes are the typical container used in collection close to the end consumer. The amount of lithium in waste battery increases and the authorities and collection systems aim for getting even more lithium-rich battery stream from residual waste collection in the battery collection. The content of flammable material in the waste battery collection will grow in the future.

Batteries contain electrical energy stored in a chemical system. The energy content depends on the capacity of the battery and the state of charge. Lithium and lithium-ion batteries can store high amounts of energy compared to size and mass. This energy can be converted into thermal energy and result in a temperature rise. Since the mechanisms are fundamentally different, thermal runaways of lithium-based batteries and a heat release of other battery type will be discussed separately.

In literature usually the effects are studied for batteries in the operational phase and not end of life. The basic mechanisms are the same, but the properties of waste batteries are expected to vary in a wider range. The differences will be discussed.

3.2.1. Thermal runaway of a lithium battery

The mechanisms of thermal runaways have already been discussed. The main cause is an internal short circuit following a destruction of the separator ([23]). The short circuit is followed by a temperature and pressure rise inside the battery and eventually venting or rupture of the battery. A thermal runaway is a failure mode typical for lithium batteries. The presence of lithium-based batteries can be assumed in collection bulks. Many aspects of thermal runaways are extensively studied in recent literature (compare [23]).

As potential causes for thermal runaways usually mechanical, thermal, and electrical abuse are named. In case of electrical abuse, the heat generation inside the battery leads to heat stress and the thermal runaway is caused by the thermal abuse.

The likelihood and the energy release at a thermal runaway is heavily influenced by the state of charge. Measurements by [37] show that 23.6 % of a disposed lithium batteries sample have a state of charge of above 25 % and 12.1 % above 50 %. In different experiments, thermal runaways occurred at reliable at 25 % state of charge. The lower the energy content of the battery, the lower the probability and severity of the thermal runaway become.

The thermal runaway is a serious threat for battery collection and will lead almost inevitable to a fire. If the separator can no longer fulfil its function due to thermal or mechanical destruction and the battery has a sufficient state of charge, a thermal runaway can no longer be prevented by any barriers.

3.2.1.1. Mechanical abuse

Mechanical stress can tear or pierce the separator leading to an internal short circuit and a following thermal runaway. Behaviour and failure of lithium batteries under quasi-static compression and dynamic collision have been studied by [29] and [30].

[29] introduced a model for prediction of internal short circuits and provides experimental data for comparison for 18650 cylindrical lithium-ion batteries. Four loading conditions were examined: radial compression, indentation, three-point bending, and axial compression. Table 2.1 lists the results for forces, displacements and deformation energies leading to an internal short circuit for different loading cases. Based on these values, the likelihood of thermal runaways because of mechanical abuse can be estimated.

In waste battery collection, four scenarios would lead to mechanical stress for a battery. The weight of batteries and the filling heights cause static pressures in the container. For a battery near the button of a static bulk all four loading conditions in table 2.1 can occur. In the worst case of a three-point bending, a force of 2 kN can trigger an internal short circuit. This would require a mass of about 200 kg of placed on one single battery. This force of 2 kN on a $1\text{ cm} \times 1\text{ cm}$ area of a battery would require a filling height of more than one kilometre.

When the batteries are dropped in a container or transferred into another, the batteries can fall on each other. The impact is equal for the falling battery and the one that is getting hit. For reaching the deformation energy by indentation, a 0.5 kg battery would require a drop height of more than seven metres. In the very unlikely event of a three-point bending, a drop height of around one metre would cause enough energy. The velocity must reach around 4 m s^{-1} . For more typical batteries with around 50 g, these values would have to be ten times higher. Mechanical treatment causes enough deformation, but it is done in special facilities which are out of scope in this work.

Data from [38] show that 97.57% of the batteries separately collected are not seriously damaged. This is in good accordance with the expectation of the occurrence of the required forces. The mechanical resistance of lithium batteries is high enough to withstand the expected loads. Mechanical stress is neglected as a trigger for thermal runaways in collection.

Protection against mechanical stress during collection is mandatory by Austrian legislation. Measures to avoid damage include limiting the pouring height and container sizes and proceeding with caution when tipping into other containers. The collection processes can be optimised to avoid mechanical manipulation as far as possible and to keep the container sizes small.

3.2.1.2. Thermal and electrical abuse

High temperatures inside the battery can lead to melting or degradation of the separator. Thermal stress can be caused by electrical abuse, external heat sources or malfunctions of the battery. Experiments, simulations and theoretical studies can be found in literature. [25] and [24] conducted tests with internal and external heating modes. In the experiments all batteries with a state of charge of 25% or higher performed a thermal runaway at temperatures between $100\text{ }^{\circ}\text{C}$ and $200\text{ }^{\circ}\text{C}$. When the state of charge is 0% batteries fail without a thermal runaway.

Electrical abuse [23] lists external short circuit, which means a high discharge current and overcharging as electrical abuse. When a battery gets charged with too high voltage, the separator can get damaged. High currents while charging or discharging lead to high heat release rates on the internal resistance of the battery and can cause a thermal runaway.

The voltages and energy contents of waste batteries are not sufficient to charge each other, regardless of the geometrical arrangement. Unlikely cases with many fully charged cells connected in series charging one other battery will be neglected. The effect of external short circuits are studied by [28] and [26]. Even a sharp rise in temperature was observed, the batteries did not show a thermal runaway.

The randomized geometrical arrangement of batteries in a bulk makes estimations about the likelihood for waste battery collection difficult. Lithium batteries come in shapes of standard batteries (as LR6 or 6F22), blocks or cylinders with blank contacts or as accumulators with wire connectors. The wires of the connectors are isolated and using a standardized socket which provides good short circuit prevention. For waste batteries, these parts can be damaged, but this would make short circuits before being deposited in the collection containers quite likely. For the probability of blank contacts being short circuited, no previous research could be found.

For especially dangerous battery collections ([32] §17 Abs. 5, 7 & 8) the prevention of short circuits is required. Examples for prevention methods are given in [33]. For other battery collections no regulations are in place. The collection systems and the coordination office advise end consumers to cover the contacts of accumulators. The chances of a thermal runaway caused by an electrical short circuit are unknown. When enough heat is released, no measures can be performed to prevent the thermal runaway.

Malfunctioning battery Due to the waste nature of the considered material stream, already damaged lithium-ion batteries can be placed into the collection. The characteristics of the damage have to be quite specific. On one hand, the failure has to be critical enough so the battery shows a thermal runaway without any further trigger. On the other hand, it has not shown it before disposal. Considering this, the likelihood can be assumed quite low. A previous damage can increase the likelihood of ignition if any other cause for failure occurs. Damaged batteries can be more sensitive to all kinds of stress.

For waste batteries, the previous treatment is usually not known. Visible and invisible damage can make the batteries more vulnerable for external stresses for fire. Most of the waste batteries are usually not fully charged and primary batteries are almost fully discharged ([37]). The energy content is smaller than for batteries in use and the hazardous properties are reduced.

Damaged lithium and lithium-ion batteries should be collected separately according to [32]. This cannot be ensured at unsupervised drop-off points.

External heat source When lithium or lithium-ion batteries are heated, a thermal runaway can occur. Studies on this effect are, among others, conducted by [26], [30], [25] and [24].

In waste battery collection, heat sources can be located inside or outside the container. In normal operation the temperature inside the bulk does not exceed the ambient temperature. A heat source inside the container is a direct effect of the of the investigated case, a fire in a battery bulk and will be discussed with the effects. Various heat sources like room heating, the sun or other fires cause by something else can be potentially found outside the box. The required temperatures are significantly above the expectable ambient temperatures during collection.

Depending on the material, the container can provide heat protection for the batteries inside. The law requires protection from excessive sunlight and sufficient distance to other flammable materials ([32]). When appropriate boxes for collection and suitable locations are used, then external heat sources pose little risk.

Thermal runaways are very well studied for lithium-based batteries in use. Applying some adaptations, most results can be taken for considerations for waste batteries. The overall likelihood of occurrence is rather low. The assumed low states of charge and the absence of some triggers reduce the risk.

For risk reduction, lithium and lithium-ion batteries are sorted out at some collection centres. Special safety measures are taken for the resulting pure lithium battery collection. Obviously damaged lithium accumulators and ones above 0.5 kg should not be thrown into collection boxes for portable batteries.

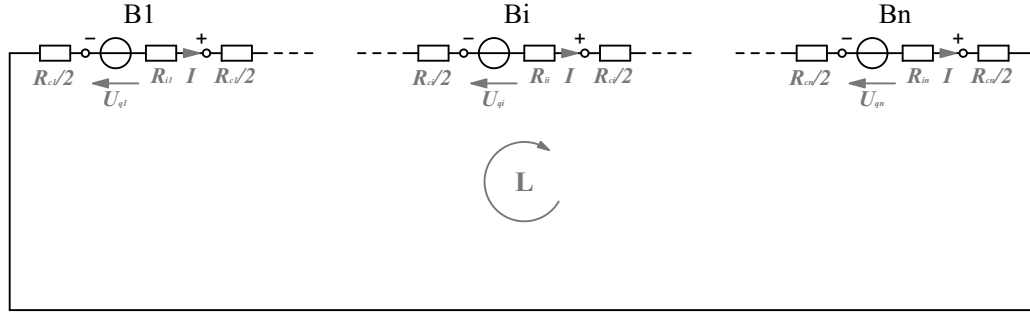
When a battery in the bulk starts a thermal runaway, no measures are present for prevention or warning. When a fire starts inside the bulk because of another reason, the thermal runaway can be a consequence that amplifies the effects.

3.2.2. Heat release of a battery

Due to their ability to provide electrical energy, all batteries can generate heat without a thermal runaway. The most common battery types have blank contacts, which are not recessed on the surface. This can lead to short-circuits of single or multiple batteries if the geometrical arrangement is right. The released heat can cause fire. No publications on the probability and effects of short circuits in battery bulks were found within the scope of this work. The positioning of the battery poles varies considerably depending on the type. A dependency on the composition and on the origin of the collected batteries can be expected.

The risk of a battery getting ignited by getting short circuited depends on the electrical current and the heat release on the internal resistance. Two idealised formations, a large serial connection and a large parallel connection of many batteries are investigated mathematically.

3.2.2.1. Serial short circuit of many batteries

Figure 3.1.: Serial connection of n batteries

For a serial connection of n batteries, as shown in figure 3.1, equation (2.5) gives

$$\sum_{i=0}^n \left(I \cdot \frac{R_{ci}}{2} - U_{qi} + I \cdot R_{ii} + I \cdot \frac{R_{ci}}{2} \right) = 0 \quad (3.1)$$

The electrical current through all batteries is equal and $I_i = I$ and \dot{Q}_i can be calculated by

$$I = \frac{\sum_{i=0}^n U_{qi}}{\sum_{i=0}^n (R_{ci} + R_{ii})} = \frac{n \cdot \bar{U}_q}{n \cdot (\bar{R}_c + \bar{R}_i)} = \frac{\bar{U}_q}{\bar{R}_c + \bar{R}_i} \quad (3.2)$$

$$\dot{Q}_i = \frac{\bar{U}_q^2 \cdot (R_{ci} + R_{ii})}{(\bar{R}_c + \bar{R}_i)^2} \quad (3.3)$$

In the whole serial connection, the heat release rate is then

$$\dot{Q}_{total} = \sum_{i=0}^n \dot{Q}_i = \frac{\bar{U}_q^2}{\bar{R}_c + \bar{R}_i} \cdot n \quad (3.4)$$

The current and the heat release of a battery do not depend on the number of batteries in the short circuit and the total heat release is just the sum of all batteries. These equations show, that large, even infinite, serial connections of batteries do not pose a higher risk than each of the batteries being short circuited separately. The size of serial connection does not matter, just the number and types of the batteries.

3.2.2.2. Parallel short circuit of many batteries

A parallel connection of n batteries is shown in figure 3.2. The batteries are short circuited with an external resistance R .

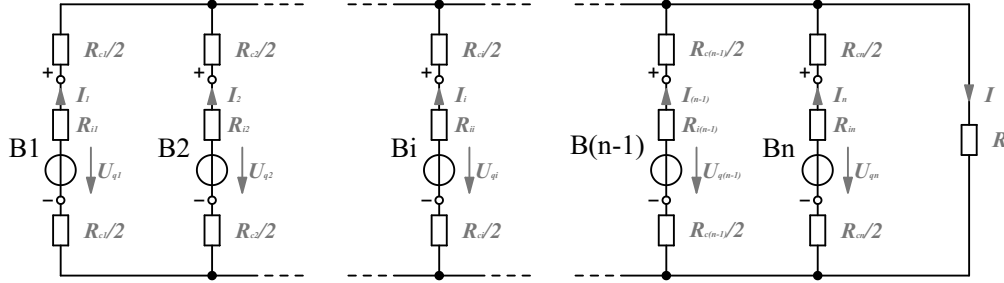


Figure 3.2.: Parallel connection of n batteries

The voltage law can be written for each battery i by

$$I_i \cdot \frac{R_{ci}}{2} - U_{qi} + R_{ii} \cdot I_i + I_i \cdot \frac{R_{ci}}{2} + R \cdot I = 0 \quad (3.5)$$

and the circuit law is

$$\sum_{i=0}^n I_i = I \quad (3.6)$$

These equation give for I_i of the battery i and I for the external resistance

$$I = \frac{\sum_{i=0}^n \frac{U_{qi}}{R_i}}{1 + R \cdot \sum_{i=0}^n \frac{1}{R_{ii} + R_{ci}}} = \frac{n \cdot \overline{\left(\frac{U_q}{R_i + R_c} \right)}}{1 + R \cdot n \cdot \overline{\left(\frac{1}{R_i + R_c} \right)}} \quad (3.7)$$

$$I_i = \frac{U_{qi}}{R_{ii} + R_{ci}} - I \cdot \frac{R}{(R_{ii} + R_{ci})} \quad (3.8)$$

For the theoretical case of $n \rightarrow \infty$ a finite electrical current of

$$I_{n \rightarrow \infty} = \frac{\overline{\left(\frac{U_q}{R_i + R_c} \right)}}{R \cdot \overline{\left(\frac{1}{R_i + R_c} \right)}} \quad (3.9)$$

Assuming that all batteries are equal and $U_{qi} = \bar{U}_q, R_{ii} = \bar{R}_i$ and $R_{ci} = \bar{R}_c$, equation (3.9) get simplified to

$$I_{n \rightarrow \infty} = \frac{\bar{U}_q}{R} \quad (3.10)$$

In this case, each battery has a current of

$$I_{i,n \rightarrow \infty} = \frac{U_{qi} - \frac{U_q}{\frac{R_i + R_c}{1}}}{R_i + R_c} = 0 \quad (3.11)$$

In parallel connection, the dependencies are a bit more complicated, but the more batteries are connected, the lower the current gets. For a theoretical infinite connected network, all heat release will be on the external resistance R .

In some collection centres, the contacts of block batteries are precautionary isolated. Coin batteries are sometimes collected separately. Studies on the effectiveness of these measures have not been found.

3.2.3. Fire causing input material

A heat source could be placed by accident or for arson. Both cases are unlikely since most public battery collection places have personal around at daytime and are not easily accessible during night. For both cases it is hard to imagine why someone would choose a battery collection container. This case is considered to have a low probability.

3.3. Effects

The Firefighting threat assessment matrix provides a systematic approach to evaluate hazards in case of fires. The scheme can be applied to humans and goods. Nuclear threats, diseases and collapse will be neglected for obvious reasons. While the basic threats come from electricity, the voltage itself does not cause any harm for people since the expectable battery types in device battery collection have low voltage.

The severity of the effects of a fire depends on the energy release, the duration and the ambient conditions. The consequences are further determined by the location. For example, private households and the municipal collection points have very different vulnerabilities in case of fires.

Again, most published research study the behaviour of new batteries or in use. The lower state of charge will lower the amount of released heat and lead to less harsh consequences. The occurrence of not used batteries in waste collection is expected.

3.3.1. Fear and panic reactions

When fire and smoke appear, people can react in panic and take unexpected actions. Collection boxes are often in highly frequented, public areas inside building. However, as these areas generally, have an appropriate fire protection concept and sufficient escape routes, this will normally not occur.

3.3.2. Release of toxic gases

As many other fuels, batteries release smoke and toxic gases when burning. These gases are a threat to people nearby and can cause property damage. The gas composition lithium-based batteries release has been studied by [39].

Since the amount of burning batteries and fire gases is usually small compared to the available space, this is not expected to be a major threat. Especially in all publicly accessible areas, fire protection concepts are usually designed for larger fires.

3.3.3. Spread inside the battery bulk

Most batteries withstand fires without getting ignited and will not add any heat value. Inflammable miscasts like plastic bags, isolation tape or cardboard can start burning and increase the heat load. A thermal runaway of lithium-based batteries as described before can be triggered. A chain reaction, where one battery ignites the next can start. If the container is made of a inflammable material it can also catch fire. For this thesis there was no literature about the propagation of fires in battery bulks available. [33] mentions the problem of on thermal runaway triggering another one and state the complexity of this problem.

The main impact factor for the spread inside the container is the container material, the content of lithium and miscast. Without any more fuel, a small fire in the bulk will go out by itself. At high fractions of inflammable substances inside the box, the resulting fire will accelerate burning and grow bigger.

The propagation of the fire inside the battery bulk is a main impact factor of the overall effect a triggered fire will show. All other effects scale with the amount of burning material and the total amount of energy released. [32] just regulates measures to prevent other effects of fires if the lithium content exceeds 10 m%.

3.3.4. Expansion out of the container

When the heat load of the burning bulk gets high enough, objects around the container can get ignited by heat convection, conduction and radiation. The rising hot gases pose a danger for materials above the box. Inflammable materials in contact with the container can start burning because of heat conduction. At high temperatures the heat radiation can set objects in some distance on fire. Lithium-based batteries can rupture, vent or get accelerated and get thrown several metres ('rocketing') and spread the fire there.

While [32] and fire protection concepts required by the authorities give clear instruction on the placement of inflammable materials close to battery boxes from the collection centres till the final treatment, for private households there are just recommendations. Depending on the used material, some boxes can prevent a fire spread up to a certain heat load.

The expansion of the fire out of the container is considered a worst case. Further consideration, what effect a fire will have in different locations in collection are not part of this thesis.

3.3.5. Release of chemical substances

Depending on the chemical system, batteries contain corrosive, caustic and flammable substances. If the battery gets destroyed, these substances can spread. In small containers the total amount is low and therefore can be neglected. For larger masses the container must be able to retain the chemicals, according to [32]. These containers are typically made from metal and will withstand a fire. The wider spread of chemicals and threats to people can be neglected.

3.3.6. Explosion

Explosions are characterized by a rapid release of energy, resulting in an overpressure in the surrounding areas. An explosion inside a collection vessel can occur when the case of a lithium battery fails or when vented gases in the container create an explosive atmosphere. [40] found explosion limits for venting gases of lithium-ion batteries from 5 to 35 %. Although explosions are a threat for larger energy storages, the composition of battery types in the portable battery collection makes actual explosions quite unlikely.

3.4. Results and discussion of the risk analysis

The results of the risk analysis are shown in figure 3.3 in the form of a bow-tie analysis. On the left-hand side are the direct causes of a fire, as well as their upstream triggers. On the right side the possible effects can be found. The Austrian laws impose measures for the prevention of fires and the limitation of their consequences. These are implemented in the analysis in the form of barriers.

The Bow-Tie analysis represents a qualitative approach to find causes and effects of a main event. To assess the risk quantitatively, the branches must be evaluated in terms of probability and severity. This can be done, among other things, through statistical evaluation of cases of damage or through mathematical modelling and description.

Although no corresponding data was found, the probability of the input of burning materials is considered unlikely. Presumably, this type of ignition can be neglected. For the evaluation of the mechanical stress, experimental data on the load limits of lithium batteries and analyses on the degree of damage of the collected quantities are available. Legal regulations prescribe protection against mechanical stress. The available data indicate the effectiveness of these measures and thermal runaways because of mechanical stress in battery collection are unlikely. In contrast to the use phase, the lack of sufficiently powerful energy sources makes electrical abuse by overcharging impossible. This trigger for a thermal runaway can be excluded.

Experiments with lithium batteries in ovens provide data on the influence of heat sources inside and outside the container. The container wall, which can represent a barrier depending on its material, can be easily described mathematically. No data or estimates are available on the spread of fires within battery packings. The probability that a burning battery will ignite another cannot yet be adequately described with the known correlations.

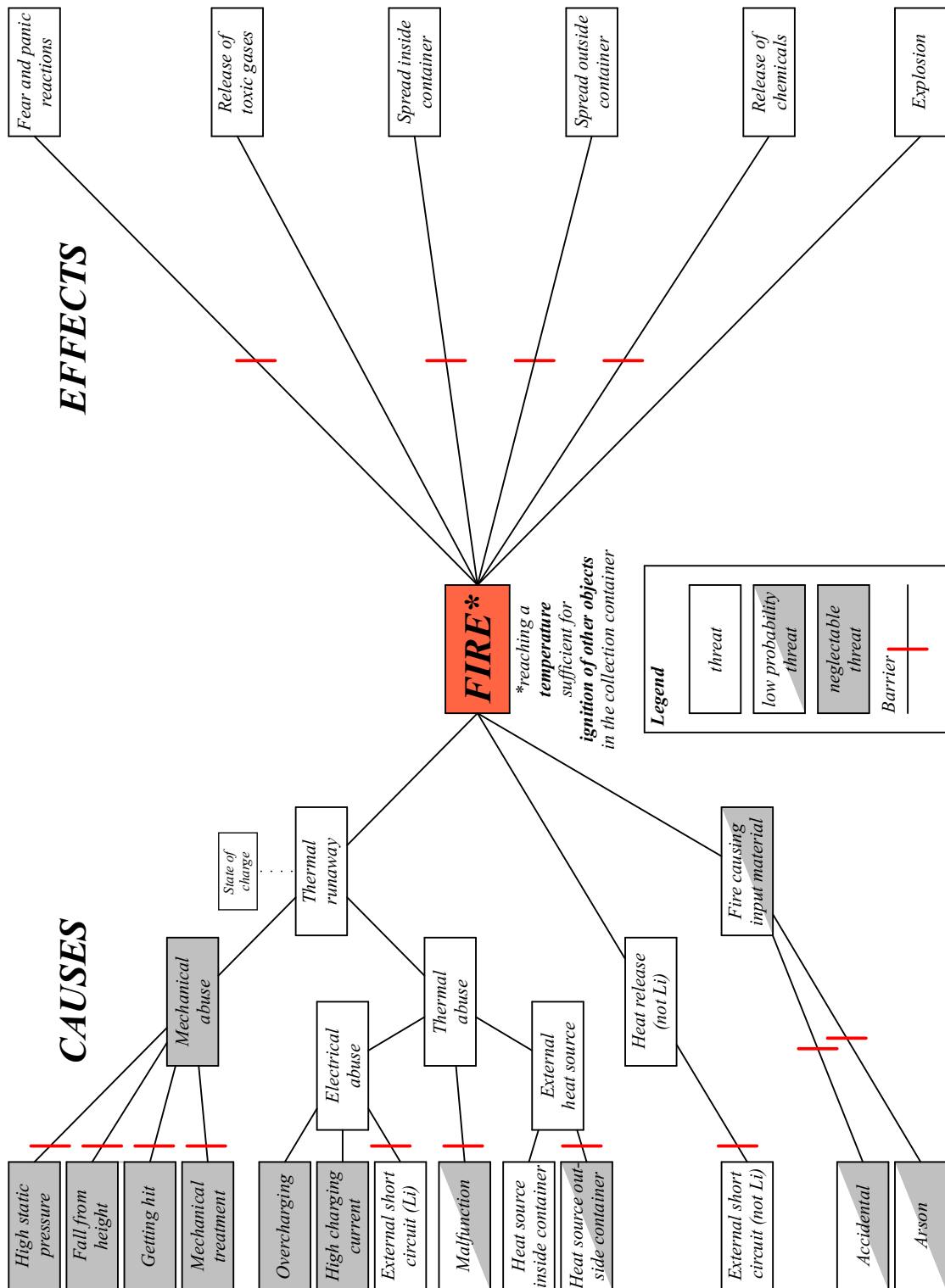


Figure 3.3.: Results of the risk analysis presented as Bow-Tie-analysis

The case of a defective battery starting a fire in a bulk material is considered unlikely, but more detailed analyses of which internal battery mechanisms can trigger this type of thermal runaway have not been found. The influence of the internal state of lithium-based batteries on possible fires cannot be quantified or described mathematically with the literature reviewed. Consequently, the effectiveness of the legally prescribed measures cannot be assessed.

The external short-circuit of batteries in bulk has not been studied so far. Statistical, geometric, numerical or experimental investigations or estimations could not be found. Lithium and lithium-ion batteries are available in dedicated shapes for accumulators or in the same designs as other primary batteries. Therefore, approximations for non-lithium based batteries would be partially transferable to them. No statement can be made at present about the influence of short circuits on the fire risk. Whether taping off poles or sorting out button cells is an improvement with regard to the fire hazard cannot be judged either.

For the effects of typical fires, a set of methods for evaluation is provided by fire protection engineering. Information about heat loads and emission of toxic substances are needed for application. Experimental fire test data of waste portable battery collection samples would make a quantitative assessment of the consequences possible. The available data for some battery types and sorting analyses of the collected mixtures could be used also.

3.5. Conclusion of the risk analysis

The qualitative approach presented shows that the risk of fire depends on a number of variables. As expected, the specific characteristics of lithium-based batteries are important for the classification of the risk. The legally prescribed measures cover most of the causes and effects found. However, qualified statements on the effectiveness of these measures are only possible in a few areas.

The existing literature data are not sufficient for a quantitative assessment of the fire risk in portable battery collection. The triggering mechanisms and subsequent consequences cannot yet be adequately described. Especially the risk of short circuits, the behaviour of damaged batteries and the fire spread within and out of the container are still unknown.

The short-circuiting of batteries is a source of ignition within the collection. If a battery heats up as a result, it can ignite other flammable objects inside the container.

The geometrical arrangement within the container is random and depends on the composition of the fill and the way it is filled. Random packings, in contrast to densest packings, are not yet mathematically described for most bodies. If different shapes are placed in a container, the problem becomes even more complicated.

To enable risk assessments for collected portable batteries, the next chapter presents an approach using rigid body simulation, which enables an investigation of the frequency and type of short circuits in battery bulks. Some typical cases will be studied in more detail, to build up more knowledge about the formation of short circuits in battery bulks.

4. Numerical study on electrical short circuits in battery bulks

In waste battery collection, the batteries are placed into containers in an unclassified way and create a random packing. In these bulks, short circuits can be formed and generate heat. This can further trigger fires and thermal runaways of inflammable batteries close enough. In this chapter an approach to study the formation of short circuits in bulks is introduced.

4.1. Problem formulation

The occurrence of short circuits cannot be quantified yet. The influence parameters are mostly unknown. The properties of bulks depend on the characteristics of the particles, the used container, and the method of filling ([41]). In reality, batteries, accumulators, and various other items (miscasts) are dropped into containers with varying shapes and sizes. Most parameters of the process like the throwing, the battery type composition, and the types and amounts of miscasts are unknown.

Aim is an algorithm to generate as realistic as possible, random packing of different batteries in a specified container. The focus will be on the final arrangement of the battery pack, while the filling process will not be studied further. The generated bulk should be analysed, short circuits should be detected and described according to electrical aspects. The simulation should have acceptable computation time and stability.

4.2. Algorithm development

The following section describes the methodology, the assumptions, and the approximations made. The algorithm for creation of a random bulks is implemented in the rigid body physics module of the open-source software "blender", version 3.2.2. The programming language python was used to generate the simulation and for evaluation.

Blender is a free and open source 3D-graphics software, with a wide range of use. Among other things, physics simulations for soft and rigid bodies can be performed. In this work, the rigid body dynamics were used for generation of battery bulks. For movement calculation and collision detection blender uses the bullet physics engine.

The setup consists of an approximation of the geometrical shapes, a physical procedure to mimic the throw-in process and electrical simplifications. When the bulk is generated contact detection and electrical evaluation of the bulk is performed.

4.2.1. Geometrical models

The geometrical model contains primitive shapes for batteries and containers. Complex and concave shapes are avoided for improvement of computational time. The objects are constructed from the basic shapes plane, cuboid, and cylinder connected by constraints. The number of basic shapes per battery is kept as low as reasonable.

Small objects and large difference in size of the bodies enhance simulation instabilities. The Blender 3.2 Reference Manual ([42]) mentions 20 cm as a lower boundary for stable rigid body objects. This is far above the size of typical batteries. The whole geometry is scaled up by *scale_factor* (table 4.1). The objects stay geometrically similar and the resulting physical behaviour is expected to be similar.

Table 4.1.: Simulation parameter for the geometry model

| Symbol | Description | Unit |
|---------------------|---|-------------------|
| <i>scale_factor</i> | Scale factor for lengths in the simulation geometry | m m ⁻¹ |

4.2.1.1. Batteries

The blender objects for batteries are formed by cuboids and cylinders, bound together by constraints. The geometries are highly simplified. IEC 60086-2 ([10]) gives lower and upper limits for the battery's dimensions. Each dimension is set as normal distributed random value $l \sim \mathcal{N}(\mu, \sigma)$. μ and σ are selected to fit six standard deviations between the boundary values. The values are limited by $\mu - 3 * \sigma < l < \mu + 3 * \sigma$. Undefined dimensions are assumed based on geometry. The applied density ranges from 1823 to 4667 kg m⁻³ and is assumed by producers publications and to be isotropic within the whole battery.

Objects of any shape, limited to rigid bodies, can be included. Most electrically conductive materials are rigid in the range of expected forces, so mainly non-conductive materials are excluded. For this work, some batteries are implemented. The simplifications for batteries are shown in figures 4.1, 4.2 and 4.3. The parameters for batteries are listed in table 4.2.

Table 4.2.: Simulation parameters for the battery model

| Symbol | Description | Unit |
|-----------------|--------------------------------------|--------------------|
| h_1 | Overall height of battery | m |
| d_1 | Diameter of the battery | m |
| l_1 | Length of the battery | m |
| h_i, d_i, l_i | Dimensions required by battery shape | m |
| ρ_{batt} | Density of the battery | kg m ⁻³ |
| U_N | Nominal voltage | V |
| n_{cell} | Number of internal chemical cells | - |

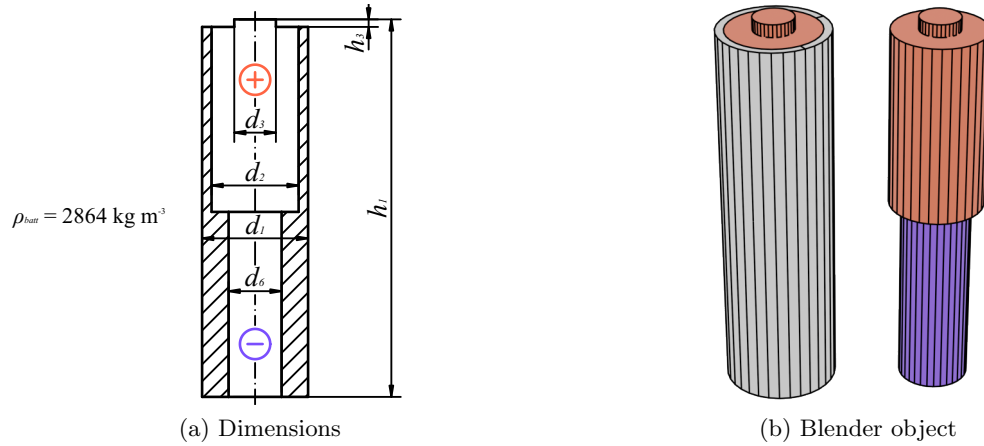


Figure 4.1.: Model for batteries IEC 60086 category 1 (LR6 as example)

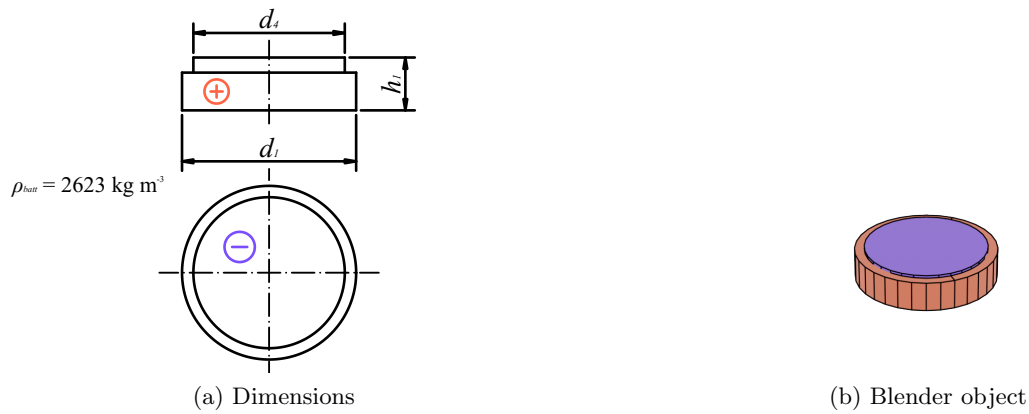


Figure 4.2.: Model for batteries IEC 60086 category 4 (CR2354 as example)

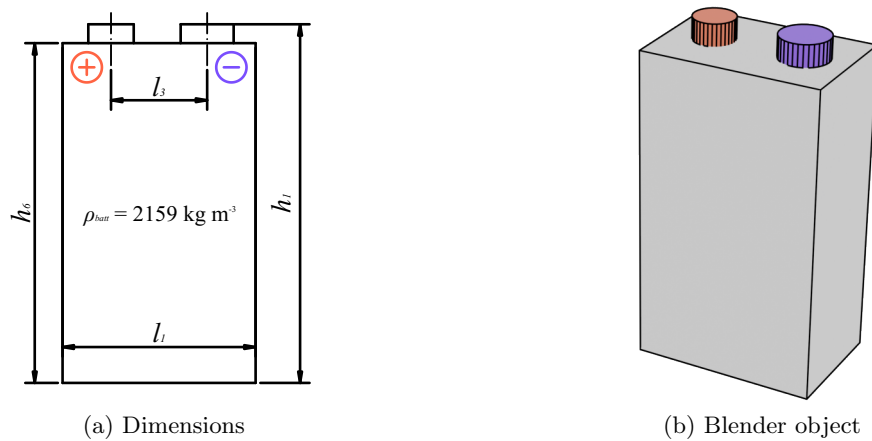


Figure 4.3.: Model for batteries IEC 60086 category 6 (6F22/6R61 as example)

4.2.1.2. Containers

In this work three simple container shapes are used,

- boxes (cuboid with $l_1 \neq l_2 \neq l_3$) (Figure 4.4),
- barrels (cylinders, regardless of size) (Figure 4.5) and
- cubes ($l_1 = l_2 = l_3$) (Figure 4.6).

The containers are created as blender objects by a python script. The object consists of just surfaces for the bottom and the side walls. All containers are open on the top side. The simulation input parameters are the dimensions of the container in table 4.3. For rectangular container types the diameter d is given as a cut of criteria for lost batteries.

The smallest container implemented in this work measures $63 \text{ mm} \times 63 \text{ mm} \times 63 \text{ mm}$. The volume is 0.25 L and the battery mass about 380 g. The maximum size is a 64 L cube with an edge length of $400 \text{ mm} \times 400 \text{ mm} \times 400 \text{ mm}$, filled with roughly 97 kg of batteries. In this case the simulation takes about 10 days for calculation. Larger bulks would be possible by the algorithm, but the computation time will grow exponentially. A list of all containers implemented yet can be found in table B.1.

Table 4.3.: Simulation parameters for the container model

| Symbol | Description | Unit |
|--------|-----------------------------------|------|
| l_1 | Length of cube and box containers | m |
| l_2 | Width of box container | m |
| l_3 | Height of box container | m |
| d | Diameter | m |

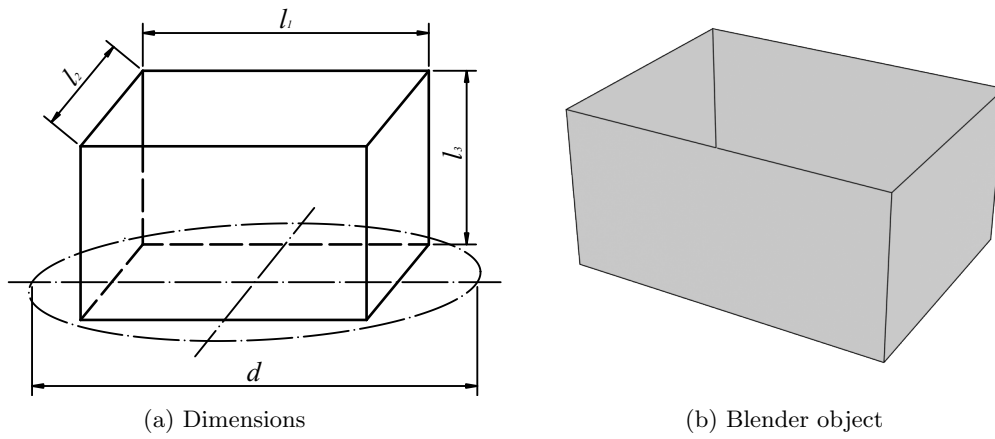


Figure 4.4.: Model for box-shaped container

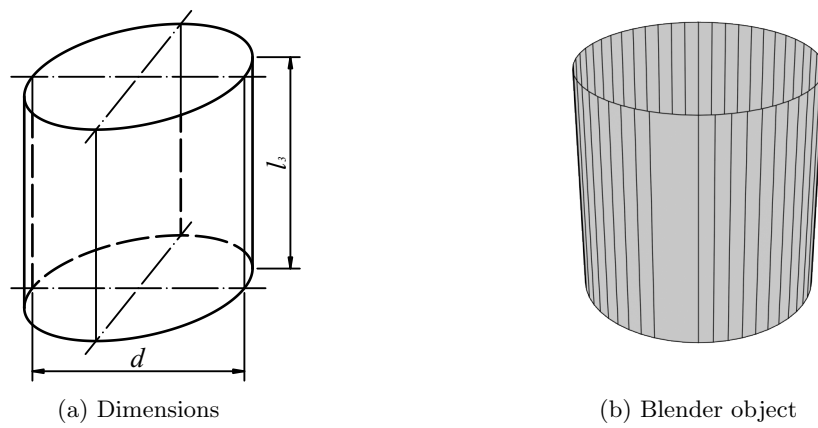


Figure 4.5.: Model for barrel-shaped container

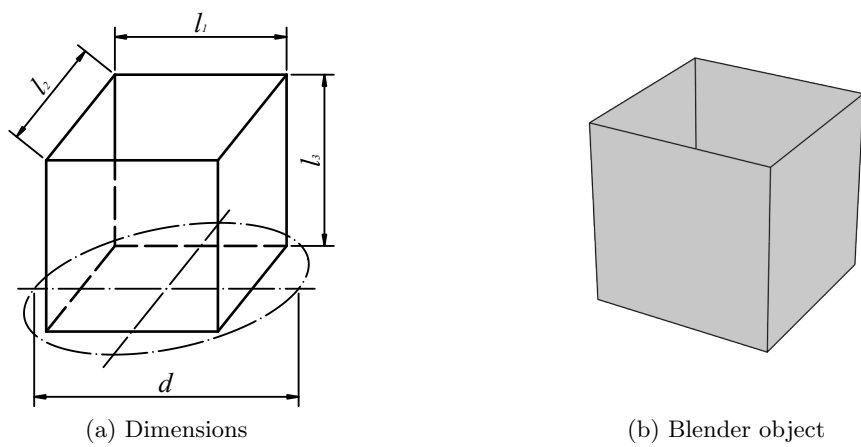


Figure 4.6.: Model for cube-shaped container

4.2.2. Physical model

The procedure of filling the container with batteries is simplified as shown in figure 4.7. The implementation in blender is presented in figure 4.8. First a battery type is selected according to a predefined distribution. The dropping point is h_d above the centre of the container floor. The orientation of the battery is randomized and a fixed initial velocity v_{0z} in z -direction is set for all batteries. The velocity along the x - and y -axes is zero. After dropping, the battery accelerate by gravity ($g = 9.81 \text{ m s}^{-2}$).

In blender all batteries are initialised at once in the beginning (figure 4.8a) and the physics engine takes over the control one by one when the battery gets thrown. The starting point is above the dropping point, because v_{0z} is set by a movement towards it before the physics is applied (figure 4.8b).

After the battery has moved for a safety distance h_{safe} and an additional safety time t_{safe} , the next battery gets thrown (figure 4.8b - 4.8e). The batteries and the container interact with each other when colliding. Collisions are calculated using values for *friction* and *restitution* in blender. Linear and angular damping are added for more stable simulation results.

The number of batteries $N_{batts,set}$ is defined in the beginning. Setting the final battery mass or a degree of filling for the container would require additional calculations during the simulation run. This was not done to improve the simulation time. After the last battery is thrown, frames for the time t_{settle} are calculated, so the batteries settle down. The resulting bulk is taken for further analysis. The required input parameters for the physical model are listed in table 4.4.

Table 4.4.: Simulation parameters for the physical model

| Symbol | Description | Unit |
|--|--|-------------------|
| h_d | Drop height | m |
| $N_{batts,set}$ | Number of batteries to throw | - |
| $\vec{v}_0 = \begin{pmatrix} 0 \\ 0 \\ v_{0z} \end{pmatrix}$ | Initial velocity vector | m s^{-1} |
| t_{safe} | Safety time after battery drop | s |
| h_{safe} | Safety distance for battery creation | m |
| t_{settle} | Settle time after last battery | s |
| <i>friction</i> | Friction parameter for physics engine | - |
| <i>restitution</i> | Restitution parameter for physics engine | - |
| <i>linear_damping</i> | Linear damping parameter for physics engine | - |
| <i>angular_damping</i> | Angular damping parameter for physics engine | - |

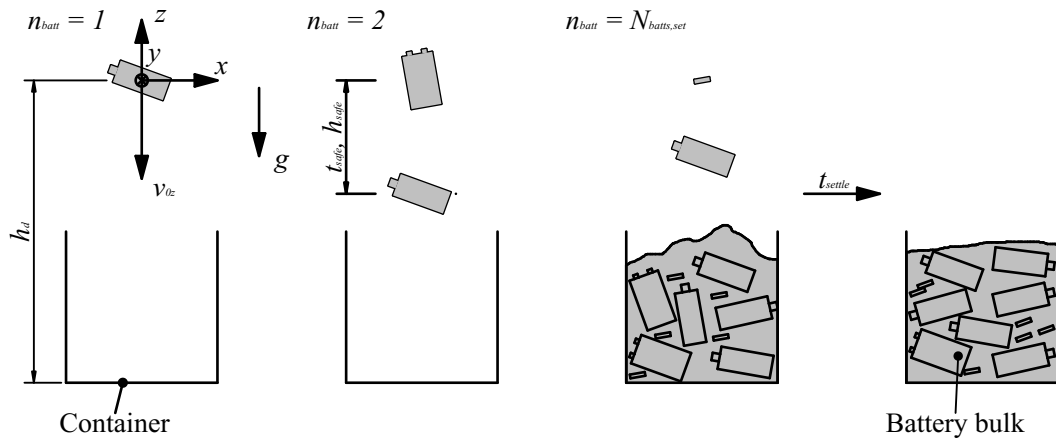


Figure 4.7.: Simplified physical model for the filling process

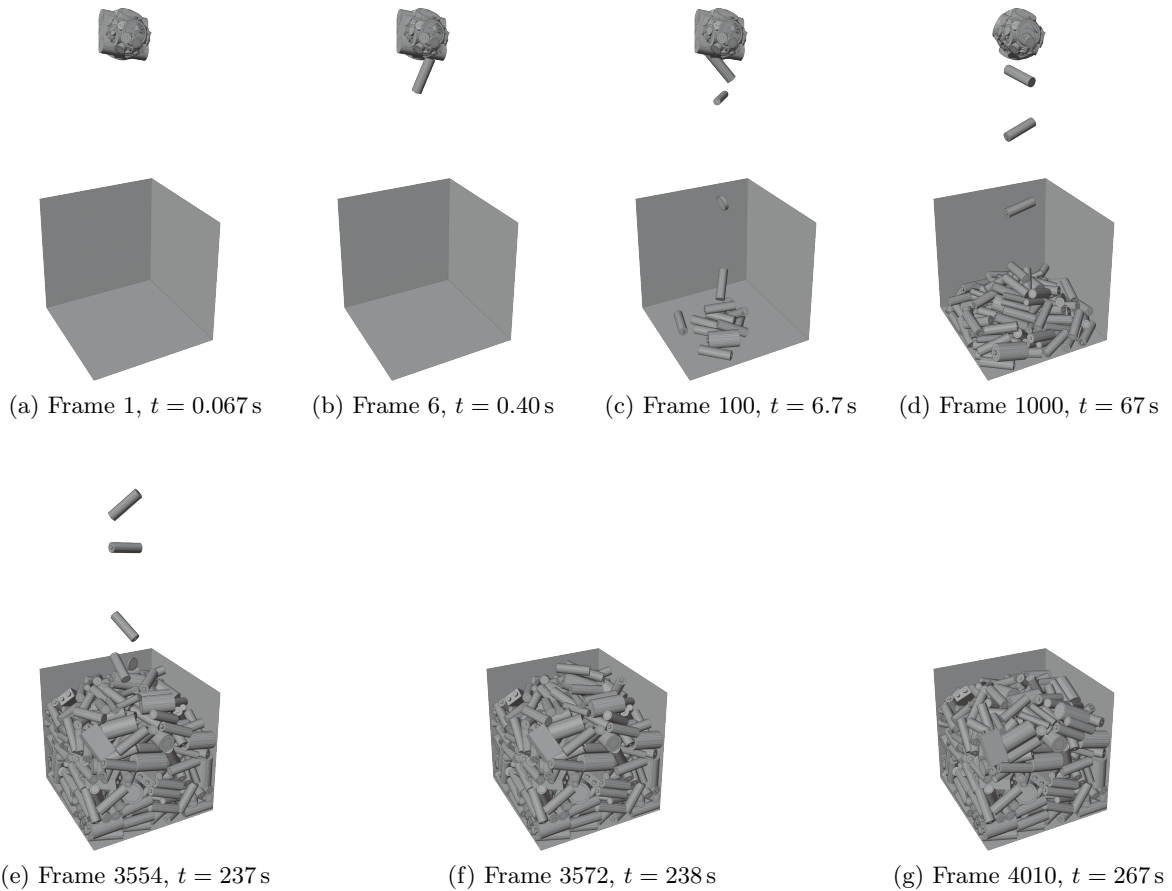


Figure 4.8.: Filling process in blender ('cube', $V_{cont} = 8$ L, $l_1 = 20$ cm, $m_{batts, bulk} = 11.6$ kg, $fps = 15$, $time_scale = 5$)

4.2.2.1. Standard battery types composition

Typically for waste streams, a wide variation in composition can be expected for waste battery collection. The type distribution is given as input parameter set into the simulation, which defines a weight factor for each battery type. This weight factor divided by the sum of all weight factors is the set share of this type in the bulk. The value refers to the number of batteries, not to the mass. For each battery thrown, a type is selected randomly, weighted by the weight factors.

Sorting analyses of battery type composition in Austrian collection were not found. A sample shown in figure 4.9 (bucket, 14.3 kg) taken in spring 2021 of 613 items (batteries and miscasts) was analysed. The results can be found in table A.1 in the appendix. The larger accumulators and the miscasts are not used for the simulation. The distribution taken as standard for the simulation is presented in figure 4.10.



Figure 4.9.: Analysed sample for battery types distribution (yellow surface approx. 1 m × 1 m)

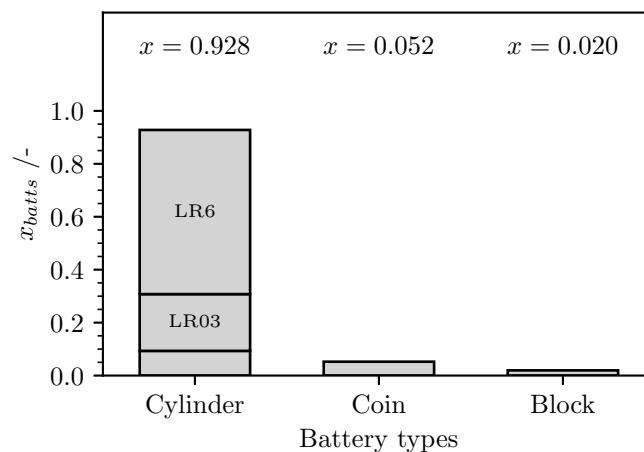


Figure 4.10.: Standard battery type distribution, simplified from sample in figure 4.9

4.2.3. Electrical model

The complexity of describing the electrical behaviour of waste batteries is discussed in chapter 2. For analysis in this work a simplified model is used. A battery cell will be substituted by an ideal voltage source in series with an internal resistor (compare figure 2.8). Discharging of the batteries will be neglected. The values for U_{batt} and $R_{i,cell}$ remain constant over time and are independent from the electrical current. The voltage is given for the whole battery, regardless of the number of cells. The internal resistance $R_{i,batt}$ is calculated by multiplying the cell resistance by the number of cells (equation (4.2)). The voltage of the internal source U_{batt} is a fraction f_U of the nominal voltage U_N :

$$U_{batt} = f_U \cdot U_N \quad (4.1)$$

$$R_{i,batt} = R_{i,cell} \cdot n_{cell} \quad (4.2)$$

The maximal voltage of the battery OCV_{max} is neglected and $0 \text{ V} \leq U_{batt} \leq U_{N,batt}$. When two electrically conduction battery parts touch, a constant contact resistance R_c is assumed. The walls of the container are considered electrically isolating.

For each battery a randomized value for f_U is generated. The values follow a normal distribution with the given parameters \bar{f}_U and σ_{fU} :

$$f_U \sim \mathcal{N}(0, 1) \cdot \sigma_{fU} + \bar{f}_U \quad (4.3)$$

The values are limited to

$$0 \leq f_U \leq 1 \quad (4.4)$$

With the known contacts between battery parts and the given electrical properties (U_{batt} , R_i , R_c) all electrical currents can be calculated, using equations (2.1), (2.3) and (2.5). Equation (2.2) can be applied to each resistance in the circuit. The resulting electrical power P_R is dissipated as thermal energy and equivalent to the heat release of the resistance \dot{Q}_R . For the battery contacts, \dot{Q}_R is divided equally to both involved batteries. The heat generation of each battery is the sum of the dissipation on the internal resistance and half of each contact resistance. The simulation input parameters for the electrical model are listed in table 4.5.

Table 4.5.: Simulation parameters for the electrical model

| Symbol | Description | Unit |
|---------------|---|-------------------|
| \bar{f}_U | Mean voltage factor | V V^{-1} |
| σ_{fU} | Standard deviation for voltage factor | V V^{-1} |
| $R_{i,batt}$ | Internal resistance of batteries | Ω |
| $R_{c,i}$ | Connective resistance of battery contacts | Ω |

Typical values for nominal voltages of batteries are 1.5 to 3 V per cell. Most battery types contain one cell. 9V-blocks have six cells with 1.5 V each.

For each bulk, the five different voltage distributions shown in table 4.6 are applied. The cumulative probability functions are represented in figure 4.11. The case $\bar{f}_U = 0, \sigma_{fU} = 0$ is neglected, because the electrical energy of the bulk would be zero and short circuits would not have any effect. $\bar{f}_U = 1, \sigma_{fU} = 0$ is a worst-case scenario, where all batteries are at nominal voltage. $R_{i,cell} = 0.3 \Omega$ and $R_c = 0.1 \text{ m}\Omega$ are assumed for all batteries, regardless of the type or the voltage.

Table 4.6.: Parameters for voltage distribution in simulation runs

| | \bar{f}_U | σ_{fU} |
|----------|-------------|---------------|
| f_{U1} | 0 | 0.2 |
| f_{U2} | 0.33 | 0.2 |
| f_{U3} | 0.66 | 0.2 |
| f_{U4} | 1 | 0.2 |
| f_{U5} | 1 | 0 |

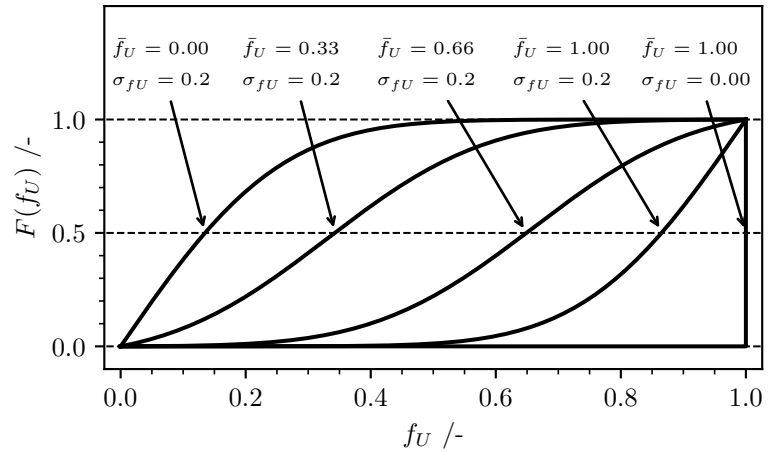


Figure 4.11.: Cumulative probability function of the applied voltage distributions

4.2.4. Time discretization and iterations

Blender calculates the physics in discrete frames. The number of frames (fps) in a certain time span (fps_base) can be set. For each frame a number of sub steps ($substeps_per_frame$) is calculated. To speed up the simulation the variable $time_scale$ is available. Settings of these values influence the computing time, the accuracy, and the stability of the simulation. The input parameters for time discretization and iterations are shown in table 4.7.

Table 4.7.: Simulation parameters for the time discretization and iterations

| Symbol | Description | Unit |
|------------------------|--|------|
| fps | Frames per fps_base seconds | - |
| fps_base | Base for fps calculation | - |
| $substeps_per_frame$ | Substeps calculated between two frames | - |
| $time_scale$ | Speed parameter for physics engine | - |
| $solver_iterations$ | Number of iterations calculated per sub step | - |

4.2.5. Analysis

When all variables for the simulation are set and the objects are created, the simulation physics is calculated. The number of required frames is given by the number of batteries, the safety time and the settling time. The result for the geometry of the last frame is analysed.

4.2.5.1. Batteries and bulk

Overfilling or instabilities in the simulation can cause batteries to end up outside the container. The position of each battery is detected and those outside the diameter d of the container or below its bottom are excluded from further considerations. For every battery, the position \vec{s}_{end} , the velocity $|\vec{v}_{end}|_{max}$ and the movement $|\Delta\vec{s}_{end}|_{max}$ are determined. Based on the randomly defined dimensions, the mass m_{batt} and the volume V_{batt} of each battery are calculated. The determined parameters can be found in table 4.8.

Table 4.8.: Evaluated output parameters for each battery

| Symbol | Description | Unit |
|---|---|-------------------|
| $\vec{s}_{end} = \begin{pmatrix} s_{end,x} \\ s_{end,y} \\ s_{end,z} \end{pmatrix}$ | Location of the batteries centre in the last simulation frame | m |
| $ \vec{v}_{end} _{max}$ | Fastest movement of the battery in the last second | m s^{-1} |
| $ \Delta\vec{s}_{end} _{max}$ | Furthest movement of the battery in the last second | m |
| m_{batt} | Mass of the battery | kg |
| V_{batt} | Volume of the battery | m^3 |

The geometrical boundaries of the bulk are defined by the smallest convex hull that includes all batteries not excluded as mentioned above. The shape of the convex hull is demonstrated in figure 4.12. The output parameters listed in table 4.9 are determined.

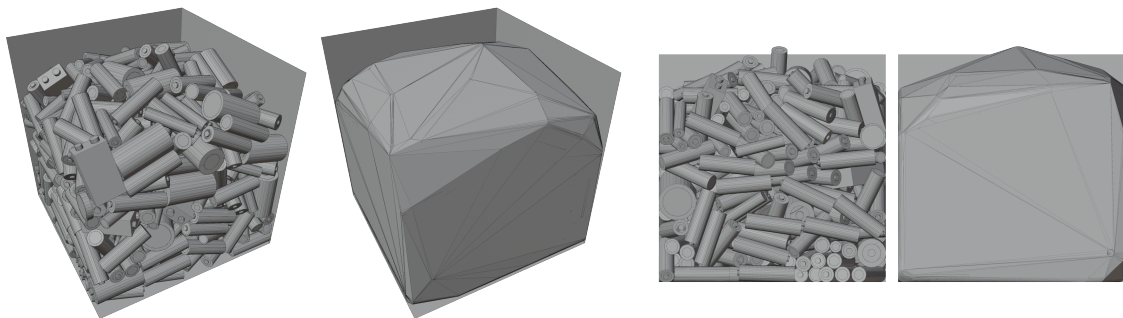


Figure 4.12.: Convex hull around batteries marking the bulk ('cube', $V_{cont} = 8\text{ L}$, $l_1 = 20\text{ cm}$, $m_{batts,bulk} = 11.6\text{ kg}$)

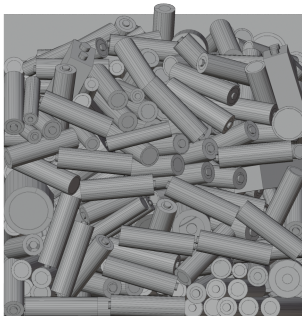
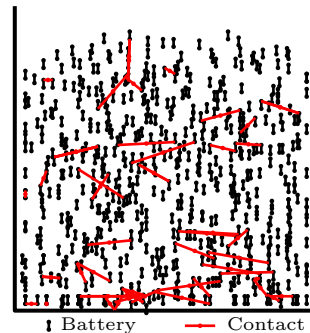
Six battery samples taken in spring 2021 with masses between 12.3 and 15.9 kg in buckets of approximately 12 L were available for comparison. The volume of the battery fill was estimated from pictures. The bulk densities are between 1400 and 1850 kg m^{-3} and 1600 kg m^{-3} on average. The example bulk in figure 4.12 contains 11.6 kg batteries in an 8 L cube. The bulk density is 1580 kg m^{-3} and $\varepsilon_{bulk} = 0.42$. The degree of filling is about 92 %.

Table 4.9.: Evaluated output parameters for the battery bulk

| Symbol | Description | Definition | Unit |
|----------------------------|---------------------------------------|--|-----------------------------|
| V_{bulk} | Volume of the battery bulk | Volume of the smallest convex hull including all batteries in the bulk | m^3 |
| $m_{batts,bulk}$ | Mass of all batteries inside the bulk | $m_{batts,bulk} = \sum^{bulk} m_{batt}$ | kg |
| $N_{batts,bulk}$ | Number of batteries inside the bulk | | - |
| ρ_{bulk} | Bulk density | $\rho_{bulk} = \frac{m_{batts,bulk}}{V_{bulk}}$ | kg m^{-3} |
| $n_{batts,bulk}$ | Number of batteries per bulk volume | $n_{batts,bulk} = \frac{N_{batts,bulk}}{V_{bulk}}$ | m^{-3} |
| ε_{bulk} | Void fracture in the bulk | $\varepsilon_{bulk} = 1 - \frac{V_{batts,bulk}}{V_{bulk}}$ | $\text{m}^3 \text{ m}^{-3}$ |
| $\varphi_{bulk,container}$ | Degree of filling of the container | $\varphi_{batts,bulk} = \frac{V_{bulk}}{V_{container}}$ | $\text{m}^3 \text{ m}^{-3}$ |

4.2.5.2. Short circuits in bulk

Contacts of battery poles are detected by checking each battery against each other one. If the centre to centre distance is closer than h_{safe} the meshes get triangulated and the triangles are checked for collision, giving a list of contacts. For the final bulk shown in figure 4.13a, the contacts are evaluated in figure 4.13b. The 557 batteries in this example form 57 connections.


 (a) Bulk at the end of t_{settle}


(b) Contacts between battery poles in the bulk

Figure 4.13.: Contact determination for battery bulk

The information about the batteries and contacts is transformed into a directed mathematical graph using the python library ‘networkx’ ([1]). Each battery pole and each contact is represented by a node. A battery is an edge pointing from the minus pole to the plus pole. One contact consists of two edges, with a node between the battery poles.

Since not all batteries are connected, the graph is separated in connected subgraphs. If a partial graph contains at least one battery inside a full cycle, it will be evaluated further. Figure 4.14 shows the relevant subgraphs for the bulk in figure 4.13. In this example N_{sc} is 2.

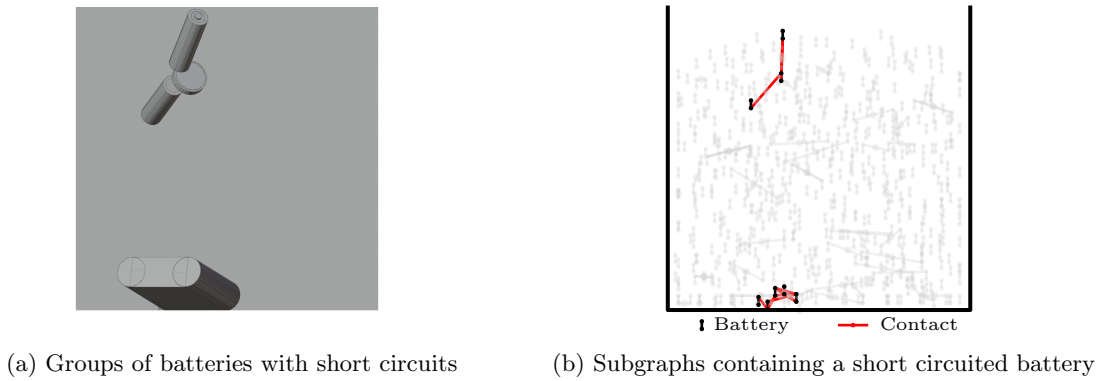


Figure 4.14.: Reduction of the graph to relevant subgraphs

The relevant batteries and their connections are rotated and enlarged in figure 4.15. In the upper group a coin battery (B7) is short circuited by the minus pole of a cylindrical cell (B8). Another cylindrical battery (B6) is in contact with the button cell, but has no electrical influence. The bottom circuit is more complicated and includes three short circuited batteries (B2, B3, B5) and two irrelevant (B1, B4). In total there are four short circuited batteries in this bulk ($N_{sc,batts} = 4$) and the maximum number of batteries in a short circuit $N_{batts,sc,max}$ is three. The output parameters for the short circuits can be found in table 4.10.

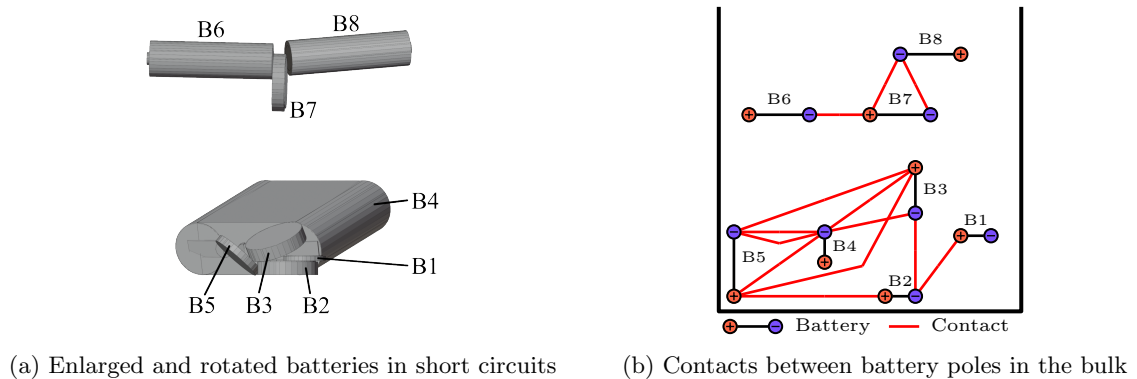


Figure 4.15.: Relevant batteries and subgraphs

Table 4.10.: Evaluated output parameters for the bulk's short circuits

| Symbol | Description | Unit |
|---------------------|---|-----------|
| N_{sc} | Total number of short circuits in bulk | - |
| $n_{sc,bulk}$ | Short circuits per bulk volume | m^{-3} |
| $b_{sc,bulk}$ | Short circuits per bulk mass | kg^{-1} |
| $N_{sc,batts}$ | Total number of batteries in short circuits in bulk | - |
| $n_{sc,batts,bulk}$ | Number of batteries in short circuits per bulk volume | m^{-3} |
| $b_{sc,batts,bulk}$ | Number of batteries in short circuits per bulk mass | kg^{-1} |
| $x_{batts,sc}$ | Fraction of batteries in short circuits | - |
| $N_{batts,sc,max}$ | Maximum number of batteries in a short circuit | - |

4.2.5.3. Electrical currents and released heat

As stated in section 4.2.3, all battery edges stand for a voltage source U_{batt} and an internal resistance R_i . The contacts edges are resistors R_c . The graph and the electrical representations contain all information needed for electrical evaluation. Figure 4.16 shows the circuit diagram for the bottom battery group of the example bulk.

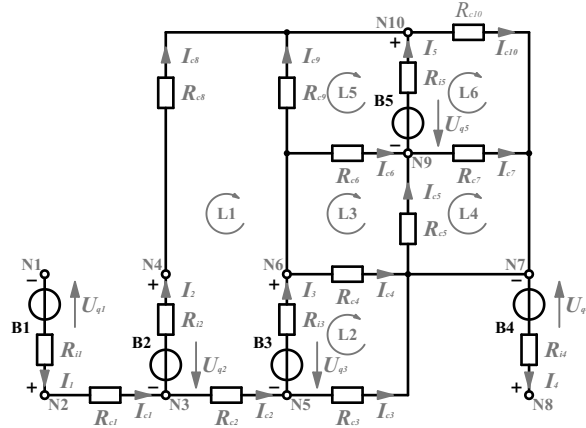


Figure 4.16.: Circuit diagram of a group of batteries in a bulk

For circuits just containing voltage sources and resistances, Kirchhoff's laws (equations (2.3) and (2.5)) give equations to solve for all electrical currents. Values for U_q , R_i and R_c are set as described in section 4.2.3. The equations can be converted in a coefficient matrix A and a result vector \vec{b} . The electrical currents are then given by

$$\vec{I} = A/\vec{b} \quad (4.5)$$

Generation and solving of the equations were performed using python. In the example bulk, five electrical currents through batteries ($I_1 \dots I_5$) and ten in contact currents ($I_{c1} \dots I_{c10}$) are unknown. Kirchhoff's circuit laws give ten linear equations for the nodes N1 ... N10 and six for the loops L1 ... L6. Since the node equations are not linear independent, one of them has to be removed (N10 in this example). The 15 equations and unknowns form a system of linear equations. The augmented matrix can be written as

$$\left(A \left| \vec{b} \right. \right) =$$

$$= \left[\begin{array}{cccccccccccccccc|cccc}
-1 & 0 & 0 & 0 & 0 & 0 & 0 & 0 & 0 & 0 & 0 & 0 & 0 & 0 & 0 & 0 & 0 & 0 & 0 \\
1 & 0 & 0 & 0 & 0 & -1 & 0 & 0 & 0 & 0 & 0 & 0 & 0 & 0 & 0 & 0 & 0 & 0 & 0 \\
0 & -1 & 0 & 0 & 0 & 1 & -1 & 0 & 0 & 0 & 0 & 0 & 0 & 0 & 0 & 0 & 0 & 0 & 0 \\
0 & 1 & 0 & 0 & 0 & 0 & 0 & 0 & 0 & 0 & 0 & 0 & 0 & -1 & 0 & 0 & 0 & 0 & 0 \\
0 & 0 & -1 & 0 & 0 & 0 & 1 & -1 & 0 & 0 & 0 & 0 & 0 & 0 & 0 & 0 & 0 & 0 & 0 \\
0 & 0 & 1 & 0 & 0 & 0 & 0 & 0 & -1 & 0 & -1 & 0 & -1 & 0 & 0 & -1 & 0 & 0 & 0 \\
0 & 0 & 0 & -1 & 0 & 0 & 0 & 1 & 1 & -1 & 0 & 1 & 0 & 0 & 0 & 1 & 0 & 0 & 0 \\
0 & 0 & 0 & 1 & 0 & 0 & 0 & 0 & 0 & 0 & 0 & 0 & 0 & 0 & 0 & 0 & 0 & 0 & 0 \\
0 & 0 & 0 & 0 & -1 & 0 & 0 & 0 & 0 & 1 & 1 & -1 & 0 & 0 & 0 & 0 & 0 & 0 & 0 \\
0 & R_{i2} & -R_{i3} & 0 & 0 & 0 & -R_{c2} & 0 & 0 & 0 & 0 & 0 & 0 & R_{c8} & -R_{c9} & 0 & 0 & -U_{q3} + U_{q2} & 0 \\
0 & 0 & R_{i3} & 0 & 0 & 0 & 0 & -R_{c3} & R_{c4} & 0 & 0 & 0 & 0 & 0 & 0 & 0 & 0 & U_{q3} & 0 \\
0 & 0 & 0 & 0 & 0 & 0 & 0 & 0 & -R_{c4} & -R_{c5} & R_{c6} & 0 & 0 & 0 & 0 & 0 & 0 & 0 & 0 \\
0 & 0 & 0 & 0 & 0 & 0 & 0 & 0 & 0 & R_{c5} & 0 & R_{c7} & 0 & 0 & 0 & 0 & 0 & 0 & 0 \\
0 & 0 & 0 & 0 & -R_{i5} & 0 & 0 & 0 & 0 & 0 & -R_{c6} & 0 & 0 & 0 & R_{c9} & 0 & 0 & -U_{q5} & 0 \\
0 & 0 & 0 & 0 & R_{i5} & 0 & 0 & 0 & 0 & 0 & 0 & -R_{c7} & 0 & 0 & 0 & R_{c10} & 0 & U_{q5} & 0
\end{array} \right]$$

The current direction is assumed to be from minus to plus pole for all batteries. If the result is negative, the battery gets charged by the others, if positive it gets discharged. The current direction in the contacts is chosen arbitrarily and the sign of the resulting current has no physical meaning.

In the example $f_U = 1$, $R_{i1} \dots R_{i5} = R_i = 0.3 \Omega$ for all batteries and $R_{c1} \dots R_{c10} = R_c = 0.1 \text{ m}\Omega$ for all contacts is assumed. The determined currents are

$$\vec{I} = \begin{bmatrix} I_1 \\ I_2 \\ I_3 \\ I_4 \\ I_5 \\ I_{c1} \\ I_{c2} \\ I_{c3} \\ I_{c4} \\ I_{c5} \\ I_{c6} \\ I_{c7} \\ I_{c8} \\ I_{c9} \\ I_{c10} \end{bmatrix} = \begin{bmatrix} 0.00 \\ 9.98 \\ 9.99 \\ 0.00 \\ 10.00 \\ 0.00 \\ -9.98 \\ -19.97 \\ 7.68 \\ 0.77 \\ 8.45 \\ -0.77 \\ 9.98 \\ -6.15 \\ 13.83 \end{bmatrix} \text{ A} \quad (4.6)$$

By equations (2.1) and (2.2) the electrical heat release rate for each resistance can be calculated. The heat generation of the contact resistors is divided to the connected batteries. The result is a heat generation \dot{Q}_{batt} of each battery.

Since the geometrical arrangement of the bulk is independent from the electrical properties of the batteries, the voltage distribution and the resistances can be varied without generation of a new bulk.

Table 4.11.: Evaluated output parameters for the bulk's electrical properties

| Symbol | Description | Unit |
|--------------------|---|--------------------|
| I_{batt} | Electrical current of a battery | A |
| \dot{Q}_{batt} | Electrical heat release of a battery | W |
| I_{max} | Maximum electrical current in bulk | A |
| \dot{Q}_{max} | Maximum heat release rate of a single battery in bulk | W |
| \dot{Q}_{bulk} | Total heat release rate of battery bulk | W |
| $\dot{q}_{m,bulk}$ | Heat release rate per bulk mass | W kg ⁻¹ |

4.2.5.4. Simulation stability and accuracy

Instabilities of the simulation can cause physical unreasonable results. The impact of these effects and the consequences should be estimated. Especially small objects, like coin batteries, can pass through the container walls in some cases. This effect is strongly correlated to the type of battery. Small types are affected more and the battery composition in the bulk can shift towards larger types. If batteries are added to the physics simulation in a way they intersect with other rigid bodies, the objects can reach very high velocities. These batteries are usually thrown far away from the container and will not end in the bulk.

Instabilities in the numerical calculation itself can show up as unexpected velocities. Resting objects can suddenly accelerate without any physical reason. Oscillations, where an object never comes to rest can occur. In some cases, the constraints between the battery parts break and geometrically impossible short circuits are detected.

Since an artificial damping of movement is added, the batteries can also start floating and not fall as in natural physics. Inaccuracies can also be a result of too low t_{settle} values. In this case the batteries are still moving and are not in a resting position.

The distribution of the final position, the maximum distance moved in the end and the velocities are taken as comparison values. The types of short circuits are checked for geometrical possibility. Stability and accuracy are also checked by studying the created videos. Table 4.12 lists output parameters for evaluation of the simulation's stability.

Table 4.12.: Evaluated output parameters for the accuracy and stability of simulation

| Symbol | Description | Unit |
|---|---|-------------------|
| $\vec{s}_{end} = \begin{pmatrix} \vec{s}_{end,x} \\ \vec{s}_{end,y} \\ \vec{s}_{end,z} \end{pmatrix}$ | Mean position of the batteries in the bulk | m |
| $(\vec{v}_{end} _{max})_{95}$ | 95 %-quantile for $ \vec{v}_{end} _{max}$ | m s^{-1} |
| $(\Delta\vec{s}_{end} _{max})_{95}$ | 95 %-quantile for $ \Delta\vec{s}_{end} _{max}$ | m |
| $f_{sc,unrealistic}$ | Fraction of detected unrealistic short circuits | - |

4.3. Design of experiments

The goal of the simulation runs presented in this thesis are the determination of suitable input parameters, getting results for some selected cases and estimate the accuracy and usability of the applied models.

To find a set of suitable input parameters for the geometrical, physical, and electrical model (tables 4.1, 4.4 and 4.5) and for time discretization (table 4.7), a non-systematic try and error approach is used. The focus is to find values to get realistic and stable simulation results, with reasonable simulation times. The size of the container, the number of batteries and the distribution are varied. For more time efficiency the runs are determined when it is obvious that the parameter set is not usable.

A set of simulation runs using the battery composition of section 4.2.2.1 for container sizes from half a litre to sixty-four litres is executed. The number of batteries is set according to the container size and the simulation parameters remain constant. Cube sizes follow a geometrical series where the volume is doubled each step. Boxes and barrels are included using the size of typical containers used in waste battery collection in Austria.

Small samples of pure button cell bulks in containers from 0.25 to 1 L are tested. The distribution of coin battery types is equal to the standard composition. The amount of coin and block batteries was varied, starting at the standard composition. After evaluation of the results, further individual tests are determined according to previous results.

To evaluate the effect of the parameter set a screening test using the Plackett-Burman design in two steps is performed. In this experiment design, all input parameters have a designated low and high value. A cube-shaped 8 L container ($0.2 \text{ m} \times 0.2 \text{ m} \times 0.2 \text{ m}$) filled with 560 batteries is used. In the first step for all parameters in tables 4.1, 4.4 and 4.7 (except $N_{batts,set}$) the high and low values are 50 % higher and lower than the standard values found before. In the second step the span is extended to $\pm 80 \%$.

4.4. Results of the numerical study

After a suitable parameter set was found, 197 simulation runs were performed. 133 195 batteries (2827 kg) were simulated and analysed. In all simulation runs using different starting conditions, 664 connected networks including 4414 short circuited batteries were detected. This section outlines the main results of the study. If not stated otherwise, the simulations were performed using the standard parameter set and the standard battery type composition.

4.4.1. Parameter tests

Table 4.13 lists the parameters found in various non-systematic test runs. The parameters produce stable simulations and the results seem to be realistic. For evaluation, the graphical animation of the simulations was used along with the output parameters in table 4.12. The values were used for further tests.

| Parameters | Value | Unit |
|---------------------------|-------|-------------------|
| <i>scale_factor</i> | 100 | m m^{-1} |
| <i>v_{0z}</i> | 1 | m s^{-1} |
| <i>t_{safe}</i> | 0.05 | s |
| <i>t_{settle}</i> | 30 | s |
| <i>h_{safe}</i> | 0.05 | m |
| <i>friction</i> | 1.6 | - |
| <i>restitution</i> | 0.5 | - |
| <i>linear_damping</i> | 0.5 | - |
| <i>angular_damping</i> | 0.5 | - |
| <i>fps</i> | 15 | - |
| <i>fps_base</i> | 1 | - |
| <i>substeps_per_frame</i> | 10 | - |
| <i>time_scale</i> | 5 | - |
| <i>solver_iterations</i> | 10 | - |

Table 4.13.: Set of input parameters used for simulation

4.4.2. Various bulk sizes with constant parameters

136 simulation runs were performed with container sizes from 0.5 up to 64 L and masses from 0.58 to 97 kg. Cubes were calculated for the whole size range from 8 to 40 cm edge length. Boxes and barrels were added in selected dimensions. Due the significant increase in computing time, more runs were conducted for smaller bulks. The distribution is shown in figure 4.17.

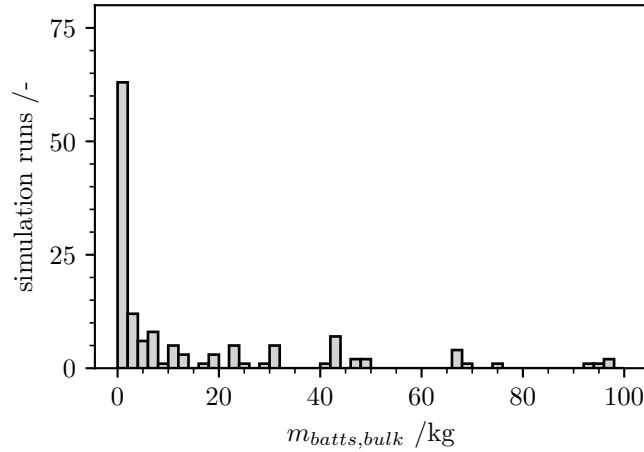


Figure 4.17.: Number of simulation runs performed for different bulk masses ($\Delta m = 2$ kg)

4.4.2.1. Bulk density ρ_{bulk}

Figure 4.18 presents ρ_{bulk} over the bulk masses. The data points show greater dispersion for masses below 5 kg. The range till 10 kg is shown enlarged in figure 4.18b. The density ranges between 1163 and 1550 kg m^{-3} for $m_{batts,bulk} \leq 2$ kg. With increasing mass, a shift towards higher values and a narrower distribution can be observed. For bulks above 10 kg the bulk density is 1624 kg m^{-3} on average with a quite narrow distribution and a slight, steady increase. A difference between the container shapes cannot be noticed.

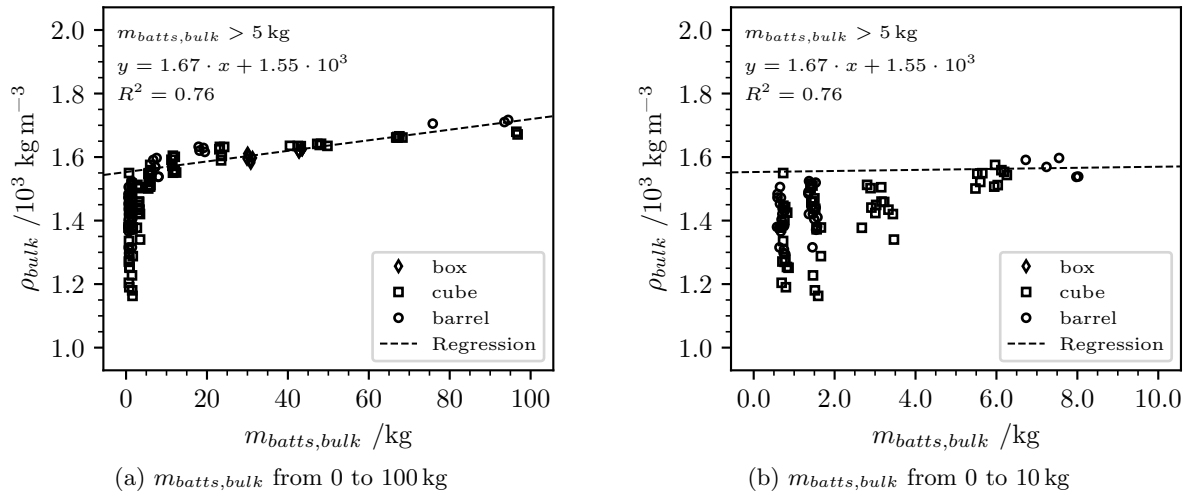


Figure 4.18.: Bulk density ρ_{bulk} of the simulated battery bulks

4.4.2.2. Bulk void fraction ε_{bulk}

Similar to ρ_{bulk} the void fraction ε_{bulk} shows a wider variation for bulk sizes below 5 kg, as shown in figure 4.19. For $m_{batts,bulk} < 2$ kg the void fraction ranges from 0.42 to 0.57. For bigger masses, ε_{bulk} decreases and the variation get narrower. Above 10 kg ε_{bulk} is about 0.40 with a slight decline towards bigger containers.

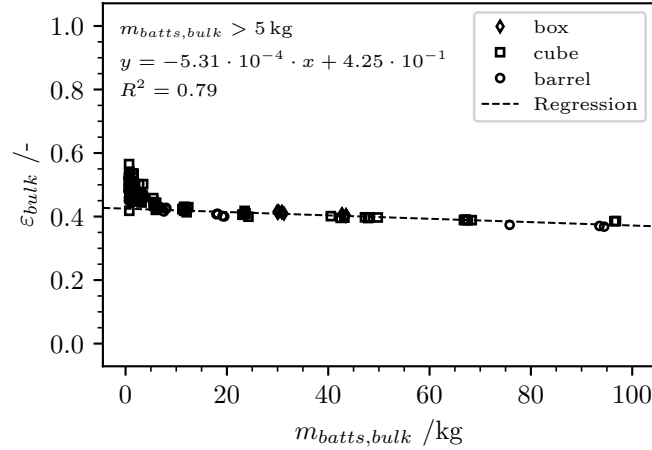


Figure 4.19.: Bulk void fraction ε_{bulk} of the simulated battery bulks

4.4.2.3. Number of batteries $N_{batts,bulk}$

The number of batteries per bulk mass found by linear regression with fixed interception is about 46 batteries per kg and is shown in figure 4.20a. The bulk contains 77 batteries per L as presented in figure 4.20b. The packing density of the batteries shows no dependency on the container shape.

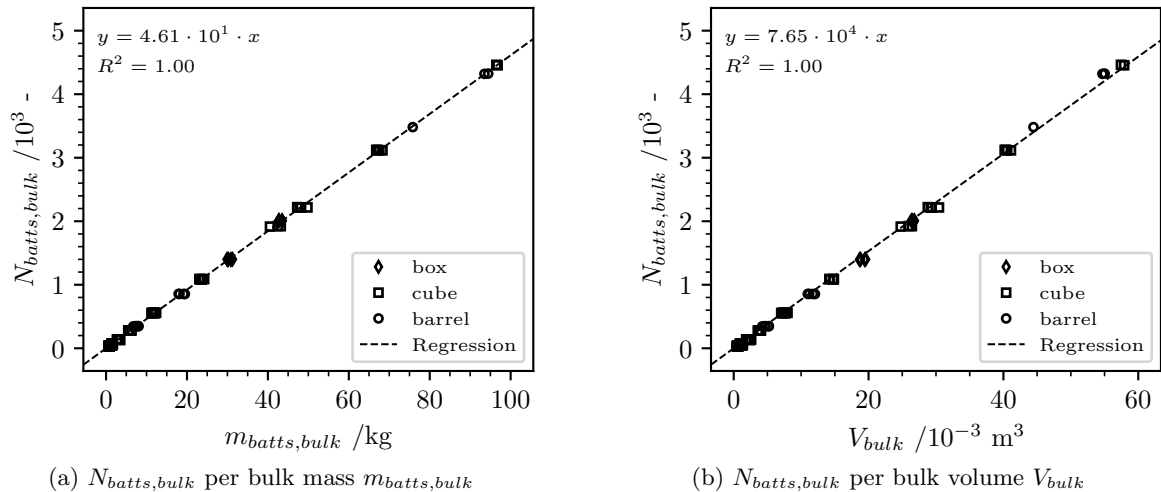


Figure 4.20.: Number of batteries $N_{batts,bulk}$ per bulk size

4.4.2.4. Movement at the end of the settle time

The residual movement of the batteries at the end of the settle time is small as shown in figure 4.21. The variation is bigger for smaller containers till around 10 kg. For larger bulks, a steady increase can be seen. The maximum moved distance in the last second before the evaluation is shown in figure 4.22. It is just a few millimetres and for bigger masses just one or two millimetres in total.

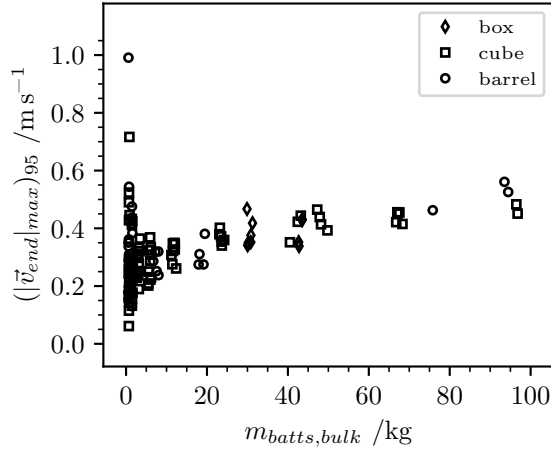


Figure 4.21.: Velocity in the last second of the settle time for different container sizes

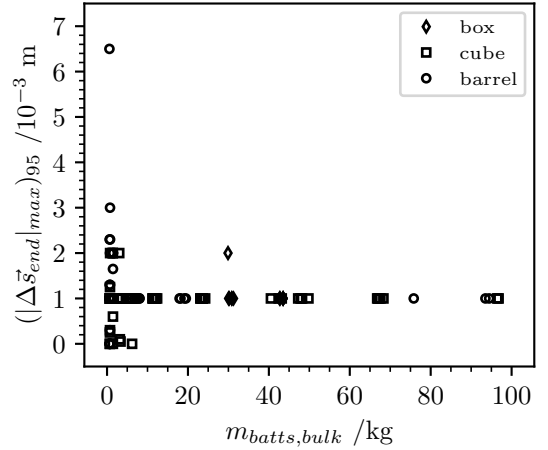


Figure 4.22.: Maximum movement in the last second of the settle time for different container sizes

4.4.2.5. Pole contacts of batteries

The absolute number of contacts between two battery poles is presented in figure 4.23. N_{con} increases linearly with the mass of batteries with about 4.3 contacts per kg of batteries. The spread increases slightly with the bulk size. The number of pole contacts per number of batteries in figure 4.24 varies for small bulks wider on a smaller level. In larger bulks the number ranges from around 7.5 to 12.5 pole contacts per 100 batteries.

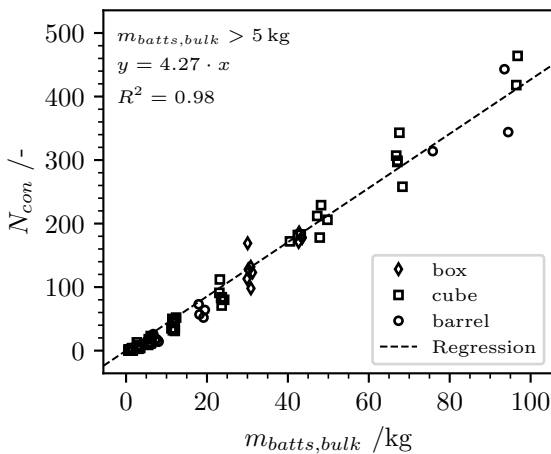


Figure 4.23.: Number of contacts between battery poles in the bulk

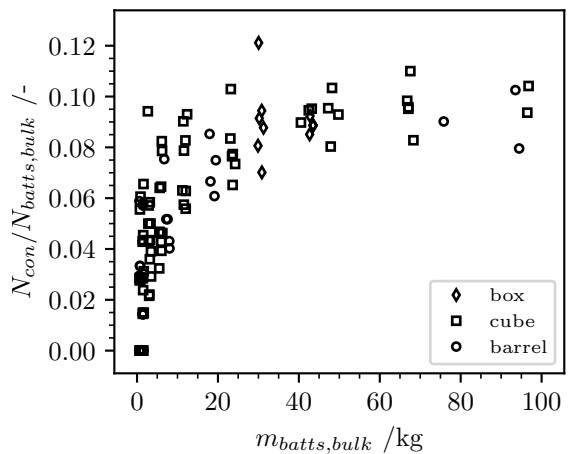


Figure 4.24.: Number of pole contacts per number of batteries in the bulk

4.4.2.6. Short circuits

The number of short circuits is presented in figure 4.25. A linear increase with the bulk size with a considerable spread can be noticed. For analysis it has to be taken in account that the number of simulation runs is far smaller for larger containers. A dependency on the container shape cannot be noticed.

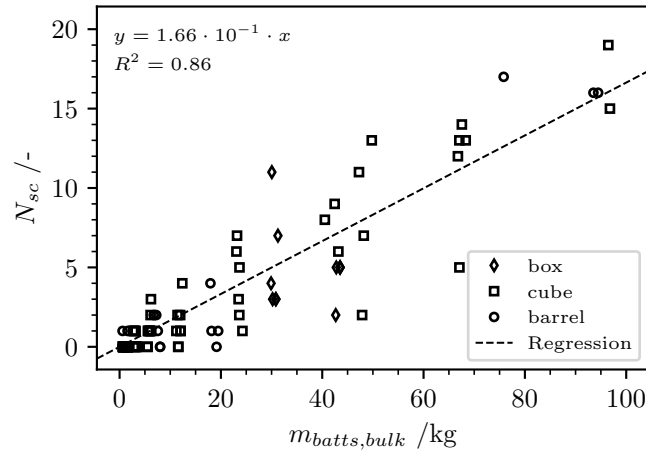


Figure 4.25.: Number of short circuits in the bulk

The number of short circuited batteries per mass shows the same pattern as the number of short circuits, shown in figure 4.26. About 18 batteries are short circuited per kg. The absolute number of short circuits is about the same as the number of short circuited batteries. Per kg the values differ for about 10 %.

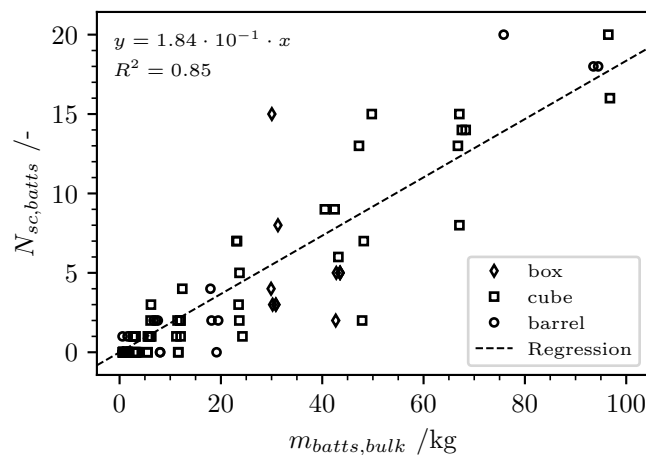


Figure 4.26.: Number of short circuited batteries

Figure 4.27 compares the number of short circuited batteries to the total number in the bulk. Linear regression with fixed interception gives 0.4% of the batteries are short circuited on average. Just one larger sample is above the line $x_{batts,sc} = 0.01$. Since the considerable spread of the data, 1% seems to be a conservative, but reasonable estimation for the fraction of short circuited batteries.

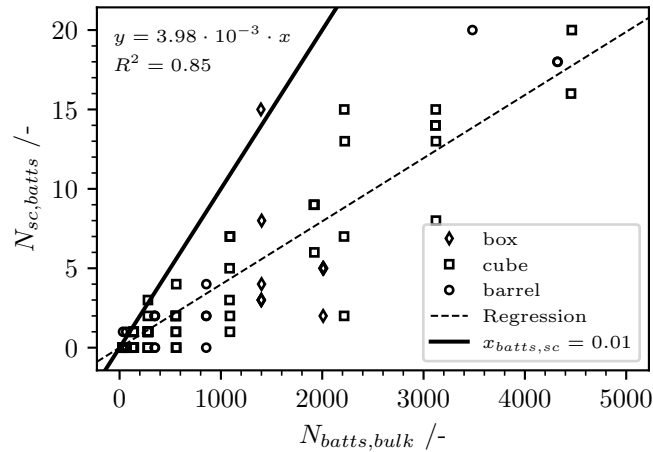


Figure 4.27.: Number of short circuited batteries to the number of batteries in the bulk

Detected short circuits can be a result of instabilities in the simulation. The fraction of short circuits $f_{sc,unreal}$, where a cylindrical battery's poles are connected by only one other battery is shown in figure 4.28. They occur in six out of 136 simulation runs. In one big bulk (96 kg) three can be found, in other cases it is just one.

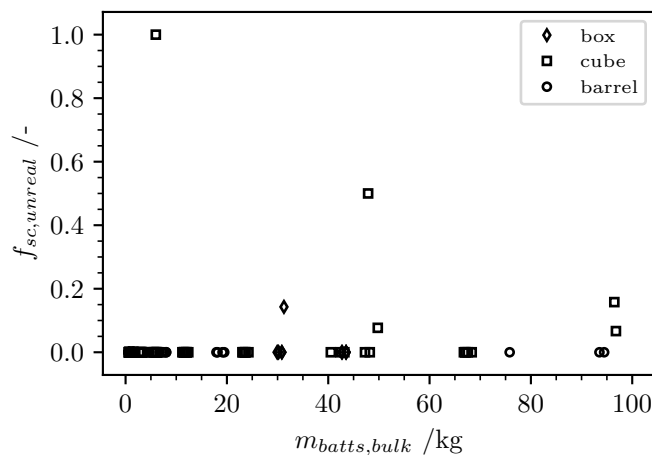


Figure 4.28.: Fraction of unrealistic short circuits

Figure 4.29 shows the battery types included in short circuits over all simulation runs in this set. Compared with the bulks type distribution in figure 4.10, where coin batteries only make around 5% of the batteries, they represent 93% of all short circuited batteries. The distribution of the different coin battery types follows the distribution in the bulk. The effect does not depend on the size of the bulk (figure 4.30).

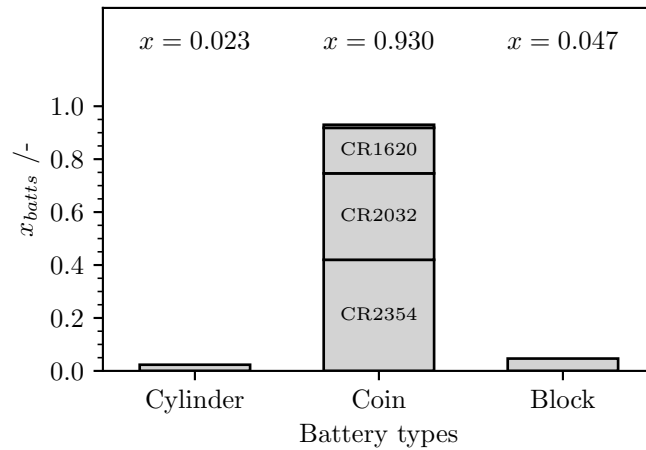


Figure 4.29.: Battery type distribution of short circuited batteries

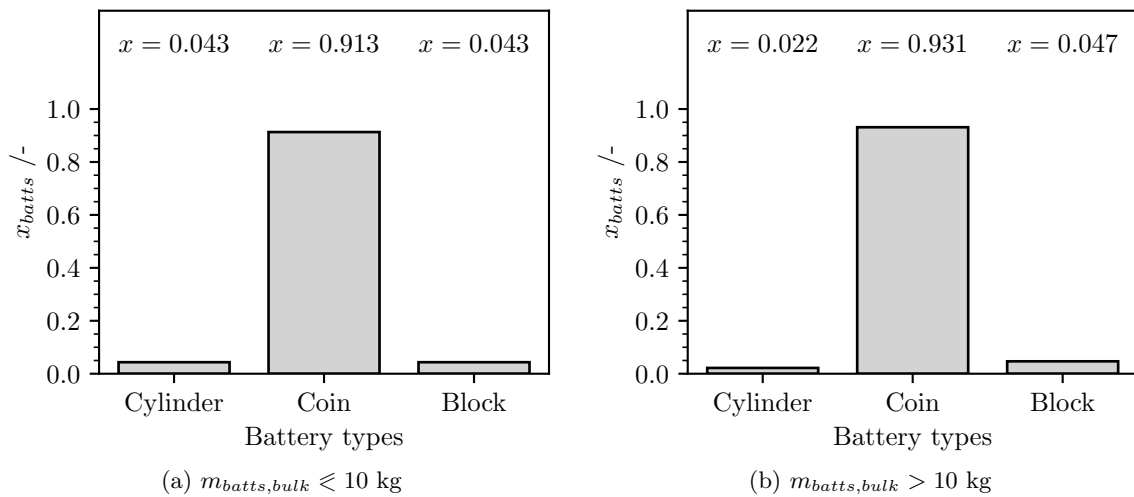


Figure 4.30.: Battery type distribution in short circuits for smaller (a) and larger (b) bulk sizes

The maximum number of batteries in one short circuit is shown in figure 4.31. The number does not indicate if the batteries are connected in series or just have one connection. In one case the maximum number was three batteries. In figure 4.32 the frequency of certain short circuit types is shown. It is mainly coin batteries that are short circuited. Usually by cylindrical or another coin battery. This most common type is equivalent to the upper circuit found in the example bulk in figure 4.15.

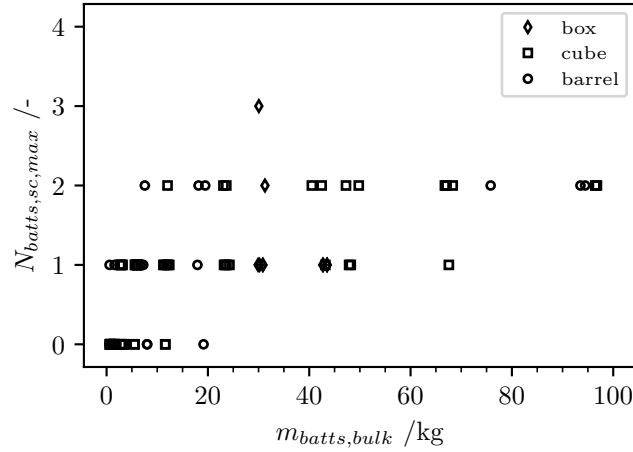


Figure 4.31.: Maximum number of batteries in one short circuit

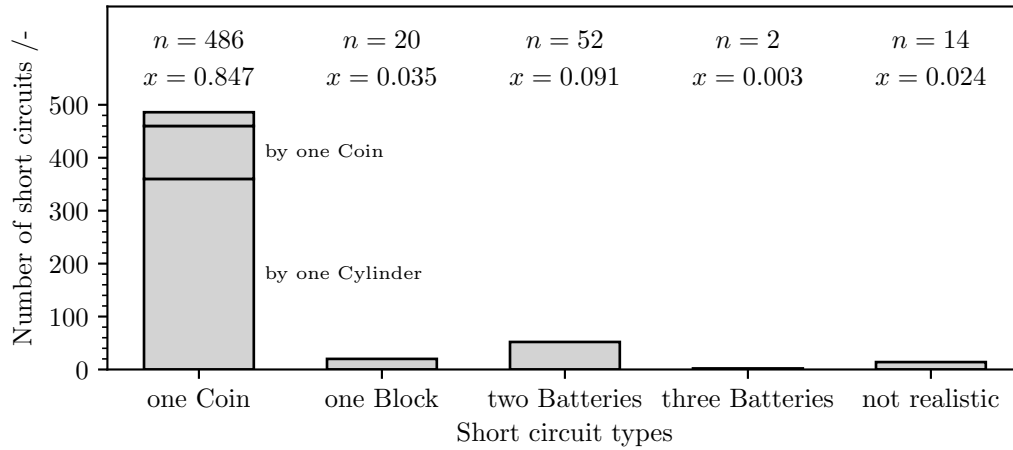


Figure 4.32.: Short circuit types by included battery types distribution

4.4.2.7. Electrical currents and heat release

The maximum initial electrical currents in the bulk by applying values for R_i , R_c and U_{batt} based on \bar{f}_U and σ_{fU} are shown in figure 4.33 for two voltage distribution. A short circuit of a fully charged button cell at $U_N = 3\text{ V}$, $R_i = 0.3\ \Omega$ and $R_c = 0.1\ \text{m}\Omega$ results in an electrical current of 10 A. The accumulation of data points in this range can be seen quite well in figure 4.33b. For voltage distributions with lower values for \bar{f}_U the resulting I_{max} is lower and wider spread (figure 4.33a). The maximum initial heat release of a battery is shown in figure 4.34. For the most common short circuit type at the assumed values, \dot{Q}_{max} is 30 W. The cluster of data points at this value is visible in figure 4.34b. The quadratic relationship in equation (2.2) leads to a decrease at lower battery voltages (figure 4.34a). The cumulative heat release in the bulk is presented in figure 4.35. Using a linear regression with fixed intercept an average specific heat release rate of $5.5\ \text{W kg}^{-1}$ for fully charged batteries and $2.5\ \text{W kg}^{-1}$ for $\bar{f}_U = 0.66$ is found. This is in good accordance with the square relation of equation 2.2.

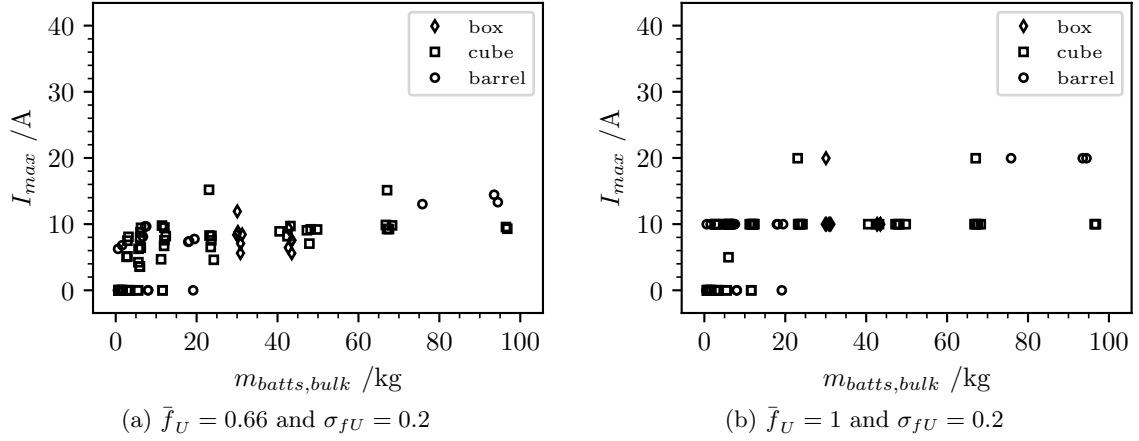


Figure 4.33.: Maximum initial electrical current in bulk using $R_i = 0.3 \Omega$ and $R_c = 0.1 \text{ m}\Omega$

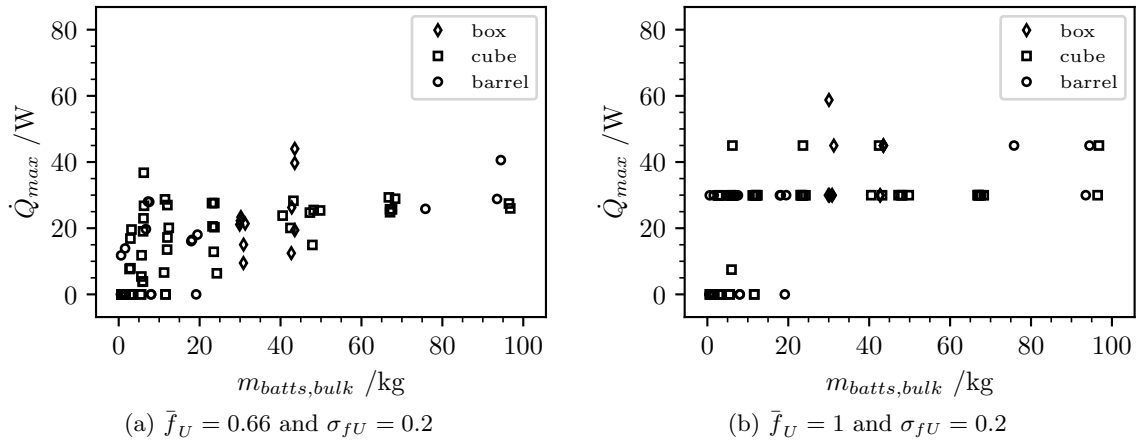


Figure 4.34.: Maximum initial heat release in one battery using $R_i = 0.3 \Omega$ and $R_c = 0.1 \text{ m}\Omega$

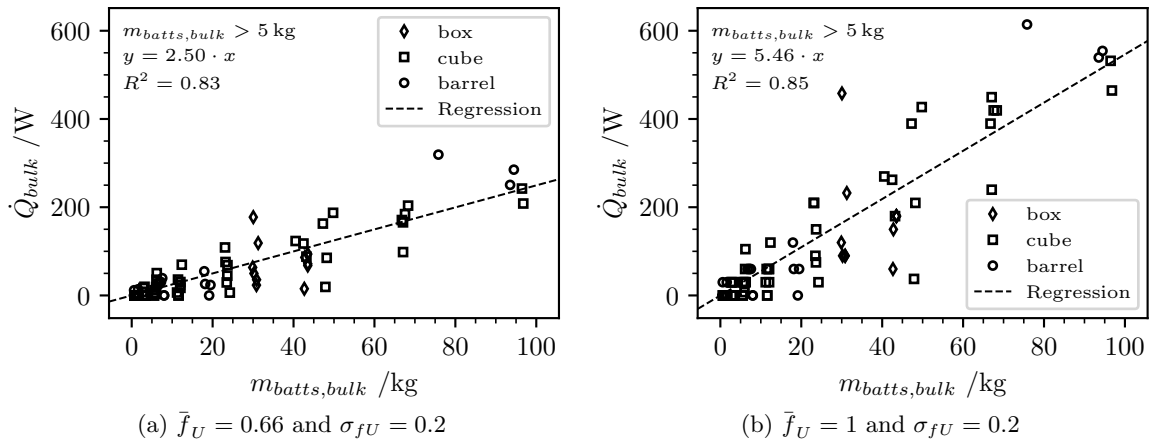


Figure 4.35.: Total initial heat release in bulk using $R_i = 0.3 \Omega$ and $R_c = 0.1 \text{ m}\Omega$

4.4.3. Pure button cell bulks

Nine simulations runs were performed using only coin batteries. The cube type containers range from 0.25 to 1 L and are filled with 0.35 to 1.7 kg batteries.

4.4.3.1. Bulk density ρ_{bulk}

The bulk density is shown in figure 4.36. The smallest bulk with about 0.35 kg can be found around 1550 kg m^{-3} . The bulk density increases with bigger masses to 1650 kg m^{-3} at 1.7 kg. The spread of the data is moderate, although the sample size is quite small.

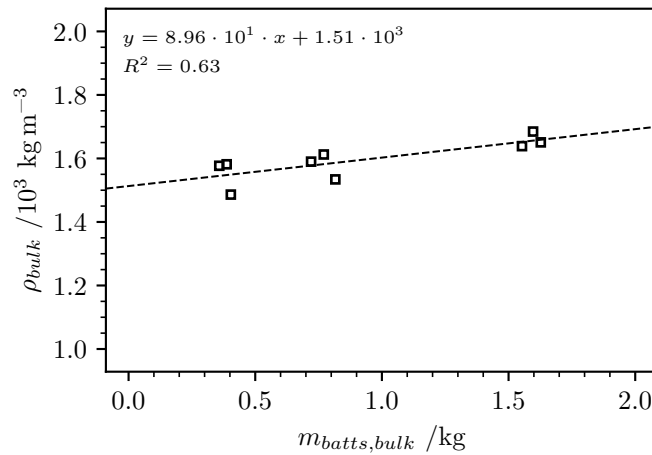


Figure 4.36.: ρ_{bulk} for different battery masses for pure coin battery bulks

4.4.3.2. Number of batteries $N_{batts,bulk}$

With 253 batteries per kg the number of batteries per bulk mass found in figure 4.37a is considerable higher than for mixed bulks. 414 batteries can be found per L bulk volume.

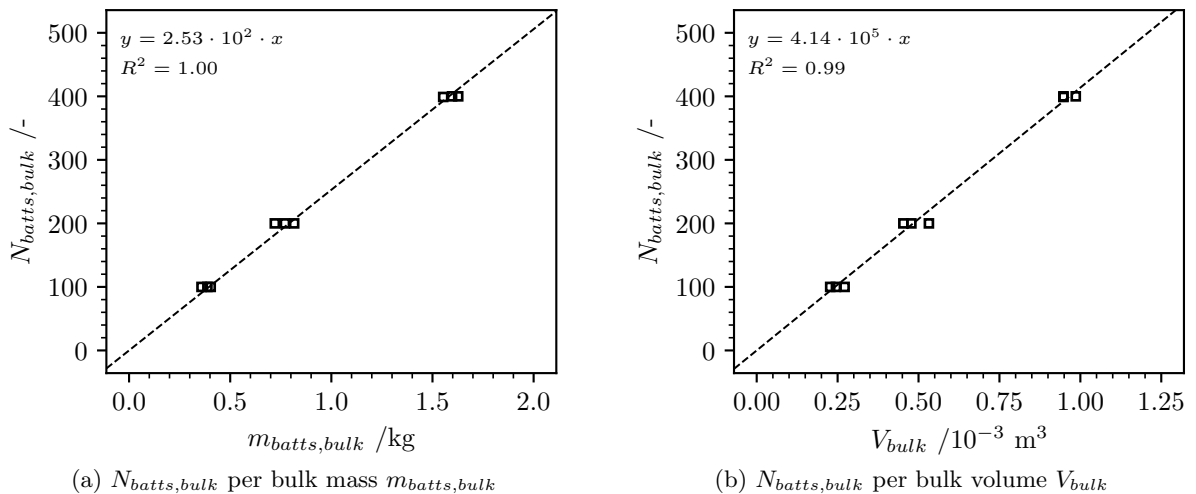


Figure 4.37.: Number of batteries $N_{batts,bulk}$ per bulk size for pure coin battery bulks

4.4.3.3. Short circuits

Different to the mixed samples, all pure coin battery bulks formed just on large short circuit where many batteries are connected. Figure 4.38 shows the maximum number of batteries in one short circuit. Compared to the mixed sample, presented in figure 4.31, the short circuits contain about 100 times the amount of batteries. As shown in figure 4.39 the fraction of batteries in short circuits is uniform for all three bulk sizes. The mean fraction is 82.7%.

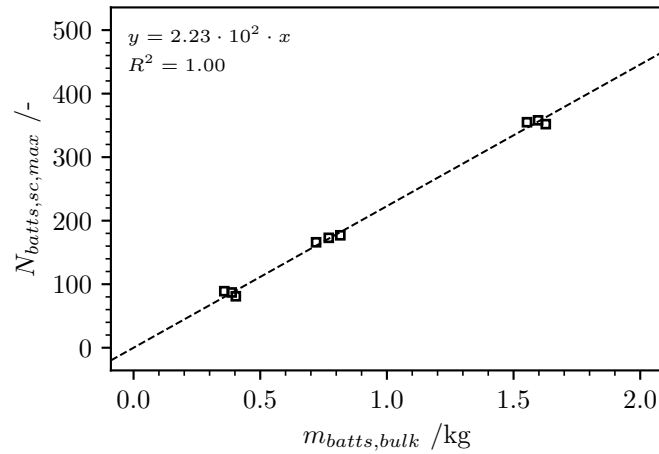


Figure 4.38.: Maximum number of batteries in one short circuit for pure coin battery bulks

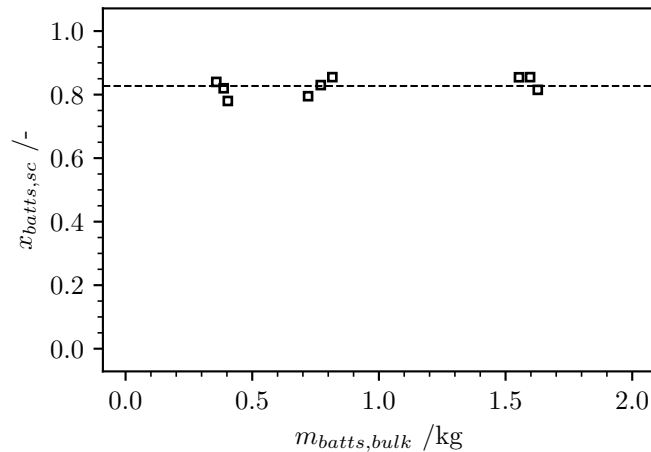
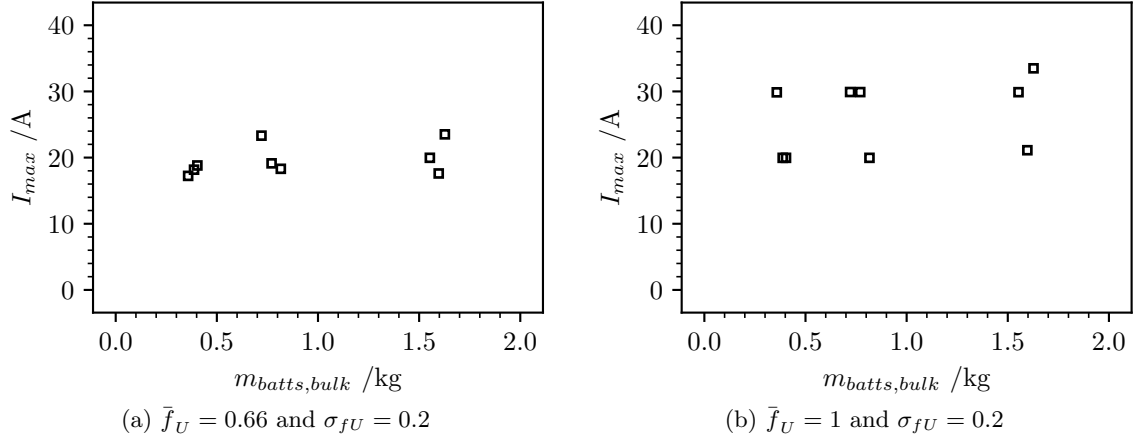
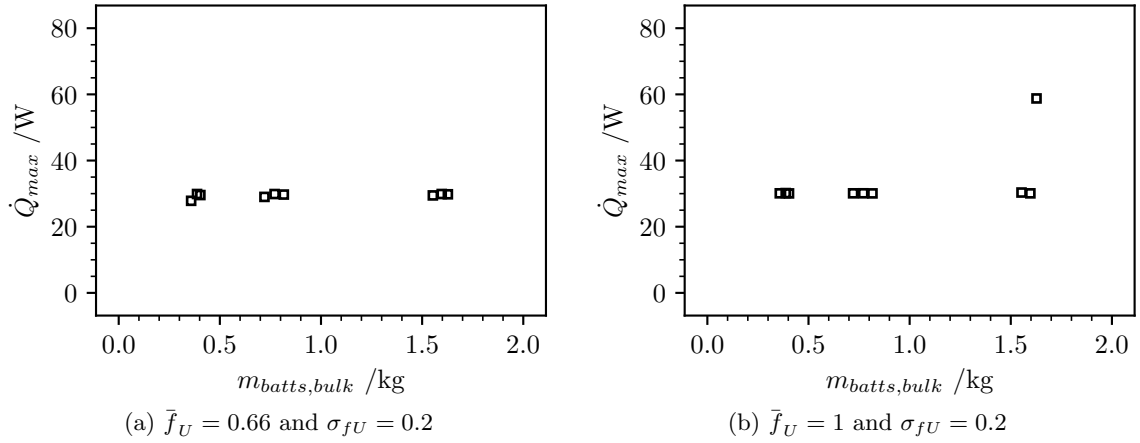
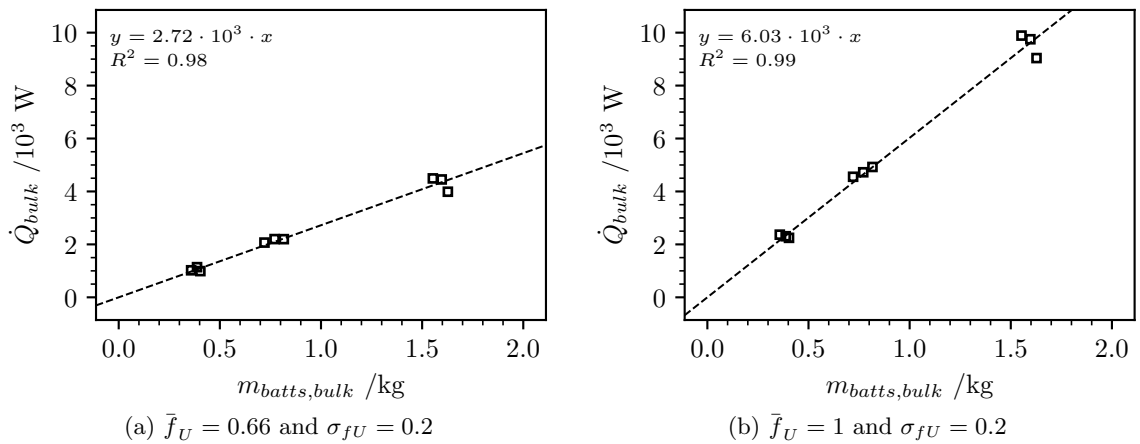


Figure 4.39.: Fraction of batteries in short circuits for pure coin battery bulks

Figures 4.40 and 4.41 show the maximum initial electrical current and heat release rate in the bulk. I_{max} and \dot{Q}_{max} are in the same range as for the mixed battery collection bulks.

The total heat release of the bulk is shown in figure 4.42. With 2.7 kW kg^{-1} and 6.0 kW kg^{-1} the found specific heat release is more the 1000 times higher than in the battery mixture.


 Figure 4.40.: I_{max} for pure coin battery bulks ($R_i = 0.3 \Omega$, $R_c = 0.1 \text{ m}\Omega$)

 Figure 4.41.: \dot{Q}_{max} for pure coin battery bulks ($R_i = 0.3 \Omega$, $R_c = 0.1 \text{ m}\Omega$)

 Figure 4.42.: \dot{Q}_{bulk} for pure coin battery bulks ($R_i = 0.3 \Omega$, $R_c = 0.1 \text{ m}\Omega$)

4.4.3.4. Distribution of heat release

The distribution of heat release within all pure coin battery simulation runs is shown in figure 4.43. The bar furthest left contains all batteries which are not short circuited or have a very low voltage. The voltages are normal distributed. The heat release rates right of the first bar show a pattern according to this distribution. $\dot{Q} = 30 \text{ W}$ is the maximum a fully charged battery with $U_N = 3 \text{ V}$ and $R_i = 0.3 \Omega$ can release.

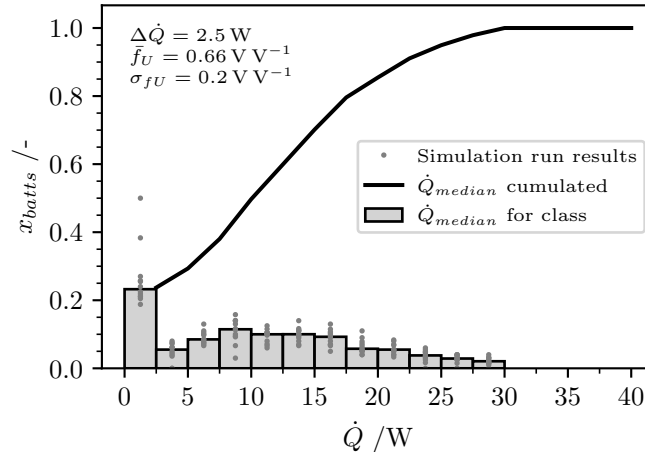


Figure 4.43.: Distribution of the heat release for coin batteries

4.4.4. Variation of battery types

Additionally, to the simulation runs using about 5 % coin batteries over a wide range of bulk sizes and the pure coin bulks, 16 simulation runs using varying coin fractions were performed. The amount of results between 5 % and 100 % button cells is low and the container sizes varies. Some trends can be recognized but results have to be taken with precaution. The fraction of short circuited batteries in the bulk is shown in figure 4.44. The fraction of short circuited batteries shows a strong positive correlation with the fraction of button cells.

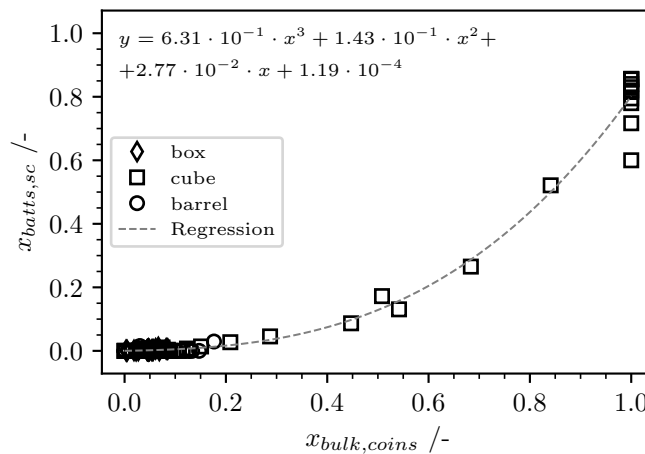


Figure 4.44.: Fraction of batteries in short circuits for variation of the button cell fraction

The maximum initial current is shown in figure 4.45. The spread of the values for 5% and 100% button cells and the low number of results between, must be taken, but a general trend of increasing electrical currents with rising coin battery fraction can be noticed. The maximum heat release of a single battery in the bulk presented in figure 4.46 does not show a clear correlation.

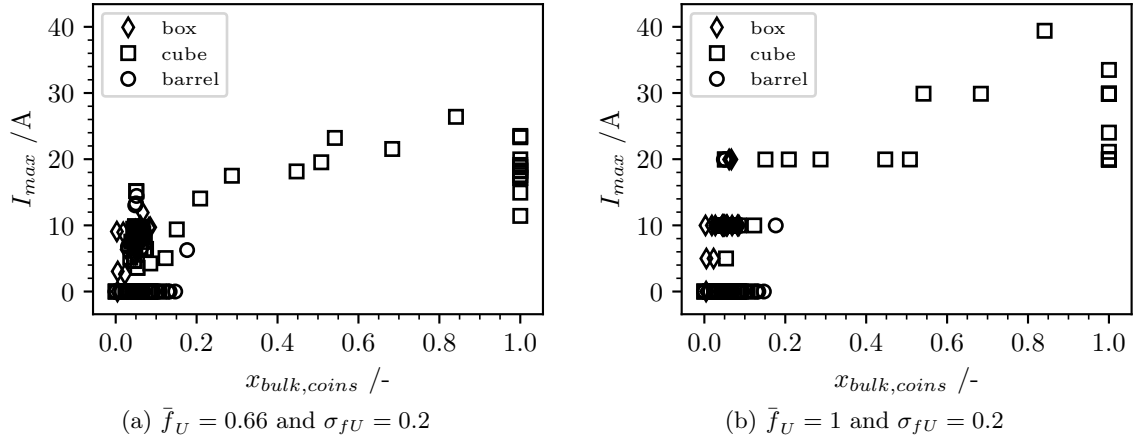


Figure 4.45.: I_{max} for varying button cell fraction ($R_i = 0.3 \Omega$, $R_c = 0.1 \text{ m}\Omega$)

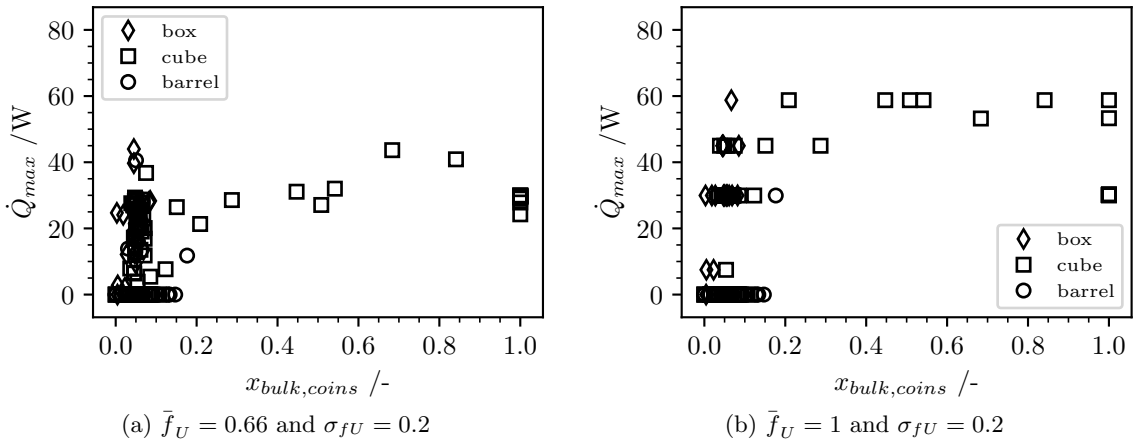
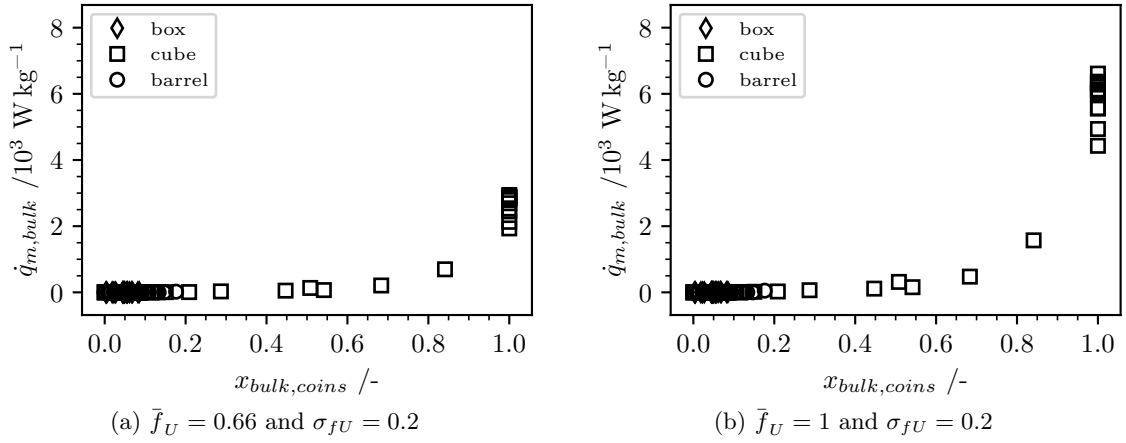


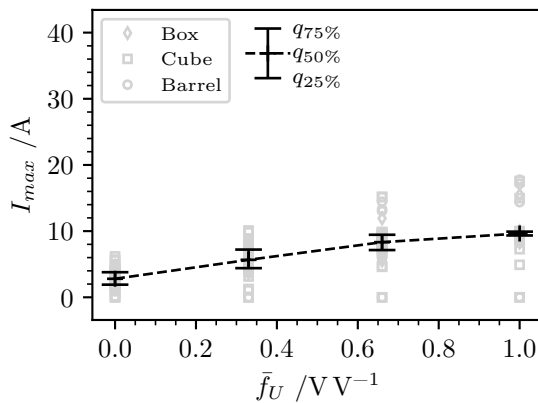
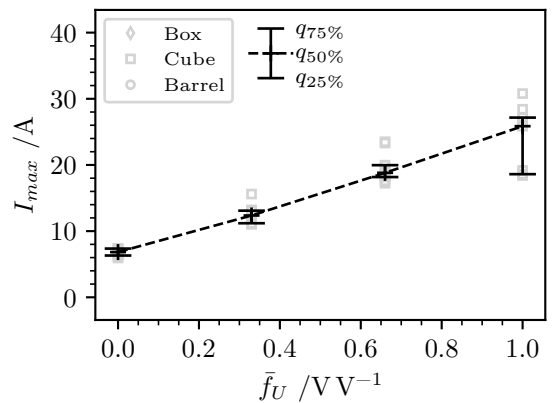
Figure 4.46.: \dot{Q}_{max} for varying button cell fraction ($R_i = 0.3 \Omega$, $R_c = 0.1 \text{ m}\Omega$)

Figure 4.47 shows the specific heat release per bulk mass at different coin battery fractions. While moderate heat generation can be noticed till about $x_{batts,coins} = 80\%$, several kilowatts are reached at higher concentrations.


 Figure 4.47.: $\dot{q}_{m,bulk}$ for varying button cell fraction ($R_i = 0.3 \Omega$, $R_c = 0.1 \text{ m}\Omega$)

4.4.5. Influence of the mean battery voltage

As explained in 4.4.2.7 for each simulation run five different voltage factor distributions were applied and calculated. Since the variation in the results is quite remarkable for smaller bulks, only bulks above 5 kg are considered in this analysis of the mixed battery bulks. Figure 4.48 presents the maximum initial electrical current in the bulk. It has to be noted, that the voltage distribution for the lowest and the highest distribution are narrower, since the cut-off at 0 V V^{-1} and 1 V V^{-1} . The average voltage factor is not \bar{f}_U . An almost linear increase of I_{max} with a rising \bar{f}_U , as expected looking at equation (2.1), can be observed. The maximum heat production in one battery \dot{Q}_{max} and the specific heat release of the bulk $\dot{q}_{m,bulk}$ is shown in figures 4.50 and 4.52. Both show the expected increase. Figures 4.49, 4.51 and 4.53 show the same data for pure coin battery bulks.


 Figure 4.48.: I_{max} for mixed battery samples using different mean voltage factors and $\sigma_{fU} = 0.2$, $m_{batts,bulk} \geq 5 \text{ kg}$

 Figure 4.49.: I_{max} for pure button cell samples using different mean voltage factors and $\sigma_{fU} = 0.2$

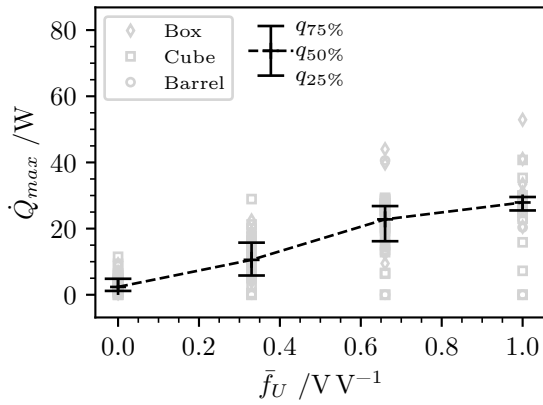


Figure 4.50.: Q_{max} for mixed battery samples using different mean voltage factors and $\sigma_{fU} = 0.2$, $m_{batts,bulk} \geq 5$ kg

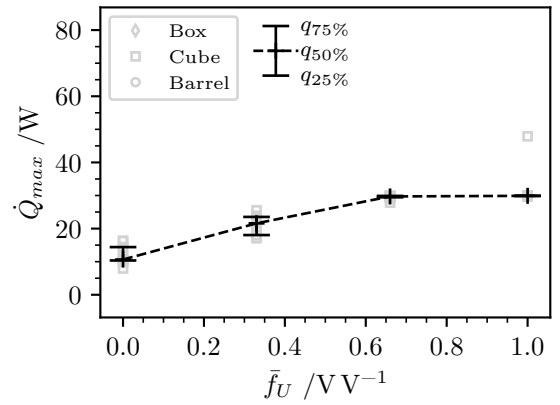


Figure 4.51.: Q_{max} for pure button cell samples using different mean voltage factors and $\sigma_{fU} = 0.2$

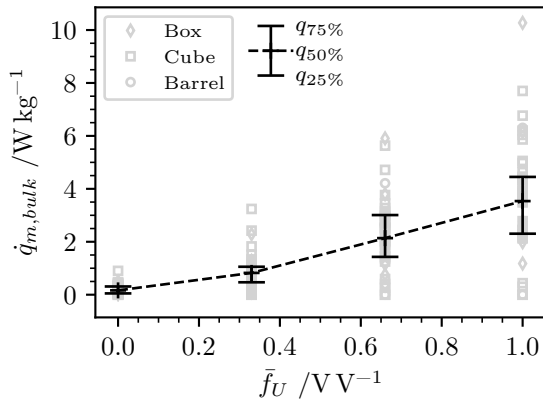


Figure 4.52.: $\dot{q}_{m,bulk}$ for mixed battery samples using different mean voltage factors and $\sigma_{fU} = 0.2$, $m_{batts,bulk} \geq 5$ kg

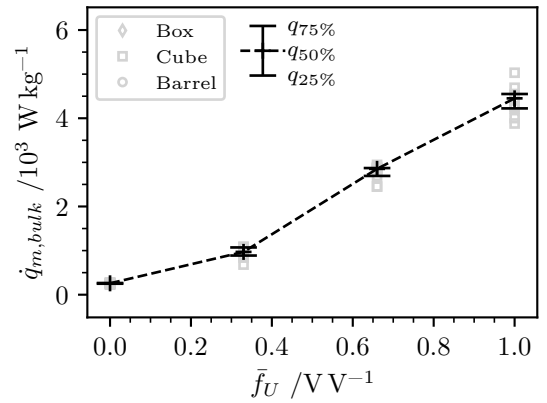


Figure 4.53.: $\dot{q}_{m,bulk}$ for pure button cell samples sample using different mean voltage factors and $\sigma_{fU} = 0.2$

4.4.6. Computational time

Figure 4.54 shows an exponentially increase for the computing time with the battery mass.

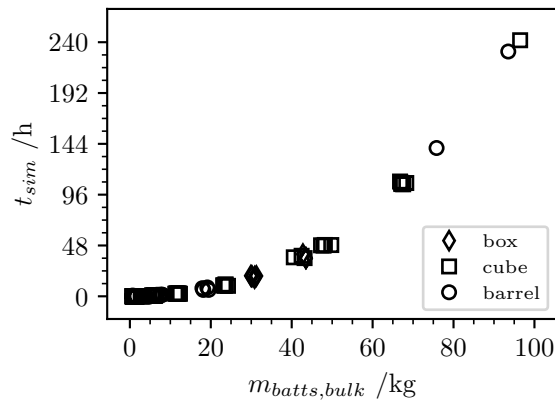


Figure 4.54.: Computing time for the simulation

4.4.7. Parameter sensitivity tests

31 simulation runs using the standard battery types composition in an 8L cube varying the simulation parameters were conducted. Since the span of $\pm 80\%$ for each input parameter is quite large, some simulation runs did not produce stable or realistic results. In eleven simulation runs, the batteries show very unrealistic behaviour, like strong overlaps, very high speeds or never getting in resting position. These results of this runs are not included in the analysis. A clear correlation which parameters produce these unstable results could not be found. A strong correlation gives the value

$$T^* = \frac{fps_base}{fps \cdot substeps_per_frame \cdot time_scale} \quad (4.7)$$

which is on average 14 times higher for unstable results. *restitution*, *safety_time* and *settle_time* show also a clear relationship to the stability. The evaluation for sensitivity was done using a linear regression for

$$\frac{\Delta y}{\bar{y}} - 1 = a \cdot \left(\frac{\Delta x}{\bar{x}} - 1 \right) + b \quad (4.8)$$

where Δx and Δy are the deviations of the input and output parameters, \bar{x} the standard value for the parameter x (table 4.13), \bar{y} the mean output value and a and b the regression parameters. Further the Coefficient of determination R^2 and the p -value for a linear approximation of the output parameter versus each simulation parameter are calculated.

Indicators for stability and accuracy are ρ_{bulk} , $(|\vec{v}_{end}|_{max})_{95}$ and $f_{sc,unrealistic}$. Tables C.1, C.2 and C.3 list the results. The sensitivity of the simulation results was analysed for $b_{sc,bulk}$, $x_{batts,sc}$, $N_{batts,sc,max}$, I_{max} and \dot{Q}_{max} . The results are shown in tables C.4, C.5 and C.6. The scale shows the most powerful effect. The influence on $x_{batts,sc}$ is depicted in figure 4.55.

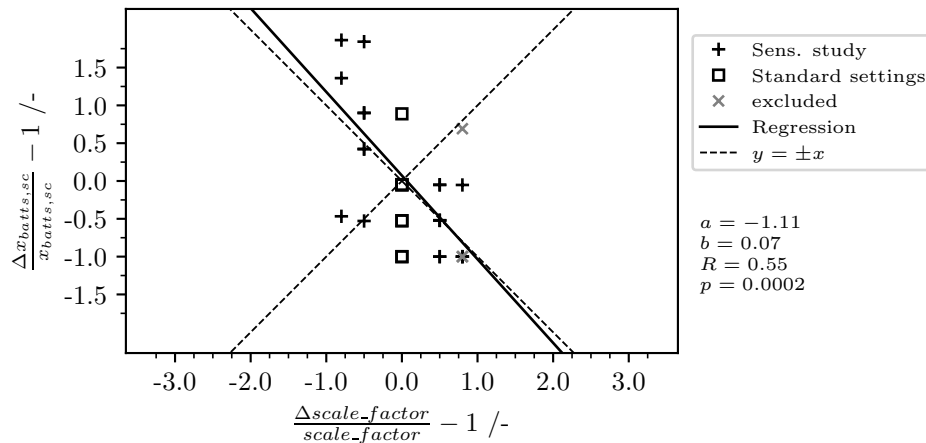


Figure 4.55.: Computing time for the simulation

4.5. Discussion of the numerical study

The novelty of the model and the few possibilities for comparison with other data make a detailed and critical examination of the model and the results necessary. The simplifications described and the stability of the simulation influence the outcome. The influence of simplifications and deviations due to the applied numerical method are discussed.

4.5.1. Approximations

To achieve a compromise between accuracy, realism and computing speed and stability, simplifications are needed. Different cases that occur in reality have been made comparable.

4.5.1.1. Rigid body simulation

In the collection of used batteries, forces that lead to a significant deformation of the batteries are considered unlikely. The typical drop and dump heights are low, and batteries have a relatively inflexible structure. It can therefore be assumed that the approximation of rigid bodies leads to appropriate results.

The sensitivity analysis shows a strongly non-linear correlation of the input parameters to the simulations stability. If certain threshold values are exceeded, the simulation becomes too unstable for further evaluation. Within the limit values, the sensitivity to most of the input parameters is little. Tables C.1 - C.3 show low correlation coefficients, effect sizes and significance levels. These values do not include the very unstable results.

The simulation results show very little hints of unstable conditions. The residual motion in the final cluster is low and very few unrealistic short circuits occur. The results indicate that useful results can be obtained in the investigated scenario by rigid body simulation.

4.5.1.2. Geometrical modelling

The geometries of the batteries and containers have been significantly simplified. In the case of the containers, the model still comes very close to reality. Especially the exact shape in the corners and edges does not play a decisive role for the accuracy of the results. The results for different container shapes show now visible differences on any scale.

In the case of the batteries, the edges are not rounded. It is possible that real batteries slide against each other in a different way, which affects the final orientation. A comparison how batteries arrange themselves in real bulks was not performed and in literature no comparable dataset was found.

The bulk densities obtained show good agreement with the available samples. The variation was wider for real life batteries. The battery type composition is different and some samples contain big accumulators. Experimental data is only available for the size range around 15 kg.

The definition of the bulk volume using a convex hull leads to strong fluctuations for bulk density when the bulk is not notable bigger than the batteries. The larger the bulk volume, the less significant the empty spaces in the peripheral zones of the convex hull become.

Button batteries are smaller, the necessary bulk size for clear results is smaller. Compaction at higher filling heights explains the increasing bulk density and decrease of void fraction for bigger bulk masses. In the analysed sample 42.8 batteries per kg and about 64 batteries per L were counted. Both values are in the range of the values determined in the simulations.

The results of the parameter study show an influence of *angular_damping* and *scale_factor* on the number of short circuits. The influence of *angular_damping* makes sense because the parameter influences the movement and therefore the arrangement.

The *scale_factor* was expected to have no influence, high values for correlation and significance level show a negative dependency. At higher scales, the number of short circuits becomes smaller. Presumably, contacts are not calculated exactly, but by a distance threshold. If this distance is not scaled as well, this leads to fewer detected contacts at higher scale factors. The type of contact detection needs to be revised for further experiments. In all simulation runs the same *scale_factor* of 100 was used, so the results are comparable. The relative effect strength is below one for all parameters.

The results of [41] on the influence of *friction* and *restitution* on the bulk density are not observed. The generated battery arrays do not show any obvious differences to real bulk. However, quantified comparisons are lacking.

4.5.1.3. Physical modelling

As shown by [41], the bulk properties depend on the type of loading. In the real case, the batteries are probably dropped into the container without special attention in most cases. Even the process is not defined, large drop heights, high velocities or orderly placement can be neglected. The forces remain within a narrow range. Emptying a smaller collection container is a possibility not represented in the algorithm. The battery type is randomly determined for each battery individually. In reality, there will probably be certain accumulations, like several items of one type at once.

The influence of miscasts, special batteries or large objects was not investigated further in this work, but is possible by adapting the developed algorithm. The addition of inert substances such as pellets is also possible.

The algorithm offers the possibility to investigate a wide range on scenarios. Adaptions in the throwing process would also be possible. In this thesis, some cases were investigated further. The procedure seems to be appropriate for studies on different scenarios.

4.5.1.4. Electrical modelling

A realistic calculation of the electrical properties of waste battery short circuits is complicated. However, the method used here provides good comparative values at low computational cost. The discharge behaviour is not taken in account. The values are therefore to be understood as an idealized initial state. Nevertheless, they represent suitable comparative quantities for many short-circuit and battery types.

The very low chosen values for R_i result in high values for the currents and heat generation. Especially discharged batteries can show orders of magnitude higher resistances. The contact resistance depends on the contact force, the geometry of the contact and the used material. In the range these properties are expected, a very low R_c can be assumed. For further usage, electrical currents and heat release should be recalculated using realistic values.

Although the interconnected networks may include many batteries, the results for I_{max} show that short circuit currents stay in the range of single short circuited batteries. In the example in section 4.2.5, five batteries are electrically connected, each one is only discharged with the current that would occur in a direct short circuit over R_c . In the experiments for the parameter study, no parameter set resulted in higher currents.

In each bulk I_{max} and \dot{Q}_{max} are extreme values. Better for comparison of bulks is the heat release distribution. In bulks with low coin battery fraction, only very few batteries are found in the range of \dot{Q}_{max} . With an increase of short circuited batteries and the voltage, the number of batteries with high heat generations rises.

4.5.2. Results of the simulation

The simulation runs show well repeatable results. For smaller containers, the small number of batteries and short circuits leads to high variations in the mass specific quantities.

The detected number of short circuits due to simulation faults or instabilities is 42 out of a total of 4414 short circuited batteries. Even if not all physically incorrect short circuits can be detected, it can still be assumed that it is not a significant amount.

An important parameter for the evaluation of the risk is $x_{batts,sc}$, the fraction of batteries that are short-circuited. The most important factor influencing $x_{batts,sc}$ is the proportion of button batteries. Figure 4.44 indicates a polynomial relationship of third degree, but the number of results between $x_{batts,sc} = 0.05$ and $x_{batts,sc} = 1$ is too small for precise statements. A linear interpolation between the mixed collection and the pure button battery mixtures yields to more conservative estimations. For bulks with very low coin fractions, the wide spread indicates, that in any case at least $x_{batts,sc} = 0.01$ should be assumed.

The model provides plausible results for all output values. In most cases the model makes conservative predictions and it can be expected that it overestimates the risk.

4.5.3. Application limits

The algorithm was developed to study specific questions about the waste battery collection in Austria. Extrapolations should be taken with precaution. Since no experimental comparison data were available, the method and all results should be used very carefully.

4.5.3.1. Limits of the model

As discussed, the approach using a rigid body simulation, is valid as long as the forces are low compared to the stiffness of the batteries. For bulks till 100 kg this seems to be valid. For bigger bulks and especially higher filling heights, the assumption has to be reconsidered.

Mechanical filling or tipping from one container in the next are not studied. This load mechanisms can create different packs than a one-by-one dropping. Waste batteries from special end-consumers, like companies, can have very different type distributions. If for example a bucket of coin batteries gets tipped in a larger container at once, results similar to pure coin bulks can be imagined, even if the overall coin fraction stays low.

4.5.3.2. Limits of interpretation of the results

Bulk masses below 5 kg show high variations and no comparison values for the bulk density were found. Most considerations in this work are just based on the larger bulks. 5 kg is about 230 batteries. This would fill a 3 L-container (edge length about 55 cm. The results should not be used for bulks far below this limit.

In all considerations, the containers are filled up to more than 90 %. This creates a relatively compacted battery bulk. Lower filling grades lead to decreasing bulk densities, which makes short circuits more unlikely. Therefor the results of this thesis would give a higher level of risk and can be taken as a conservative approach.

Investigations further than on the influence of the coin fraction have not been made. The results should not be applied to battery mixtures with a lot of block batteries or larger accumulators.

For different coin fractions just very few simulation runs were performed. The general trend seems valid, but for good quantifications, more tests are needed. The high computational time limited the number of tests for large containers. Even the number of simulation runs is quite high, most of them are in a narrow area of sizes and coin fractions.

Different containers were used for simulation, but for all of them the ratio of the side lengths was about the same. The results are maybe not valid for special container shapes.

4.6. Conclusions of the numerical study

The goal to develop an algorithm producing plausible and repeatable results with reasonable simplifications and acceptable computing time was achieved. The simulation seems to be appropriate for studies on the short circuit behaviour of battery bulks and compare different bulks. Typical cases were simulated and studied. From the generated data and the risk analysis, the main conclusions can be summarized as follows:

1. The occurrence of short circuits can be expected and described statistically.
2. Button cell batteries are the most short circuited battery type.
3. Networks of connected batteries do not generate higher currents than the same number of batteries short circuited individually.
4. The direct short circuit of a single button cell battery can be used as a model for all short circuited batteries.
5. The fraction of coin batteries is the main influence factor for the fraction of short circuited batteries.

Even there is a considerable spread, figures 4.25, 4.26, 4.39, and 4.44 show that short circuits can occur at all bulk sizes. The probability increases with mass and the coin battery fraction. Regardless of the battery type composition, studied in this work, Figures 4.29, 4.30 and 4.32 reveal that coins are by far the most frequently short circuited.

Complicated short circuits can be compared the basis of the electrical currents. These currents are equivalent to a directly short circuited battery for the vast majority of batteries. Even the large connected networks forming in pure coin collection have no currents higher. The arrangement in figure 4.56 is a valid approximation for short circuits.

A correlation of the fraction of short circuited batteries to the fraction of coin batteries is shown in figure 4.44. Other impact factors with a similar effect strength have not been found.

In order to be able to evaluate the results of the simulation, experimental, numerical or analytical comparison data are required. None could be found within the scope of this work. The results presented are plausible within the framework of the deviations discussed, but further considerations are necessary.

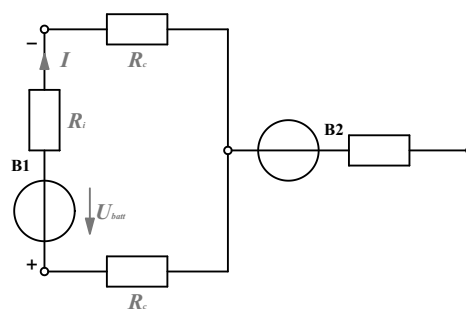


Figure 4.56.: Most common short circuit and model case for all

From the conclusions 1 to 5 follows, that the main impact factors for the risk are

- $x_{batts,coins}$, the fraction of button cell batteries,
- U_N , the nominal voltage of the typical short circuited battery type,
- \bar{f}_U and σ_{fU} , the parameters for an approximatly normal distribution of coin battery voltages,
- R_i and R_c as internal and contact resistances and
- \dot{Q}_{ignite} , the heat release of a battery sufficient for ignition.

The main risk in a bulk is a single, short circuited battery that, due to its state of charge, produces enough heat to perform a thermal runaway or ignite other inflammable bulk contents. So

$$\dot{Q}_{batt} \geq \dot{Q}_{ignite} \quad (4.9)$$

with \dot{Q}_{batt} is the heat release of a single battery. For the model case in figure 4.56 and the assumptions in section 4.2.3 for battery B1 is is

$$\dot{Q}_{batt} = \frac{U_N^2 \cdot (R_i + R_c)}{(R_i + 2 \cdot R_c)^2} \cdot f_U^2 \quad (4.10)$$

The maximum heat release \dot{Q}_{max} of the battery possible is when $f_U = 1$:

$$\dot{Q}_{max} = \frac{U_N^2 \cdot (R_i + R_c)}{(R_i + 2 \cdot R_c)^2} \quad (4.11)$$

Using the simplification that \dot{Q}_{batt} is normal distributed, the propagation of uncertainty give the parameters

$$\bar{\dot{Q}}_{batt} = \frac{U_N^2 \cdot (R_i + R_c)}{(R_i + 2 \cdot R_c)^2} \cdot \bar{f}_U^2 = \dot{Q}_{max} \cdot \bar{f}_U^2 \quad (4.12)$$

$$\sigma_{\dot{Q}} \approx \frac{\partial \dot{Q}_{batt}}{\partial f_U} \cdot \sigma_{fU} = 2 \cdot \bar{f}_U \cdot \frac{U_N^2 \cdot (R_i + R_c)}{(R_i + 2 \cdot R_c)^2} \cdot \sigma_{fU} = \dot{Q}_{max} \cdot 2 \cdot \bar{f}_U \cdot \sigma_{fU} \quad (4.13)$$

The cumulated propability density function for \dot{Q}_{batt} is then

$$x_{batts}(\dot{Q}_{batt} \leq \dot{Q}) = F(\dot{Q}) = C_1 \cdot \Phi \left(\frac{\dot{Q} - \bar{\dot{Q}}_{batt}}{\sigma_{\dot{Q}}} \right) + C_2 \text{ for } 0 \leq \dot{Q} \leq \dot{Q}_{max} \quad (4.14)$$

with $\Phi(x)$ as the cumulative standard normal distribution. It is defined for $-\infty < x < \infty$. Since f_U is limited in the range from 0 to 1, the function has to be scaled using the constants C_1 and C_2 .

Based on the assumptions, all batteries have heat release rates between 0 and \dot{Q}_{max} , so two conditions can be used for determine the constants:

$$x_{batts}(\dot{Q}_{batt} \leq 0) = 1 - x_{batts,sc} \quad (4.15)$$

$$x_{batts}(\dot{Q}_{batt} \leq \dot{Q}_{max}) = 1 \quad (4.16)$$

The final distribution for the heat generation of batteries in a bulk is

$$x_{batts}(\dot{Q}_{batt} \leq \dot{Q}) = 1 - x_{batts,sc} \cdot \frac{\Phi\left(\frac{1-\bar{f}_U^2}{2 \cdot \bar{f}_U \cdot \sigma_{fU}}\right) - \Phi\left(\frac{\frac{\dot{Q}_{max}}{2 \cdot \bar{f}_U \cdot \sigma_{fU}} - \bar{f}_U^2}{2 \cdot \bar{f}_U \cdot \sigma_{fU}}\right)}{\Phi\left(\frac{1-\bar{f}_U^2}{2 \cdot \bar{f}_U \cdot \sigma_{fU}}\right) - \Phi\left(\frac{-\bar{f}_U^2}{2 \cdot \bar{f}_U \cdot \sigma_{fU}}\right)} \quad (4.17)$$

and the fraction of ignited batteries can be calculated by

$$x_{batts}(\dot{Q}_{batt} \geq \dot{Q}_{ignite}) = 1 - x_{batts}(\dot{Q}_{batt} \leq \dot{Q}_{ignite}) = x_{batts,sc} \cdot \frac{\Phi\left(\frac{1-\bar{f}_U^2}{2 \cdot \bar{f}_U \cdot \sigma_{fU}}\right) - \Phi\left(\frac{\frac{\dot{Q}_{ignite}}{2 \cdot \bar{f}_U \cdot \sigma_{fU}} - \bar{f}_U^2}{2 \cdot \bar{f}_U \cdot \sigma_{fU}}\right)}{\Phi\left(\frac{1-\bar{f}_U^2}{2 \cdot \bar{f}_U \cdot \sigma_{fU}}\right) - \Phi\left(\frac{-\bar{f}_U^2}{2 \cdot \bar{f}_U \cdot \sigma_{fU}}\right)} \quad (4.18)$$

Equation (4.18) gives a quantitative estimation for the risk of ignition by a short circuit, based on the battery type composition and the state of charge distribution of the bulk. The limits of application in section 4.5.3 have to be noted. It must also be checked whether the assumptions in sections 4.2.3 are permissible in the application case.

Instead of the nominal voltage of the battery, also the maximum open circuit voltage OCV_{max} of the battery can be used for the Definition of f_U and equation (4.11). This would give more accurate results for fully charged batteries.

The required fraction of short circuited batteries $x_{batts,sc}$ and be estimated by the coin battery content of the bulk. The regression of a polynom of the third degree in figure 4.44 can be used for estimations:

$$x_{batts,sc}(x_{batts,coins}) = a_1 \cdot x_{batts,coins}^3 + a_2 \cdot x_{batts,coins}^2 + a_3 \cdot x_{batts,coins} + a_4 \quad (4.19)$$

with $a_1 = 6.31 \cdot 10^{-1}$, $a_2 = 1.43 \cdot 10^{-1}$, $a_3 = 2.77 \cdot 10^{-2}$ and $a_4 = 1.19 \cdot 10^{-4}$, with the consideration discussed in section 4.5.3. As a minimum value $x_{batts,sc} = 0.01$ should be used. A more conservative approach would be a linear interpolation between 1% at zero coin batteries and 82.7% for pure coin battery bulks.

The equations (4.17), (4.18) and (4.19) require just a few parameters and give a good estimation about the likelihood of short circuits which can trigger fires in battery bulks.

The introduced method should be illustrated on four example bulks. The parameters for the bulks are given in table 4.14. The first bulk is a mixed collection sample with a low but widely spread voltage distribution. Bulk 2 has the same voltages levels, but a higher coin battery fraction. Bulk 3 and 4 are pure coin battery bulks with higher voltage levels. In bulk 4 most batteries are at nominal voltage. $R_i = 0.3\Omega$ and $R_c = 0.1\text{ m}\Omega$ will be equal as used before in this work.

Table 4.14.: Parameters for example bulks

| Name | $x_{batts,coins}$ | $x_{batts,sc}$ (Eq. 4.19) | \bar{f}_U | σ_{fU} |
|--------|-------------------|------------------------------|-------------|---------------|
| Bulk 1 | 0.05 | 0.010 | 0.25 | 0.5 |
| Bulk 2 | 0.7 | 0.306 | 0.25 | 0.4 |
| Bulk 3 | 1 | 0.802 | 0.66 | 0.2 |
| Bulk 4 | 1 | 0.802 | 1 | 0.1 |

The results for the bulks are presented in figure 4.57. In bulk 1 there is almost no heat generation in any battery at all. From bulk 1 to bulk 4 the distribution shifts further to higher heat release values. In bulk 4 about 50% of the batteries have heat release values above 25 W. The risk for ignition increases from bulk 1, where it is almost zero to very high in bulk 4.

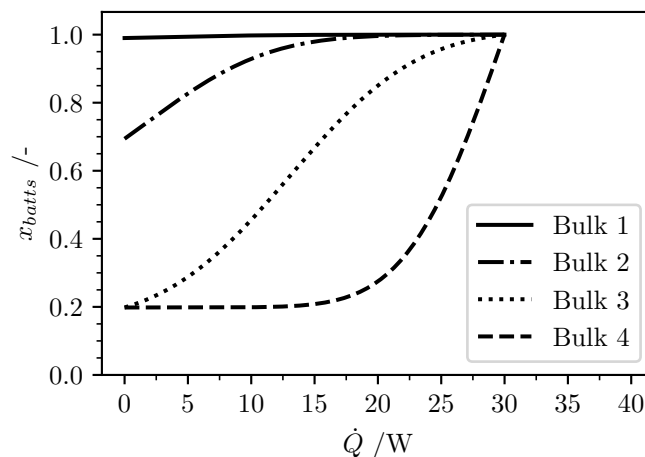


Figure 4.57.: Distribution of the heat release for example bulks

5. Conclusions

The risk analysis in chapter 3 shows the factors relevant for a fire risk assessment. The hazard potential of lithium-based battery systems differs significantly from other chemical systems. It is therefore plausible that lithium and lithium-ion batteries are considered a major risk factor by legislators. Even a lot of mandatory measures are in place to provide safety, there is a lack of scientific approaches to investigate the usefulness. Even the number of possible causes and effects is low, most branches of the Bow-tie analysis cannot be described accurately yet.

The numerical approach and the obtained data of chapter 4 provides a method for quantification of the short circuiting of batteries. The implementation is flexible in terms of battery types and states of charge. For some typical cases, the simulation give results are plausible and the obtained data can be used for investigation.

Equations 4.11, 4.18 and 4.19 require little input parameters and give a good, conservative estimation on the number of batteries igniting in a container or even a whole material stream. Suitable input parameters have to be found by experiments.

Activities for the reduction of risk are usually costly. They can feign false safety when there are many measures, but they are not suitable to reduce the risk. All efforts have to be evaluated to find a good compromise of safety and economical reason.

Typical measures against short circuits in battery bulks are the separation of coin batteries and the covering of the contacts of certain battery types, usually block batteries. Based on the results of the simulations, splitting a battery mass stream with 5% button cells in a high and a low coin stream, the percentage of batteries short circuited in both streams together increases from 0.4% to 4%. If a fully charged battery enters the stream, it has a chance of 80% being short circuited, compared to 8% without separation. Block batteries make around 3.5% of the short circuits in mixed collection. Isolating their contacts has very little effect, even if all block batteries would be covered.

Figure 3.3 indicates, that without external short circuits the risk of ignition inside the battery bulk would be very low. From the numerical study follows that keeping the coin fraction in a bulk low would reduce this risk. This could be achieved by not collecting them separately. Assuming the added electrically isolated material, like pellets or similar, have a similar effect as cylindrical batteries on the short circuits, they could be used for risk reduction in collection places with usually high button cell fractions.

6. Outlook and Suggestions

The proposed model provides a method for quantitatively describing the risk of ignition by short circuits. This enables a so far little understood branch of the risk analysis to be described in detail based on specified parameters. Comparison with experimental data on the frequency of short circuits in battery bulks would give more meaning to the presented results.

More detailed data on the compositions of the equipment battery collection, on states of charge, voltages, and internal resistances, as well as on the type and frequency of miscasts, can serve as a basis for further investigations. If these data are provided by geographical region, type of collection point and possible other social, infrastructural, and economic factors, detailed risk assessments can be carried out for different parts of the collection.

Using the presented algorithm, more detailed investigations of the risk situation in different areas of the collection can be carried out. This can be applied to specific features of the collected batteries as well as to the different stations along the collection path. Due to the relatively simple structure in free software, the algorithm can be adapted for many different use cases.

Looking at the risk analysis in figure 3.3, the spread of the fire within the container is another subject that has been little studied so far. Since the model can be used to create realistic geometries of battery piles, the system can in principle be extended to study this issue. In addition, a chemical model would have to be developed of how different batteries behave after ignition and at higher temperatures. The heat propagation through heat conduction, convection and radiation within the bulk would have to be modelled. Subsequently, the expected risks could be described in very comprehensively. By knowing the influencing parameters and their impact, an estimation of the risk situation can be made in advance if conditions change.

Circular economy and the recovery of raw materials are important issues. For this, safety for the end user and all stakeholders along the collection route is crucial. Changing compositions of material flows make forward-looking risk assessments necessary. The increasing use of lithium-based energy storage devices and the resulting rise in collection volumes require constant attention to risks.

6.1. Suggestions for further work

The risk analysis and the numerical study offer several options for further investigations. The ones considered most important are presented in this section.

1. For comparative data an experimental Setup should be developed for investigation of bulk properties and short circuit formation. The obtained data should be compared to the simulation results for further improvement of the data model.
2. The composition of the portable battery collection should be analysed by battery types and miscasts. The fraction of lithium-based or other hazardous batteries and the flammability of the miscasts should be evaluated. The data should be separated by geographical regions, type of collection point and other impact factors. Further information about the process when the end-consumer places the batteries in the container should be documented.
3. The results indicate that button cells are short circuited quite often in random bulks. A detailed analysis on the short circuit behaviour of button cells should be conducted. The currents and heat release rates sufficient for ignition should be measured in experiments for different types and states of charge.
4. The process after ignition of a button cell should be investigated by experiments to get information about the heat release and duration of burning.
5. The heat propagation inside a bulk of batteries and miscasts, including follow-up ignition and thermal runaways should be performed. Experimental and numerical approaches seem to be possible. For example the batteries can be modelled by heat sources and thermal resistances, which makes similar solution methodes possible as used for electrical calculations in this work.
6. When the data in this thesis is backed up by experimental results and the fire propagation inside can be described in a similar manner, a comprehensive risk assessment based on figure 3.3 using quantitative data to describe the risks in portable battery collection seems to be possible.

Nomenclature

Greek Symbols

| | |
|--------------------------------|--|
| ε_{bulk} | Void fracture in the bulk in $\text{m}^3 \text{m}^{-3}$ |
| μ | Mean value of a normal distributed randomized variable |
| $\Phi(x)$ | Cumulative function of the standard normal distribution |
| ρ_{batt} | Density of the battery in kg m^{-3} |
| ρ_{bulk} | Bulk density in kg m^{-3} |
| σ | Standard deviation of a normal distributed randomized variable |
| σ_{f_U} | Standard deviation parameter for the normal distribution of f_U in V V^{-1} |
| $\varphi_{bulk,container}$... | Degree of filling of the container in $\text{m}^3 \text{m}^{-3}$ |

Mathematical Symbols

| | |
|----------------------------------|--|
| $\mathcal{N}(0, 1)$ | Random standard normal distributed variable |
| $\mathcal{N}(\mu, \sigma)$ | Random normally distributed variable with the distribution parameters μ and σ |

Roman Symbols

| | |
|----------------------------|--|
| A | Coefficient matrix of a system of linear equations |
| a | Slope coefficient for linear regression models |
| <i>angular_damping</i> | Angular damping parameter for physics engine |
| \vec{b} | Result vector of a system of linear equations |
| B | Battery |
| b | Interception coefficient for linear regression models |
| $b_{sc,batts,bulk}$ | Number of batteries in short circuits per bulk mass in kg^{-1} |
| $b_{sc,bulk}$ | Short circuits per bulk mass in kg^{-1} |
| CCV | Closed circuit voltage of a battery in V |
| d | Diameter in m |
| d_1 | Diameter of the battery in m |
| d_i | Required diameter of the battery in m |
| E_{deform} | Energy of deformation in J |
| EV | End-point-voltage of a battery in V |
| \bar{f}_U | Mean value parameter for the normal distribution of f_U in V V^{-1} |
| F | Force in N |
| f_U | Voltage factor of a battery in V V^{-1} |
| $f_{sc,unrealistic}$ | Fraction of detected unrealistic short circuits |
| f_{ps} | Frames per f_{ps_base} seconds parameter for the physics engine |
| f_{ps_base} | Base for fps calculation parameter for the physics engine |

| | |
|---------------------------|--|
| <i>friction</i> | Friction parameter for physics engine |
| <i>g</i> | Acceleration due to gravity in m s^{-2} |
| h_1 | Overall height of battery in m |
| h_d | Drop height in m |
| h_i | Required height of battery in m |
| h_{safe} | Safety distance for battery creation in m |
| \vec{I} | Vector of calculated electrical currents I in A |
| I | Electrical current in A |
| I_{batt} | Electrical current of a battery in A |
| I_{max} | Maximum electrical current in bulk in A |
| $I_{sc,max}$ | Maximum short circuit current of a battery in A |
| L | Loop in an electrical circuit |
| l | length in m |
| l_1 | Length of the battery in m |
| l_i | Required length of the battery in m |
| l_1 | Length of cube and box containers in m |
| l_2 | Width of box container in m |
| l_3 | Height of box container in m |
| <i>linear_damping</i> | Linear damping parameter for physics engine |
| $m_{batts,bulk}$ | Mass of all batteries inside the bulk in kg |
| m_{batt} | Mass of the battery in kg |
| N | Junction or node in an electrical circuit |
| $N_{batts,bulk}$ | Number of batteries inside the bulk |
| $n_{batts,bulk}$ | Number of batteries per bulk volume in m^{-3} |
| $N_{batts,sc,max}$ | Maximum number of batteries in a short circuit in |
| $N_{batts,set}$ | Drop height in m |
| n_{cell} | Number of internal chemical cells |
| N_{con} | Number of contacts between two battery poles |
| $n_{sc,batts,bulk}$ | Number of batteries in short circuits per bulk volume in m^{-3} |
| $N_{sc,batts}$ | Total number of batteries in short circuits in bulk |
| $n_{sc,bulk}$ | Short circuits per bulk volume in m^{-3} |
| N_{sc} | Total number of short circuits in bulk |
| OCV | Open circuit voltage of a battery in V |
| OCV_{max} | Maximum open circuit voltage of a battery in V |
| P | Electrical power in W |
| p | p -value for linear regression models |
| \dot{Q} | Heat release rate in W |
| \dot{Q}_{batt} | Electrical heat release of a battery in W |
| \dot{Q}_{bulk} | Total heat release rate of battery bulk in W |
| \dot{Q}_{ignite} | Heat release rate of a battery sufficient for ignition in W |
| $\dot{q}_{m,bulk}$ | Heat release rate per bulk mass in W kg^{-1} |

| | |
|---|---|
| \dot{Q}_{max} | Heat release rate of a battery at nominal voltage in W |
| \dot{Q}_{max} | Maximum heat release rate of a single battery in bulk in W |
| Q | Voltage source |
| R | Resistance in Ω |
| R^2 | Coefficient of determination for linear regression models |
| R_i | Internal resistance of a battery in Ω |
| R_L | Load resistance in Ω |
| R_c | Resistance of a battery to battery contact in Ω |
| $R_{i,batt}$ | Internal resistance of a battery in Ω |
| $R_{i,cell}$ | Internal resistance of one battery cell in Ω |
| <i>restitution</i> | Restitution parameter for physics engine |
| $\bar{s}_{end,x}, \bar{s}_{end,y}, \bar{s}_{end,z}$ | Mean positions in all directions of the batteries in the bulk in m |
| \bar{s}_{end} | Mean position of the batteries in the bulk in m |
| \vec{s}_{end} | Location of the batteries centre in the last simulation frame in m |
| $s_{end,x}, s_{end,y}, s_{end,z}$ | Locations in all directions of the batteries centre in the last simulation frame in m |
| <i>scale_factor</i> | Scale factor for lengths in the simulation geometry in $m m^{-1}$ |
| <i>SOC</i> | State of charge of a battery |
| <i>solver_iterations</i> | Number of iterations calculated per sub step parameter for the physics engine |
| <i>substeps_per_frame</i> | Substeps calculated between two frames parameter for the physics engine |
| T^* | Comparison value for time discretization of the physics engine |
| t_{safe} | Safety time after battery drop in s |
| t_{settle} | Settle time after last battery in s |
| t_{sim} | Computational time of the simulation in h |
| <i>time_scale</i> | Speed parameter for the physics engine |
| U | Voltage in V |
| U_N | Nominal voltage of a battery in V |
| U_q | Voltage of the voltage source Q in V |
| U_R | Voltage drop across the resistor R in V |
| U_T | Voltage measured on the terminals of battery in V |
| U_{batt} | Voltage of the modelled voltage source in a battery in V |
| \vec{v}_0 | Initial velocity vector in $m s^{-1}$ |
| v_{0z} | Initial velocity in z -direction in $m s^{-1}$ |
| V_{batt} | Volume of the battery in m^3 |
| V_{bulk} | Volume of the battery bulk in m^3 |
| $x_{batts,coins}$ | Fraction of button cell batteries in the bulk |
| $x_{batts,sc}$ | Fraction of batteries in short circuits |
| x_{batts} | Fraction of batteries in the bulk |

Bibliography

- [1] ARIC A. HAGBERG ; DANIEL A. SCHULT ; PIETER J. SWART: Exploring Network Structure, Dynamics, and Function using NetworkX. In: GAËL VAROQUAUX (Hrsg.) ; TRAVIS VAUGHT (Hrsg.) ; JARROD MILLMAN (Hrsg.): *Proceedings of the 7th Python in Science Conference*. Pasadena, CA USA, 2008, S. 11–15
- [2] CROMPTON, T. R.: *Battery Reference Book*. 3rd ed. Jordan Hill : Elsevier Science & Technology Books, 2000 <https://ebookcentral.proquest.com/lib/kxp/detail.action?docID=313582>. – ISBN 9780080499956
- [3] BUNDESMINISTERS FÜR LAND- UND FORSTWIRTSCHAFT, UMWELT UND WASSERWIRTSCHAFT: *Verordnung des Bundesministers für Land- und Forstwirtschaft, Umwelt und Wasserwirtschaft über die Abfallvermeidung, Sammlung und Behandlung von Altbatterien und -akkumulatoren (Batterienverordnung): BGBl. II Nr. 159/2008 as amended by BGBl. II Nr. 311/2021*
- [4] THE EUROPEAN PARLIAMENT AND THE COUNCIL: *Directive 2006/66/EC of 6 September 2006 on batteries and accumulators and waste batteries and accumulators and repealing Directive 91/157/EEC*
- [5] IEC 61951-1:2017: *Secondary cells and batteries containing alkaline or other non-acid electrolytes - Secondary sealed cells and batteries for portable applications - Part 1: Nickel-Cadmium*
- [6] IEC 61951-2:2017: *Secondary cells and batteries containing alkaline or other non acid electrolytes - Secondary sealed cells and batteries for portable applications - Part 2: Nickel-metal hydride*
- [7] IEC 61960-3:2017: *Secondary cells and batteries containing alkaline or other non-acid electrolytes - Secondary lithium cells and batteries for portable applications - Part 3: Prismatic and cylindrical lithium secondary cells and batteries made from them*
- [8] IEC 61960-4:2020: *Secondary cells and batteries containing alkaline or other non-acid electrolytes - Secondary lithium cells and batteries for portable applications - Part 4: Coin secondary lithium cells, and batteries made from them*
- [9] IEC 60086-1:2021: *Primary batteries - Part 1: General*
- [10] IEC 60086-2:2021: *Primary batteries - Part 2: Physical and electrical specifications*
- [11] STIFTUNG GRS BATTERIEN: *Erfolgskontrolle gemäß § 15 (1) Batteriegesetz 2021*
- [12] STIFTUNG GRS BATTERIEN: *Erfolgskontrolle gemäß § 15 (1) Batteriegesetz 2020*
- [13] DURACELL INC.: *Product safety datasheet - Duracell Lithium HPL Cells and Batteries, 2022*

-
- [14] ENERGIZER HOLDINGS, INC.: *Product datasheet - Lithium CRV3*. <https://data.energizer.com/pdfs/crv3.pdf>. – checked on 16/11/2022 15:00
- [15] ENERGIZER HOLDINGS, INC.: *Product datasheet - Energizer L522 Ultimate Lithium*. <https://data.energizer.com/pdfs/1522.pdf>. – checked on 16/11/2022 15:00
- [16] ENERGIZER HOLDINGS, INC.: *Product datasheet - Energizer L91 Ultimate Lithium*. <https://data.energizer.com/pdfs/191.pdf>. – checked on 16/11/2022 15:00
- [17] ENERGIZER HOLDINGS, INC.: *Product datasheet - Energizer L92 Ultimate Lithium*. <https://data.energizer.com/pdfs/192.pdf>. – checked on 16/11/2022 15:00
- [18] ADVANCED POWER SOLUTIONS NV: *Panasonic Batteriekatalog 2021*. <https://www.panasonic-batteries.com/sites/default/files/Panasonicproductcatalogue2021-ENGwoAPB-RZ.pdf>. Version: 2021. – checked on 16/11/2022 15:00
- [19] VARTA MICROBATTERY GMBH: *Product Overview 2022*. https://www.varta-ag.com/fileadmin/varta/industry/downloads/products/VARTA_Product_Overview_2022.pdf. Version: 2022. – checked on 16/11/2022 15:00
- [20] KANAMURA, Kiyoshi: Electrolytes for lithium batteries. Version: 2005. <http://dx.doi.org/10.1016/B978-008044472-7/50039-4>. In: NAKAJIMA, Tsuyoshi (Hrsg.) ; GROULT, Henry (Hrsg.): *Fluorinated materials for energy conversion*. Amsterdam and San Diego, CA and Oxford : Elsevier, 2005. – DOI 10.1016/B978-008044472-7/50039-4. – ISBN 9780080444727, S. 253–266
- [21] LOGAN, E. R. ; TONITA, Erin M. ; GERING, K. L. ; LI, Jing ; MA, Xiaowei ; BEAULIEU, L. Y. ; DAHN, J. R.: A Study of the Physical Properties of Li-Ion Battery Electrolytes Containing Esters. In: *Journal of The Electrochemical Society* 165 (2018), Nr. 2, A21-A30. <http://dx.doi.org/10.1149/2.0271802jes>. – DOI 10.1149/2.0271802jes. – ISSN 1945–7111
- [22] NOH, Hyung-Joo ; YOUN, Sungjune ; YOON, Chong S. ; SUN, Yang-Kook: Comparison of the structural and electrochemical properties of layered Li[NixCoyMnz]O2 ($x = 1/3, 0.5, 0.6, 0.7, 0.8$ and 0.85) cathode material for lithium-ion batteries. In: *Journal of Power Sources* 233 (2013), S. 121–130. <http://dx.doi.org/10.1016/J.JPOWSOUR.2013.01.063>. – DOI 10.1016/J.JPOWSOUR.2013.01.063. – ISSN 0378–7753
- [23] SHAHID, Seham ; AGELIN-CHAAB, Martin: A review of thermal runaway prevention and mitigation strategies for lithium-ion batteries. In: *Energy Conversion and Management: X* 16 (2022), S. 100310. <http://dx.doi.org/10.1016/j.ecmx.2022.100310>. – DOI 10.1016/j.ecmx.2022.100310. – ISSN 25901745
- [24] ZHAO, Chunpeng ; SUN, Jinhua ; WANG, Qingsong: Thermal runaway hazards investigation on 18650 lithium-ion battery using extended volume accelerating rate calorimeter. In: *Journal of Energy Storage* 28 (2020), S. 101232. <http://dx.doi.org/10.1016/j.est.2020.101232>. – DOI 10.1016/j.est.2020.101232. – ISSN 2352152X
- [25] WU, Tangqin ; CHEN, Haodong ; WANG, Qingsong ; SUN, Jinhua: Comparison analysis on the thermal runaway of lithium-ion battery under two heating modes. In: *Journal of*

- hazardous materials* 344 (2018), S. 733–741. <http://dx.doi.org/10.1016/j.jhazmat.2017.11.022>. – DOI 10.1016/j.jhazmat.2017.11.022
- [26] SPOTNITZ, R. ; FRANKLIN, J.: Abuse behavior of high-power, lithium-ion cells. In: *Journal of Power Sources* 113 (2003), Nr. 1, S. 81–100. [http://dx.doi.org/10.1016/S0378-7753\(02\)00488-3](http://dx.doi.org/10.1016/S0378-7753(02)00488-3). – DOI 10.1016/S0378-7753(02)00488-3. – ISSN 0378-7753
- [27] KIM, Sin W. ; PARK, Soo G. ; LEE, Eui J.: Assessment of the explosion risk during lithium-ion battery fires. In: *Journal of Loss Prevention in the Process Industries* 80 (2022), S. 104851. <http://dx.doi.org/10.1016/j.jlp.2022.104851>. – DOI 10.1016/j.jlp.2022.104851. – ISSN 09504230
- [28] LEISING, Randolph A. ; PALAZZO, Marcus J. ; TAKEUCHI, Esther S. ; TAKEUCHI, Kenneth J.: Abuse Testing of Lithium-Ion Batteries: Characterization of the Overcharge Reaction of LiCoO₂/Graphite Cells. In: *Journal of The Electrochemical Society* 148 (2001), Nr. 8, S. A838. <http://dx.doi.org/10.1149/1.1379740>. – DOI 10.1149/1.1379740. – ISSN 0013-4651
- [29] WANG, Lubing ; YIN, Sha ; XU, Jun: A detailed computational model for cylindrical lithium-ion batteries under mechanical loading: From cell deformation to short-circuit onset. In: *Journal of Power Sources* 413 (2019), S. 284–292. <http://dx.doi.org/10.1016/j.jpowsour.2018.12.059>. – DOI 10.1016/j.jpowsour.2018.12.059. – ISSN 0378-7753
- [30] ZHU, Feng ; DU, Xianping ; LEI, Jianyin ; AUDISIO, Lorenzo ; SYPECK, David: Experimental study on the crushing behaviour of lithium-ion battery modules. In: *International Journal of Crashworthiness* 26 (2021), Nr. 6, S. 598–607. <http://dx.doi.org/10.1080/13588265.2020.1766397>. – DOI 10.1080/13588265.2020.1766397. – ISSN 1358-8265
- [31] *Bundesgesetz über eine nachhaltige Abfallwirtschaft (Abfallwirtschaftsgesetz 2002 - AWG 2002): BGBl. I Nr. 102/2002 as amended by BGBl. I Nr. 200/2021*
- [32] BUNDESMINISTERS FÜR LAND- UND FORSTWIRTSCHAFT, UMWELT UND WASSERWIRTSCHAFT: *Verordnung des Bundesministers für Land- und Forstwirtschaft, Umwelt und Wasserwirtschaft über Abfallbehandlungspflichten (AbfallBPV) Abfallbehandlungspflichten (AbfallBPV): BGBl. II Nr. 102/2017*
- [33] BUNDESMINISTERIUM FÜR NACHHALTIGKEIT UND TOURISMUS: *Erläuterungen zur Verordnung Abfallbehandlungspflichten - Stand April 2018*
- [34] BUNDESMINISTERIN FÜR KLIMASCHUTZ, UMWELT, ENERGIE, MOBILITÄT, INNOVATION UND TECHNOLOGIE: *Verordnung der Bundesministerin für Klimaschutz, Umwelt, Energie, Mobilität, Innovation und Technologie über ein Abfallverzeichnis (Abfallverzeichnisverordnung 2020): BGBl. II Nr. 409/2020*
- [35] ECONOMIC COMMISSION FOR EUROPE INLAND TRANSPORT COMMITTEE: *Agreement Concerning the International Carriage of Dangerous Goods by Road (ADR) Volume I applicable as from 1 January 2021*
- [36] ECONOMIC COMMISSION FOR EUROPE INLAND TRANSPORT COMMITTEE: *Agreement Concerning the International Carriage of Dangerous Goods by Road (ADR) Volume II applicable as from 1 January 2021*

- [37] NIGL, Thomas ; BÄCK, Tanja ; STUHLPFARRER, Stefan ; POMBERGER, Roland: The fire risk of portable batteries in their end-of-life: Investigation of the state of charge of waste lithium-ion batteries in Austria. In: *Waste management & research : the journal of the International Solid Wastes and Public Cleansing Association, ISWA* 39 (2021), Nr. 9, S. 1193–1199. <http://dx.doi.org/10.1177/0734242X211010640>. – DOI 10.1177/0734242X211010640
- [38] NIGL, Thomas ; BALDAUF, Mirjam ; HOHENBERGER, Michael ; POMBERGER, Roland: Lithium-Ion Batteries as Ignition Sources in Waste Treatment Processes—A Semi-Quantitate Risk Analysis and Assessment of Battery-Caused Waste Fires. In: *Processes* 9 (2021), Nr. 1, S. 49. <http://dx.doi.org/10.3390/pr9010049>. – DOI 10.3390/pr9010049
- [39] ZHANG, Qingsong ; NIU, Jianghao ; ZHAO, Ziheng ; WANG, Qiong: Research on the effect of thermal runaway gas components and explosion limits of lithium-ion batteries under different charge states. In: *Journal of Energy Storage* 45 (2022), S. 103759. <http://dx.doi.org/10.1016/j.est.2021.103759>. – DOI 10.1016/j.est.2021.103759. – ISSN 2352152X
- [40] WANG, Shunli ; XIE, Yanxin ; GUERRERO, Josep M.: Market batteries and their characteristics. Version: 2022. <http://dx.doi.org/10.1016/B978-0-323-91134-4.00010-8>. In: *Nano Technology for Battery Recycling, Remanufacturing, and Reusing*. Elsevier, 2022. – DOI 10.1016/B978-0-323-91134-4.00010-8. – ISBN 9780323911344, S. 3–31
- [41] MOGHADDAM, Elyas M. ; FOUMENY, Esmail A. ; STANKIEWICZ, Andrzej I. ; PADDING, Johan T.: Rigid Body Dynamics Algorithm for Modeling Random Packing Structures of Nonspherical and Nonconvex Pellets. In: *Industrial & engineering chemistry research* 57 (2018), Nr. 44, S. 14988–15007. <http://dx.doi.org/10.1021/acs.iecr.8b03915>. – DOI 10.1021/acs.iecr.8b03915. – ISSN 0888–5885
- [42] BLENDER DOCUMENTATION TEAM: *Blender 3.2 Reference Manual*. <https://docs.blender.org/manual/en/3.2/index.html>. Version: 2021. – checked on 16/11/2022 15:00

List of Figures

| | | |
|-------|--|----|
| 2.1. | Symbol for an ideal electrical resistor (EN 60617-2) | 3 |
| 2.2. | Symbol for an ideal voltage source (EN 60617-2) | 3 |
| 2.3. | Electrical currents entering and leaving the junction | 4 |
| 2.4. | Sum of all voltages around a loop equals zero | 5 |
| 2.5. | Schematic structure of the chemical system of a battery | 6 |
| 2.6. | Symbol for a battery (EN 60617-2) | 7 |
| 2.7. | Terminal voltage of a battery under a load R_L | 7 |
| 2.8. | Internal resistance model of a battery | 9 |
| 3.1. | Serial connection of n batteries | 26 |
| 3.2. | Parallel connection of n batteries | 27 |
| 3.3. | Results of the risk analysis presented as Bow-Tie-analysis | 31 |
| 4.1. | Model for batteries IEC 60086 category 1 (LR6 as example) | 35 |
| 4.2. | Model for batteries IEC 60086 category 4 (CR2354 as example) | 35 |
| 4.3. | Model for batteries IEC 60086 category 6 (6F22/6R61 as example) | 35 |
| 4.4. | Model for box-shaped container | 37 |
| 4.5. | Model for barrel-shaped container | 37 |
| 4.6. | Model for cube-shaped container | 37 |
| 4.7. | Simplified physical model for the filling process | 39 |
| 4.8. | Filling process in blender ('cube', $V_{cont} = 8\text{ L}$, $l_1 = 20\text{ cm}$, $m_{batts,bulk} = 11.6\text{ kg}$, $fps = 15$, $time_scale = 5$) | 39 |
| 4.9. | Analysed sample for battery types distribution (yellow surface approx. $1\text{ m} \times 1\text{ m}$) | 40 |
| 4.10. | Standard battery type distribution, simplified from sample in figure 4.9 | 40 |
| 4.11. | Cumulative probability function of the applied voltage distributions | 42 |
| 4.12. | Convex hull around batteries marking the bulk ('cube', $V_{cont} = 8\text{ L}$, $l_1 = 20\text{ cm}$, $m_{batts,bulk} = 11.6\text{ kg}$) | 43 |
| 4.13. | Contact determination for battery bulk | 44 |
| 4.14. | Reduction of the graph to relevant subgraphs | 45 |
| 4.15. | Relevant batteries and subgraphs | 45 |
| 4.16. | Circuit diagram of a group of batteries in a bulk | 46 |
| 4.17. | Number of simulation runs performed for different bulk masses ($\Delta m = 2\text{ kg}$) | 51 |
| 4.18. | Bulk density ρ_{bulk} of the simulated battery bulks | 51 |
| 4.19. | Bulk void fraction ε_{bulk} of the simulated battery bulks | 52 |
| 4.20. | Number of batteries $N_{batts,bulk}$ per bulk size | 52 |
| 4.21. | Velocity in the last second of the settle time for different container sizes | 53 |

| | |
|--|----|
| 4.22. Maximum movement in the last second of the settle time for different container sizes | 53 |
| 4.23. Number of contacts between battery poles in the bulk | 53 |
| 4.24. Number of pole contacts per number of batteries in the bulk | 53 |
| 4.25. Number of short circuits in the bulk | 54 |
| 4.26. Number of short circuited batteries | 54 |
| 4.27. Number of short circuited batteries to the number of batteries in the bulk . . . | 55 |
| 4.28. Fraction of unrealistic short circuits | 55 |
| 4.29. Battery type distribution of short circuited batteries | 56 |
| 4.30. Battery type distribution in short circuits for smaller (a) and larger (b) bulk sizes | 56 |
| 4.31. Maximum number of batteries in one short circuit | 57 |
| 4.32. Short circuit types by included battery types distribution | 57 |
| 4.33. Maximum initial electrical current in bulk using $R_i = 0.3 \Omega$ and $R_c = 0.1 \text{ m}\Omega$. | 58 |
| 4.34. Maximum initial heat release in one battery using $R_i = 0.3 \Omega$ and $R_c = 0.1 \text{ m}\Omega$ | 58 |
| 4.35. Total initial heat release in bulk using $R_i = 0.3 \Omega$ and $R_c = 0.1 \text{ m}\Omega$ | 58 |
| 4.36. ρ_{bulk} for different battery masses for pure coin battery bulks | 59 |
| 4.37. Number of batteries $N_{batts,bulk}$ per bulk size for pure coin battery bulks | 59 |
| 4.38. Maximum number of batteries in one short circuit for pure coin battery bulks . | 60 |
| 4.39. Fraction of batteries in short circuits for pure coin battery bulks | 60 |
| 4.40. I_{max} for pure coin battery bulks ($R_i = 0.3 \Omega$, $R_c = 0.1 \text{ m}\Omega$) | 61 |
| 4.41. \dot{Q}_{max} for pure coin battery bulks ($R_i = 0.3 \Omega$, $R_c = 0.1 \text{ m}\Omega$) | 61 |
| 4.42. \dot{Q}_{bulk} for pure coin battery bulks ($R_i = 0.3 \Omega$, $R_c = 0.1 \text{ m}\Omega$) | 61 |
| 4.43. Distribution of the heat release for coin batteries | 62 |
| 4.44. Fraction of batteries in short circuits for variation of the button cell fraction . . | 62 |
| 4.45. I_{max} for varying button cell fraction ($R_i = 0.3 \Omega$, $R_c = 0.1 \text{ m}\Omega$) | 63 |
| 4.46. \dot{Q}_{max} for varying button cell fraction ($R_i = 0.3 \Omega$, $R_c = 0.1 \text{ m}\Omega$) | 63 |
| 4.47. $\dot{q}_{m,bulk}$ for varying button cell fraction ($R_i = 0.3 \Omega$, $R_c = 0.1 \text{ m}\Omega$) | 64 |
| 4.48. I_{max} for mixed battery samples using different mean voltage factors and $\sigma_{fU} =$ 0.2, $m_{batts,bulk} \geq 5 \text{ kg}$ | 64 |
| 4.49. I_{max} for pure button cell samples using different mean voltage factors and $\sigma_{fU} =$ 0.2 | 64 |
| 4.50. Q_{max} for mixed battery samples using different mean voltage factors and $\sigma_{fU} =$ 0.2, $m_{batts,bulk} \geq 5 \text{ kg}$ | 65 |
| 4.51. Q_{max} for pure button cell samples using different mean voltage factors and $\sigma_{fU} = 0.2$ | 65 |
| 4.52. $\dot{q}_{m,bulk}$ for mixed battery samples using different mean voltage factors and $\sigma_{fU} =$ 0.2, $m_{batts,bulk} \geq 5 \text{ kg}$ | 65 |
| 4.53. $\dot{q}_{m,bulk}$ for pure button cell samples sample using different mean voltage factors and $\sigma_{fU} = 0.2$ | 65 |
| 4.54. Computing time for the simulation | 65 |
| 4.55. Computing time for the simulation | 66 |
| 4.56. Most common short circuit and model case for all | 71 |
| 4.57. Distribution of the heat release for example bulks | 74 |

List of Tables

| | |
|--|-----|
| 2.1. Forces, displacement and approximate deformation energy for internal short circuits of 18650 cylindrical lithium-ion batteries [29] | 11 |
| 2.2. Relevant legislation on the collection of waste batteries in Austria | 13 |
| 2.3. Classification of waste batteries in Austria (Abfallverzeichnisverordnung 2020 Annex 1) | 15 |
| 4.1. Simulation parameter for the geometry model | 34 |
| 4.2. Simulation parameters for the battery model | 34 |
| 4.3. Simulation parameters for the container model | 36 |
| 4.4. Simulation parameters for the physical model | 38 |
| 4.5. Simulation parameters for the electrical model | 41 |
| 4.6. Parameters for voltage distribution in simulation runs | 42 |
| 4.7. Simulation parameters for the time discretization and iterations | 42 |
| 4.8. Evaluated output parameters for each battery | 43 |
| 4.9. Evaluated output parameters for the battery bulk | 44 |
| 4.10. Evaluated output parameters for the bulk's short circuits | 46 |
| 4.11. Evaluated output parameters for the bulk's electrical properties | 48 |
| 4.12. Evaluated output parameters for the accuracy and stability of simulation . . . | 49 |
| 4.13. Set of input parameters used for simulation | 50 |
| 4.14. Parameters for example bulks | 74 |
| A.1. Battery type distribution in analysed sample | I |
| B.1. Sizes of containers implemented in this work | II |
| C.1. R^2 for the stability and accuracy indicators to the simulation input parameters | III |
| C.2. a for the stability and accuracy indicators to the simulation input parameters . | III |
| C.3. p -values for the stability and accuracy indicators to the simulation input parameters | IV |
| C.4. R^2 for the results to the simulation input parameters | IV |
| C.5. a for the results to the simulation input parameters | V |
| C.6. p -values for the results to the simulation input parameters | V |

A. Standard battery distribution from sample

Table A.1.: Battery type distribution in analysed sample

| IEC 60086-2 category | IEC 60086-2 designation | Trade names | Number |
|----------------------|-----------------------------------|-----------------|--------|
| 1 | R03, LR03, HR03 | AAA, Micro | 148 |
| 1 | R6, LR6, HR6 | AA, Mignon | 379 |
| 1 | R14, LR14 | C, Baby | 25 |
| 1 | R20, LR20 | D, Mono | 9 |
| 2 | CR17345 | | 3 |
| 4 | CR1025 | Button cell | 1 |
| 4 | CR1620 | Button cell | 1 |
| 4 | CR2032 | Button cell | 10 |
| 4 | CR2354 | Button cell | 17 |
| 5 | 8LR932 | | 2 |
| 5 | 4LR44 | | 1 |
| 6 | 3LR12 | Lantern battery | 2 |
| 6 | 6R61, 6LR61, 6F22 | 9-volt battery | 10 |
| | Larger batteries and accumulators | | 4 |
| | Miscasts | | 1 |

B. Implemented container sizes and types

Table B.1.: Sizes of containers implemented in this work

| V_{cont} | container type | $m_{batts,bulk}$ (estimate) | container size |
|------------|----------------|-----------------------------|--------------------------|
| 0.25 L | cube | 0.4 kg | 63 mm × 63 mm × 63 mm |
| 0.5 L | barrel | 0.8 kg | ∅86 mm × 86 mm |
| 0.5 L | cube | 0.8 kg | 80 mm × 80 mm × 80 mm |
| 1 L | barrel | 1.5 kg | ∅108 mm × 108 mm |
| 1 L | cube | 1.5 kg | 100 mm × 100 mm × 100 mm |
| 2 L | cube | 3 kg | 126 mm × 126 mm × 126 mm |
| 4 L | cube | 6 kg | 159 mm × 159 mm × 159 mm |
| 5 L | barrel | 7.5 kg | ∅185 mm × 185 mm |
| 8 L | cube | 12 kg | 200 mm × 200 mm × 200 mm |
| 10.7 L | cube | 16 kg | 220 mm × 220 mm × 220 mm |
| 12.3 L | barrel | 19 kg | ∅250 mm × 250 mm |
| 15.6 L | cube | 24 kg | 250 mm × 250 mm × 250 mm |
| 20 L | box | 31 kg | 260 mm × 360 mm × 215 mm |
| 21 L | barrel | 32 kg | ∅300 mm × 300 mm |
| 27 L | cube | 40 kg | 300 mm × 300 mm × 300 mm |
| 28.9 L | box | 44 kg | 285 mm × 375 mm × 270 mm |
| 32 L | cube | 48 kg | 317 mm × 317 mm × 317 mm |
| 44 L | cube | 66 kg | 352 mm × 352 mm × 352 mm |
| 50 L | barrel | 75 kg | ∅348 mm × 526 mm |
| 60 L | barrel | 90 kg | ∅366 mm × 568 mm |
| 64 L | cube | 97 kg | 400 mm × 400 mm × 400 mm |

C. Sensitivity parameters

Table C.1.: R^2 for the stability and accuracy indicators to the simulation input parameters

| | ρ_{bulk} | $(\vec{v}_{end} _{max})_{95}$ | $f_{sc,unreal}$ |
|---------------------------|---------------|--------------------------------|-----------------|
| <i>time_scale</i> | 0.23 | 0.09 | 0.05 |
| <i>fps</i> | 0.10 | 0.07 | 0.03 |
| <i>substeps_per_frame</i> | 0.06 | 0.21 | 0.00 |
| <i>solver_iterations</i> | 0.05 | 0.01 | 0.04 |
| <i>friction</i> | 0.16 | 0.02 | 0.03 |
| <i>restitution</i> | 0.03 | 0.00 | 0.04 |
| <i>linear_damping</i> | 0.07 | 0.05 | 0.04 |
| <i>angular_damping</i> | 0.13 | 0.01 | 0.04 |
| <i>scale_factor</i> | 0.15 | 0.07 | 0.04 |
| <i>safety_distance</i> | 0.13 | 0.00 | 0.06 |
| <i>safety_time</i> | 0.04 | 0.00 | 0.06 |
| v_{0z} | 0.25 | 0.00 | 0.02 |
| <i>settle_time</i> | 0.05 | 0.06 | 0.05 |

Table C.2.: a for the stability and accuracy indicators to the simulation input parameters

| | ρ_{bulk} | $(\vec{v}_{end} _{max})_{95}$ | $f_{sc,unreal}$ |
|---------------------------|---------------|--------------------------------|-----------------|
| <i>time_scale</i> | 0.08 | 0.66 | 1.51 |
| <i>fps</i> | -0.05 | 0.55 | 1.17 |
| <i>substeps_per_frame</i> | -0.04 | -1.21 | 0.56 |
| <i>solver_iterations</i> | 0.04 | -0.22 | -1.48 |
| <i>friction</i> | -0.06 | -0.32 | 1.26 |
| <i>restitution</i> | 0.03 | -0.10 | 1.48 |
| <i>linear_damping</i> | 0.04 | -0.48 | -1.33 |
| <i>angular_damping</i> | -0.06 | -0.20 | -1.33 |
| <i>scale_factor</i> | -0.06 | 0.58 | -1.48 |
| <i>safety_distance</i> | 0.06 | -0.03 | -1.76 |
| <i>safety_time</i> | -0.03 | 0.12 | -1.76 |
| v_{0z} | 0.08 | 0.02 | 1.03 |
| <i>settle_time</i> | 0.04 | -0.53 | -1.58 |

Table C.3.: p -values for the stability and accuracy indicators to the simulation input parameters

| | ρ_{bulk} | $(\vec{v}_{end} _{max})_{95}$ | $f_{sc,unreal}$ |
|---------------------------|---------------|--------------------------------|-----------------|
| <i>time_scale</i> | 0.032 | 0.194 | 0.367 |
| <i>fps</i> | 0.178 | 0.278 | 0.484 |
| <i>substeps_per_frame</i> | 0.319 | 0.040 | 0.785 |
| <i>solver_iterations</i> | 0.326 | 0.669 | 0.375 |
| <i>friction</i> | 0.085 | 0.530 | 0.450 |
| <i>restitution</i> | 0.452 | 0.852 | 0.375 |
| <i>linear_damping</i> | 0.246 | 0.343 | 0.422 |
| <i>angular_damping</i> | 0.126 | 0.690 | 0.422 |
| <i>scale_factor</i> | 0.096 | 0.251 | 0.375 |
| <i>safety_distance</i> | 0.119 | 0.958 | 0.298 |
| <i>safety_time</i> | 0.376 | 0.827 | 0.298 |
| v_{0z} | 0.025 | 0.965 | 0.543 |
| <i>settle_time</i> | 0.335 | 0.302 | 0.346 |

Table C.4.: R^2 for the results to the simulation input parameters

| | $b_{sc,bulk}$ | $x_{batts,sc}$ | $N_{batts,sc,max}$ | I_{max} | \dot{Q}_{max} |
|---------------------------|---------------|----------------|--------------------|-----------|-----------------|
| <i>time_scale</i> | 0.00 | 0.00 | 0.01 | 0.00 | 0.01 |
| <i>fps</i> | 0.07 | 0.06 | 0.10 | 0.14 | 0.11 |
| <i>substeps_per_frame</i> | 0.01 | 0.03 | 0.16 | 0.14 | 0.14 |
| <i>solver_iterations</i> | 0.01 | 0.00 | 0.00 | 0.01 | 0.00 |
| <i>friction</i> | 0.04 | 0.03 | 0.10 | 0.19 | 0.08 |
| <i>restitution</i> | 0.08 | 0.06 | 0.02 | 0.04 | 0.08 |
| <i>linear_damping</i> | 0.06 | 0.05 | 0.00 | 0.02 | 0.00 |
| <i>angular_damping</i> | 0.25 | 0.16 | 0.20 | 0.38 | 0.34 |
| <i>scale_factor</i> | 0.56 | 0.55 | 0.46 | 0.33 | 0.40 |
| <i>safety_distance</i> | 0.00 | 0.00 | 0.00 | 0.03 | 0.06 |
| <i>safety_time</i> | 0.03 | 0.02 | 0.06 | 0.10 | 0.11 |
| v_{0z} | 0.03 | 0.06 | 0.10 | 0.02 | 0.01 |
| <i>settle_time</i> | 0.02 | 0.07 | 0.06 | 0.02 | 0.02 |

Table C.5.: a for the results to the simulation input parameters

| | $b_{sc,bulk}$ | $x_{batts,sc}$ | $N_{batts,sc,max}$ | I_{max} | \dot{Q}_{max} |
|---------------------------|---------------|----------------|--------------------|-----------|-----------------|
| <i>time_scale</i> | 0.01 | 0.01 | 0.09 | 0.03 | -0.08 |
| <i>fps</i> | -0.36 | -0.38 | -0.36 | -0.36 | -0.32 |
| <i>substeps_per_frame</i> | -0.14 | -0.33 | -0.55 | -0.42 | -0.44 |
| <i>solver_iterations</i> | 0.15 | 0.10 | -0.06 | -0.08 | -0.06 |
| <i>friction</i> | -0.29 | -0.24 | -0.37 | -0.40 | -0.27 |
| <i>restitution</i> | -0.40 | -0.36 | -0.16 | -0.20 | -0.28 |
| <i>linear_damping</i> | 0.34 | 0.35 | -0.07 | -0.13 | -0.01 |
| <i>angular_damping</i> | -0.70 | -0.60 | -0.50 | -0.57 | -0.56 |
| <i>scale_factor</i> | -1.04 | -1.11 | -0.78 | -0.54 | -0.62 |
| <i>safety_distance</i> | 0.02 | -0.03 | 0.01 | 0.17 | 0.24 |
| <i>safety_time</i> | -0.23 | -0.19 | -0.28 | -0.31 | -0.34 |
| v_{0z} | 0.23 | 0.36 | 0.37 | 0.14 | 0.09 |
| <i>settle_time</i> | -0.21 | -0.40 | -0.28 | 0.12 | 0.12 |

Table C.6.: p -values for the results to the simulation input parameters

| | $b_{sc,bulk}$ | $x_{batts,sc}$ | $N_{batts,sc,max}$ | I_{max} | \dot{Q}_{max} |
|---------------------------|---------------|----------------|--------------------|-----------|-----------------|
| <i>time_scale</i> | 0.981 | 0.987 | 0.748 | 0.906 | 0.734 |
| <i>fps</i> | 0.273 | 0.283 | 0.180 | 0.098 | 0.161 |
| <i>substeps_per_frame</i> | 0.732 | 0.435 | 0.079 | 0.111 | 0.109 |
| <i>solver_iterations</i> | 0.648 | 0.782 | 0.826 | 0.709 | 0.784 |
| <i>friction</i> | 0.376 | 0.487 | 0.165 | 0.057 | 0.232 |
| <i>restitution</i> | 0.224 | 0.308 | 0.554 | 0.374 | 0.223 |
| <i>linear_damping</i> | 0.296 | 0.321 | 0.807 | 0.571 | 0.950 |
| <i>angular_damping</i> | 0.024 | 0.078 | 0.050 | 0.004 | 0.007 |
| <i>scale_factor</i> | 0.000 | 0.000 | 0.001 | 0.008 | 0.003 |
| <i>safety_distance</i> | 0.948 | 0.934 | 0.981 | 0.456 | 0.299 |
| <i>safety_time</i> | 0.489 | 0.595 | 0.305 | 0.169 | 0.147 |
| v_{0z} | 0.493 | 0.307 | 0.169 | 0.537 | 0.719 |
| <i>settle_time</i> | 0.533 | 0.257 | 0.300 | 0.594 | 0.607 |